Eugene Goss
COMMISSIONER OF HIGHWAYS

COMMONWEALTH OF KENTUCKY
DEPARTMENT OF HIGHWAYS
FRANKFORT, KENTUCKY 40601

February 26, 1970

H - 2 - 38

MEMORANDUM TO: A. O. Neiser, State Highway Engineer
Chairman, Research Committee

SUBJECT: Research Report (Interim); "Rheological and Ultimate-Strength Properties of Cohesive Soils;" KYHPR-65-38; HPR-1(5), Part II.

The report enclosed herewith was delayed a long time in the review stage. It presents a unique but perhaps controversial approach to the measurement of strength of cohesive soils. The method permits the complete Mohr failure envelope to be developed from a single specimen of soil rather than from a series of specimens. Further validation of the method is needed and will be forthcoming. Correlations thus far with respect to conventional triaxial tests have been excellent.

Respectfully submitted,

Jas. H. Havens
Director of Research

JHH:cel
Attachment
cc's: Research Committee

Assistant State Highway Engineer, Research and Development
Assistant State Highway Engineer, Planning and Programming
Assistant State Highway Engineer, Pre-Construction
Assistant State Highway Engineer, Construction
Assistant State Highway Engineer, Staff Services
Assistant Pre-Construction Engineer
Assistant Operations Engineer
Executive Director, Office of Computer Services
Executive Director, Office of Equipment and Properties
Director, Division of Bridges
Director, Division of Construction
Director, Division of Design
Director, Division of Maintenance
Director, Division of Materials
Director, Division of Photogrammetry
Director, Division of Planning
Director, Division of Right of Way
Director, Division of Roadside Development

Director, Division of Rural Roads
Director, Division of Traffic
Division Engineer, Bureau of Public Roads
Chairman, Department of Civil Engineering, University of Kentucky
Associate Dean for Continuing Education, College of Engineering
All District Engineers

Research Report

RHEOLOGICAL AND ULTIMATE STRENGTH PROPERTIES OF COHESIVE SOILS

INTERIM REPORT
KYHPR-65-38; HPR-1(4), Part II

by

Gordon D. Scott
Research Engineer Principal

Division of Research
DEPARTMENT OF HIGHWAYS
Commonwealth of Kentucky

in cooperation with the
U. S. Department of Transportation
Federal Highway Administration
Bureau of Public Roads

February 1969

INTRODUCTION

In recent years, there have been considerable advances made in rheological theory and its application to various materials. There has not been, however, nearly as much work done toward applying rheology to soil mechanics as the successes of others would seem to indicate. For instance, it has been shown *(11, 21, 22)* that a variety of stress and deflection problems considering the application of a load by means of an elastic plate to an elastic foundation can be extended to include rate effects through the application of linear viscoelastic theory. Before this theory can be applied to foundation design, however, two questions must be answered: 1) do soils generally conform to linear viscoelastic behavior? and 2) how can the design parameters be determined? A better knowledge of the long-term deformation properties of cohesive soils also would be invaluable in the analysis of the stability of slopes. For example, it has been determined from creep tests that, at loads less than those required to cause failure in triaxial shear tests, failure may occur after an extended period of loading.

Alfrey *(1)*, Alfrey and Gurnee *(3)*, and Leaderman *(13)* gave very good discussions of linear viscoelastic theory and pointed out the general behavior of viscoelastic materials. Lee *(14, 15)* reviewed viscoelastic stress analysis and discussed further developments needed to aid in appling the theory. Hoskins and Lee *(11)*, Pister and Williams *(22)*, and Pister *(21)* have shown how some solutions based on elastic theory can be extended to include rate effects with the aid of viscoelastic theory. Ferry *(6)* reviewed the measurement techniques which have been used on viscoelastic materials and pointed out the difficulties which arise in instrumentation.

Schiffman *(24)* has indicated the procedure for solving viscoelastic boundary value problems of the types generally encountered in soil tests. The procedure was illustrated by general solutions based on various simple types of viscoelasticity. Biot *(4, 5)* has developed a general theory of deformation of porous materials. Thermodynamic principles were used to derive operational relations between stress, deformation, fluid content, and fluid pressure. According to Biot, Tan was the first to apply viscoelastic analysis procedures to clay materials. Tan *(25, 26)* performed creep and relaxation tests on tubular as well as cylindrical soil specimens. His studies show that clay, under shear stress, may exhibit instantaneous deformation followed by a retarded deformation and, ultimately, continuous flow. He stated that there exists an upper yield stress in some clays above which accelerating flow occurs. Folgue *(7)* studied the rheological model, consisting of a spring and friction element in parallel with a Maxwell element, which

represented the relaxation and constant-rate-of-strain test results accurately but which was not adequate to describe creep test results.

Murayama and Shibata *(20)* and Mitchell *(18)* discussed the application of rate process theory to qualitatively describe the effects of temperature, etc on the response to various loading patterns. Murayama and Shibata also observed an upper yield value as reported by Tan. Their results indicate that stiff clays tend to fail at almost the same strain irrespective of the applied constant stress, but failure occured sooner for high stresses. They proposed a rheological model similar to the one suggested by Folgue. Corresponding studies by others *(29, 8)* have indicated similar results. Lara-Thomas *(12)* illustrated a procedure for transforming experimental creep curves to mechanical models for tubular soil specimens in shear. Similar studies *(19)* have been reported for bituminous materials. Tan *(27)* and Lo *(17)*, for instance, have used models to represent creep in long-term consolidation tests. Leonards and Girault *(16)*, however, have shown that the load increment ratio (stress history) has a profound effect on the time-dependent response.

In 1955 Havens and Daniels *(9)* re-emphasized the necessity of determining the basic rheological properties of materials, rather than empirical relationships, in order to make satisfactory correlations between material composition and behavior. Mossbarger *(19)* presented a basic preliminary study of viscoelastic principles from the standpoint of their derivation through tensor notations and their application to semi-solid materials.

For the study of soil problems, it is necessary to have a knowledge of the stress-strain-time characteristics of the material. The validity of a theoretical approach must be measured against the exactness of the soil parameters required. Any mathematical model must be reproducible approximately by experiment on the material, and the quantities which go to make up the model must be amenable to independent measurement in order for the theory to be useful.

Settlement of embankments and foundations built on plastic, residual, limestone-derived clays and the instability of slopes in shale areas are common problems in Kentucky. In 1963 two research studies involving field observations were initiated to develop better procedures for constructing bridge approaches and for correcting troublesome landslides. These experiences indicated the need for more basic knowledge concerning the factors that affect time-dependent behavior of soils.

Reported herein are the results of a laboratory study to determine ultimate strength and rheological properties of some cohesive soils, and to correlate strength test data with response to non-destructive, rheological tests.

Stress relaxation tests on small cylindrical specimens using modified triaxial equipment were conducted. The specimens were quickly strained a small amount and held at that strain while the load and pore pressure were measured. The duration of the stress relaxation test was on the order of one hour. After the relaxation test was completed, the sample was unloaded (unstrained) and allowed to rebound for a few minutes. A conventional triaxial test with pore pressure measurements was then conducted.

Data resulting from the stress relaxation tests are presented in the form of relaxation modulus-time and pore pressure-time curves. Triaxial test data are presented as conventional stress-strain and pore pressure-strain curves and failure envelopes. Correlations were made by plotting relaxation modulus versus failure stress and pore pressure from the relaxation test versus pore pressure at failure.

To develop a single, unique correlation curve relating each pair of soil parameters and valid for all soils would, of course, be the ideal goal. With such curves, a Mohr's envelope could be defined by performing stress relaxation tests upon a single specimen at various consolidation pressures. For example, a specimen could be consolidated to a low pressure (say 10 psi) overnight and a relaxation test could be performed. The specimen could again be consolidated to a higher pressure (say 30 psi) until late afternoon, when another relaxation test could be performed. The specimen could again be consolidated overnight at a still higher pressure (say 50 psi) and a third relaxation test performed the following morning. With the aid of the correlation curves, a Mohr's circle could be obtained from the results of each separate relaxation test, and thus a failure envelope would result from tests on only one sample with only one setup. Verification of the last point on the failure envelope could easily be made by performing a conventional triaxial test after the third relaxation test.

It was anticipated, however, that soils having different moisture contents, consistencies, and plasticities would exhibit different correlation curves. On the other hand, if a family of curves could be established, the test procedure described above -- with the triaxial test to failure -- would establish which particular curve applies to the specimen and would permit the correct failure envelope to be constructed. The development of a family of curves, therefore, and a demonstration that they can be used to obtain an accurate failure envelope through a testing program involving a single specimen was the objective of this research.

The initial testing was performed on undisturbed samples as part of another research study. Conventional triaxial tests with pore pressure measurements were being performed on Shelby tube samples obtained from landslides and sites of proposed construction of major highway embankments for the purpose of making stability analyses. Thus, it occurred to the author that some significant data applicable to this study could

be obtained at little extra effort by performing stress relaxation tests on the triaxial specimens just prior to performing the triaxial test. In this way, stress relaxation data would be made available for a wide variety of soil types, mositure contents, and consistencies. Moreover, ultimate strength data would also be available for the same specimens for comparison.

The majority of the testing was performed on remolded specimens prepared by extrusion. Stress relaxation tests followed by conventional triaxial tests were used to establish correlation curves and conventional failure envelopes. Then, using a single specimen and the correlation curves, a testing program involving relaxation tests at various consolidation pressures followed by a triaxial test were used to construct the failure envelope for comparison.

The significance of this research lies mainly in the possibility of eliminating the effect on the failure envelope of non-identical specimens rather than in the possibility of reducing the number of tests. In most cases, samples that are obviously not identical must be included in the testing program in order to have enough points to construct the failure envelope. The effect of sample differences cannot be evaluated in each case due to other unknown errors (the development of a leak after the test is started, for instance) but it is known that these differences can have a tremendous influence upon test results.

Schmertmann and Osterberg *(23)* described the development of a "curve hopping" test procedure designed to permit the determination of a Mohr's envelope from test results on a single specimen. The test is performed at an extremely slow rate of strain, and during the test the effective major principal stress is alternated between two predetermined values by varying the pore pressure in such a way that two stress-strain curves can be plotted -- one for each value of effective major principal stress. Terzaghi *(28)* stated that, "... *The determination of the shear characteristics of cohesive soils in an undisturbed state requires a considerable number of samples of practically identical materials which, in most cases, cannot be obtained. If the procedure proposed by Schmertmann and Osterberg should prove to be sufficiently reliable, this difficulty would disappear, because the procedure would make it possible to obtain the essential data from triaxial tests on a single specimen...* "

However, considerable correlation work remains to be done before Sclunertmann and Osterberg's procedure can be adapted to the solution of real problems since their test procedure does not yield the conventional shear strength parameters. That is, Schmertmann and Osterberg's values of cohesion and friction for a particular material do not agree with values obtained by conventional test procedures on practically identical materials. Wilson and Dietrich *(30)*, however, have found very good correlation between modulus of elasticity and failure strength of one clay soil.

METHODOLOGY

Soils

Soils used in this research consisted of both undisturbed and remolded specimens. The initial testing was performed on undisturbed samples as part of another research study -- conventional triaxial tests with pore pressure measurements were being performed on Shelby tube samples obtained from landslides and sites of proposed construction of major highway embankments for the purpose of making stability analyses.

Undisburbed Soil Specimens

The undisturbed samples were obtained from three highway embankment construction sites -- one in Jefferson County, Kentucky; one in Lyon County, Kentucky; and one in Webster and McLean Counties, Kentucky.

Undisturbed samples were obtained essentially in accordance with ASTM D 1587, Thin-Walled Tube Sampling of Soils. Thin-walled tubes, 2 3/8 inches inside diameter and 30 to 36 inches in length, were used to secure the samples. The drilling was performed with hollow stem augers using size "A" drill rods and a pilot bit. At five-foot intervals of depth, the drill rods were removed and a Shelby tube attached in place of the pilot bit. The sample tube was then lowered into the hole through the hollow augers and was pushed the length of the tube into the soil. After waiting approximately ten minutes, the tube was rotated about one turn to separate the sample from the soil below. The drill rods were then pulled and the sample tube removed. The Shelby tubes were immediately sealed with wax and covered with a plastic wrapping to minimize any loss of moisture. The tubes were then marked as to the hole and depth from which they were obtained. Tube samples were carefully transported to the laboratory by car.

Immediately upon arrival at the laboratory, the samples were removed from the Shelby tubes, using a horizontal hydraulic extractor, and identified by ASTM D 2488, Description of Soils (Visual-Manual Procedure). To remove soil which may have been seriously disturbed during sampling, material was trimmed from each end of the tube sample and discarded. The remainder of each sample was cut into specimens approximately four inches long, dipped in melted wax for protection and to maintain the moisture contents at natural conditions, and stored at approximately 70^{o}F until tested. Triaxial and unconfined compression

tests were performed to define the shear strength of the embankment foundations and consolidation tests were performed to define the settlement characteristics. Stress relaxation tests were performed on the triaxial specimens just prior to performing the triaxial strength tests. A summary of test results is given in Table 1.

Remolded Soil Specimens

It was desirable to have available a large number of specimens with as high a degree of saturation as possible and with the clay structure duplicated as closely as possible. This included void ratio, degree of saturation, particle orientation, mineralogy, and composition of the pore water. Such duplication in a large numbers of specimens could only be hoped for in remolded specimens. A "Vac-Aire" extrusion machine capable of extruding bars of clay up to three inches in diameter was used. The soil was mixed in a vacuum and forced by augers through a die of desired size and shape. Mixing in a vacuum produced a high degree of uniformity and saturation.

The remolded specimens were prepared from samples of four naturally occuring Kentucky soils and one commercial clay. The commercial clay was a kaolinite purchased from the Edgar Plastic Kaolin Company, Edgar, Florida. Classification test data are shown in Table 2. The Kentucky soils were obtained from pits in Adair, Clark, Fayette, and Fulton Counties. All four soils were cohesive, ranging from clay to silty loam. Engineering classification tests were performed on the actual samples obtained and the results are summarized in Table 3. Approximately 20 specimens of each of the natural Kentucky soils and 60 kaolinite specimens were prepared.

The Kentucky soils investigated were first allowed to air dry and were pulverized and passed through a Number 10 sieve. The plus 10 size material was discarded. A jar mill with rubber covered rods was used to pulverize the soil. Distilled water was added to the sample, to bring the moisture content to the desired value, and mixed for a few minutes by hand. The mixture was sealed in plastic bags and allowed to cure overnight. The moist soil was then run through the extrusion machine at least twice to insure complete and uniform mixing. The material was again run through the extrusion apparatus, and the rod of extruded soil was cut into specimens approximately four inches long and immediately immersed in melted wax for protection until testing. Cylindrical specimens two inches in diameter were used in this research.

The kaolinite was received in a dry, powdered form. It was then mixed with distilled water in its "as received" form and specimens were prepared in the same manner as described for the naturally occurring

Table 1. Summary of Laboratory Test Results -- Undisturbed Soils.

Project	Location	Description	Depth (feet)	Shelby Tube Moisture Content (%)	Atterberg Limits LL (%)	Atterberg Limits PL (%)	Specific Gravity	Dry Unit Weight After Test (lbs/ft³)	Confining Pressure (psi)	Pore Pressure (psi)	Maximum (σ1-σ3) (psi)	Cohesion (psi)	Effective Angle (°)
I 264, Jefferson County	Sta 314+50	Yellow, sandy clay Yellow sand	8-10.5 13-15				2.68						
	Sta 317+00	Silty blue clay	5-7		31.8	19.7	2.68						
	Sta 320+00	Silty blue clay Sand and gravel	0-15.5 15.5-16		22.6	16.9	2.65						
	Sta 320+00 (50 feet right)	Silty blue clay	5-7.5					86.1 87.0 85.5	5 30 55	16.377 24.844 38.794	0.575 8.950 31.13	1.0	26
		Silty blue clay	10-12.5				2.68	83.1 88.0 88.8	50 35 20	47.763 34.275 53.036	35.50 21.88 -1.650	3.5	32
	Sta 320+00 (50 left)	Silty blue clay	5-7.5 10-12.5		25.8	16.1	2.71	85.5 83.5 82.6 85.6	5 20 35 50	12.325 16.481 18.480 36.217	0.000 16.65 32.50 35.13	1.6	30
	Sta 323+00	Silty blue clay Sand and gravel	0-20 20-21		47.0	25.1	2.65						
I 24, Lyon County	Sta 3692+00	Moist, reddish-brown, silty clay Wet, soft, organic clay Gray, saturated, organic clay Light brown, saturated, organic clay	8.5 13.5 18.5 35.0	44.0 41.1 56.2 62.3			2.64 2.60 2.62						
	Sta 3688+00	Reddish-brown, saturated, organic clay	10.0	35.5					5 25 50	0.75 15.50 21.25	10.25 27.50 41.85	1.0	28
		Blue-gray, wet, organic clay Reddish-gray, saturated, dense sand Gray, wet organic silt (shells present)	15.0 20.0 28.0	17.2 23.9 34.5			2.62 2.56 2.68		25 55	20.70 24.00	14.80 72.00	1.5	31
		Dark tan, saturated, sandy clay	34.5	30.8					5 30	2.75 11.50	9.75 39.10		
	Sta 3684+00	Reddish-tan, saturated, organic clay Reddish-brown, saturated, organic, silty clay Red, saturated, organic silt (with sand lenses)	7.0 12.0 17.0	34.7 23.6 26.3									
	Sta 3691+00 (50 feet right)	Reddish-brown, saturated, organic clay	8.0	29.5					5 30 55	1.90 11.90 17.50	8.40 28.70 73.60	1.0	28
		Tan, wet, organic silt	13.0	23.1			2.67		10 25 45 65	2.50 10.00 7.50 36.00	17.00 36.40 57.75 72.00	0.0	34
		Tan, wet, organic silt Bluish-gray, saturated, organic clay Bluish-gray, wet, organic silt Reddish-tan, saturated, organic clay	18.0 23.0 28.0 33.0	27.0 24.3 18.8			2.65 2.66 2.64						
	Sta 3686+00 (57 feet left)	Reddish-brown, saturated, organic silt Reddish-gray, saturated, organic silt Saturated, organic silt Reddish-gray, saturated, organic silt Dark tan, saturated, organic silt Bluish-gray, saturated, organic clay	8.0 13.0 18.0 23.0 28.0 33.0	25.6 43.4 36.6 25.9 28.3									
Webster - McLean Counties	Sta 115+00	Brown clay	10-12.5	22.2				100.3 105.9	5 15 30 55	-5.13 -2.50 12.10 13.38	27.48 33.98 42.08 51.76	1.0	31.0
	Sta 125+00	Brown clay	5-7.5	18.1				101.7 105.7 103.5	5 30 55	-2.90 6.05 23.88	35.40 53.14 84.16	0.5	34.5
	Sta 125+00	Brown, silty clay	15-17.5	20.0				100.7 101.3 103.4	15 30 54	3.76 13.10 18.50	30.49 36.23 57.41	3.0	21.0
	Sta 125+00	Brown, sandy clay	20-22.5	24.0				100.8 102.3 106.3	5 30 55	-2.19 19.15 35.00	20.21 26.61 42.20	2.0	28.5
	Sta 125+00	Brown sand	25-27.5	26.8				97.7 101.1 98.5	5 30 50	-0.47 11.0 32.50	16.76 54.25 37.04	1.2	31.5

Table 2

Descriptive Data (Kaolinite)

		Percent Finer Than		
Liquid Limit	54%			
Plastic Limit	33%	200 sieve	50μ	2μ
Specific Gravity	2.61	100	100	60
Unified Classification	MH			

Table 3. Summary of Classification Test Results -- Kentucky Soils.

County	Liquid Limit (%)	Plastic Limit (%)	Specific Gravity	Standard Proctor Density (lbs/ft^3)	Optimum Moisture (%)	Kentucky CBR	Classifications			
							Unified	AASHO	Agricultural	Textural
Adair	61	27	2.768	96	24	5.0	MH	A-7-5(19)	Baxter Cherty Silt Loam	Clay
Clark	37	25	2.705	96	22	6.5	CL	A-6(13)	Eden Silty Clay Laom	Silty Caly
Fayette	35	21	2.685	101	20	9.5	CL	A-6(12)	Maury Silt Loam	Clay Loam
Fulton	26	NP	2.657	106	16	10.0	ML	A-4(8)	Calloway Silt Loam	Silty Loam

County	Percent Finer Than													
	1"	3/4"	3/8"	4	10	20	40	60	140	200	.05 mm	.02 mm	.005 mm	.002 mm
Adair	100	95	93	92	91	90	89	89	88	88	82	74	58	50
Clark	100	100	100	100	99	98	98	97	94	91	88	75	44	31
Fayette	100	100	100	100	99	96	94	92	85	79	76	61	30	20
Fulton	100	100	100	100	99	98	98	97	87	78	79	40	17	13

soils.

Adair County -- The soil from Adair County was a clay. Its Unified classification was CH and the AASHO classification was A-7-5(19). The agricultural classification was Baxter cherty silty loam. Baxter soils are widespread and well drained and occupy sloping upland areas. They are developed in residuum from cherty limestones.

Clark County -- The soil from Clark County was a silty clay. Its Unified classification was CL and the AASHO classification A-6(13). The agricultural classification was Eden silty clay loam. The Eden series consists of moderately deep, somewhat excessively drained soils underlain by calcareous shale and thin-bedded limestone. These soils are found on ridge tops and sideslopes in the uplands and are the most extensive soils of the Hills of the Bluegrass (Eden Hills). The subsoil is thin, yellowish-brown clay, and it overlies parent material of variegated, plastic clay. The number of rock slabs throughout the profile ranges from none to many; most of the slabs are in the lower part of the subsoil. The profile ranges from neutral in the upper part to calcareous in the lower.

Fayette County -- The soil from Fayette County was a clay loam. Its Unified classification was CL and the AASHO classification A-6(12). The soil was classified agriculturally as a Maury silt loam. The Maury series consists of nearly level to strongly sloping, deep, well-drained soils on uplands. These soils form mostly in material weathered from phosphatic limestone but partly in a mantle of silt. Maury soils are found only in the Inner Bluegrass but is extensively mapped there.

Fulton County -- The soil from Fulton County was a silty loam. Its Unified classification was ML and the AASHO classification was A-4(8). The agricultural classification was Calloway silt loam. The Calloway series consists of somewhat poorly drained soils on uplands and stream terraces where slopes range from 0 to 6 percent. These soils develop in thick loess and cover a large area.

Test Equipment

The sample trimming equipment used by the Division of Research consists of a cylindrical cutter held in vertical alignment inside a frame (see Figure 1). This equipment includes appropriate trimming and carving tools, vernier calipers capable of measuring the length and diameter of the specimen to the nearest 0.01 inch, an end-trimming cradle, and a sample extruder. The inside diameter of the cutter is approximately 0.005 inch larger than the desired diameter of the test specimen, except for a 1/8- inch length at the cutting

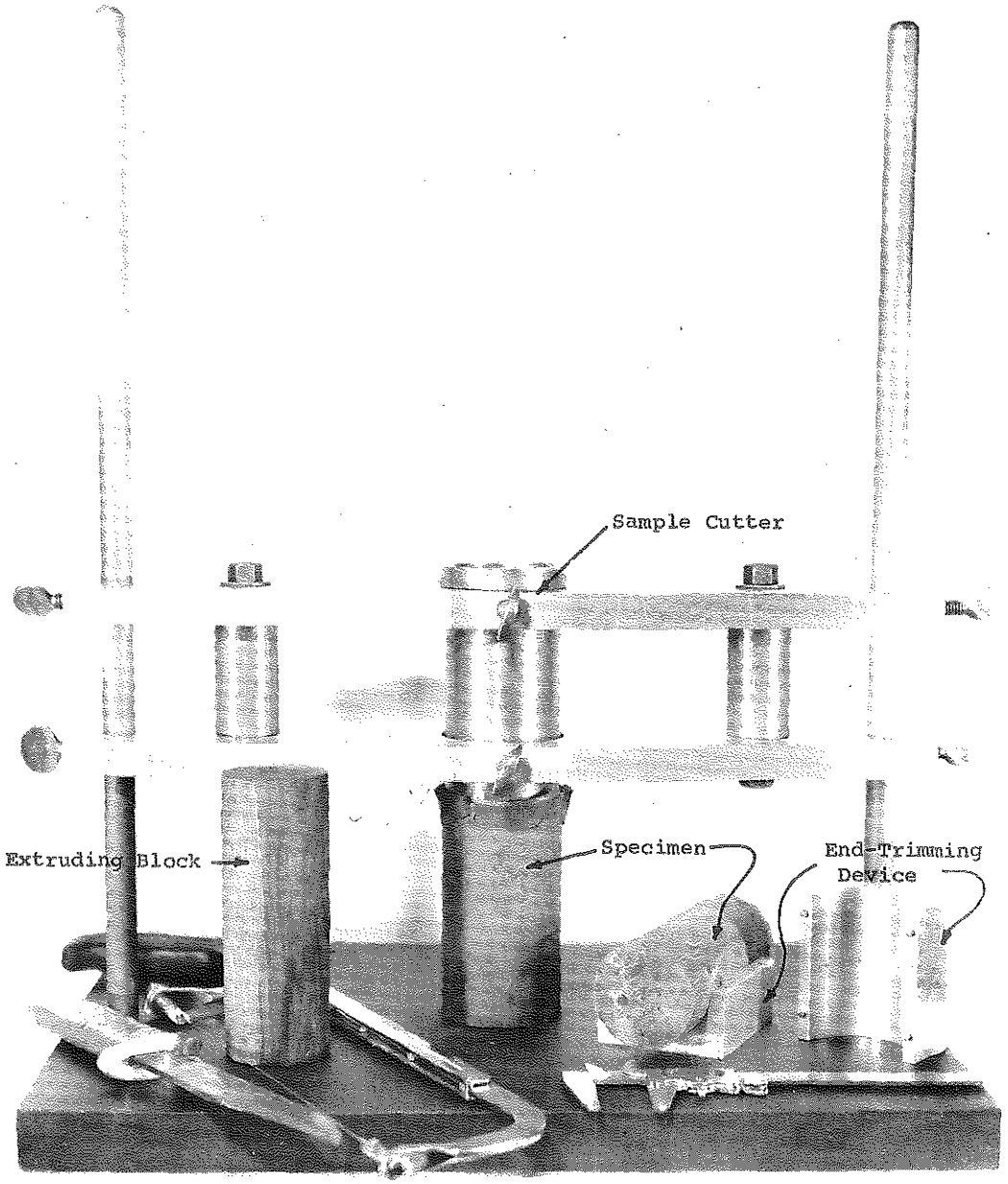

Figure 1. Sample Trimming Equipment.

end, where the diameter is equal to the specimen diameter.

The commercially available triaxial equipment (see Figures 2 and 3) used by the Division of Research was modified to increase the ease and reliability of pore pressure and consolidation measurements. The pressure chambers were equipped with two-inch base pedestals and headers. The bottom pedestal was provided with a relatively fine grained porous stone 1.9 inches diameter by 0.1 inch thick fitted snugly into an indentation. Two drainage lines -- 1/16-inch O. D. nylon tubing -- lead from outside the chamber to the bottom pedestal. Thus water could be circulated through the lines and porous stone to purge the system of air. The drainage lines were continuous, i.e., there were no fittings between the outside of the chamber and the porous stone as they might be difficult to deair completely.

One of the lines was provided with a no-volume-change valve outside the chamber which could be connected to a burette and back pressure system. The other line could be connected to a pore pressure transducer. Water was used as the confining fluid and both the chamber pressure and back pressure were controlled by precision air pressure regulators. The confining air pressure was applied to the upper part of the chamber -- above the specimen -- which was not filled with water. A continuous supply of dry, filtered air was required. The supply pressure was not permitted to drop below 120 psi nor rise above 150 psi.

The load was applied to the top cap through a 3/4-inch steel piston guided through the top of the chamber by two Thompson ball bushings and a rubber "quad-ring" pressure seal. A variable speed drive forced the chamber containing the specimen up against the piston, which was fixed to the top of the loading frame. The rate of deformation could be controlled to as low as 0.0002 inches per minute through the use of a 100:1 reduction gear box. The load was measured with strain gage load cells mounted inside the chambers, eliminating the effect of piston friction. Pore pressures were measured with strain gage pressure transducers. Deformation was usually indicated on dial extensometers, or linear variable differential transformers could be used if it was desired to record the data.

Test loads and pore pressures were monitored on either a Sanborn Model 321 dual channel oscillograph or a Brush Recorder Mark II with a dual strain gage amplifier.

Testing Procedure

The trimming of specimens, whenever possible, was done in a controlled-humidity room to minimize any change in moisture content of the soil. The sample was centered under the cutter, which was lowered to the

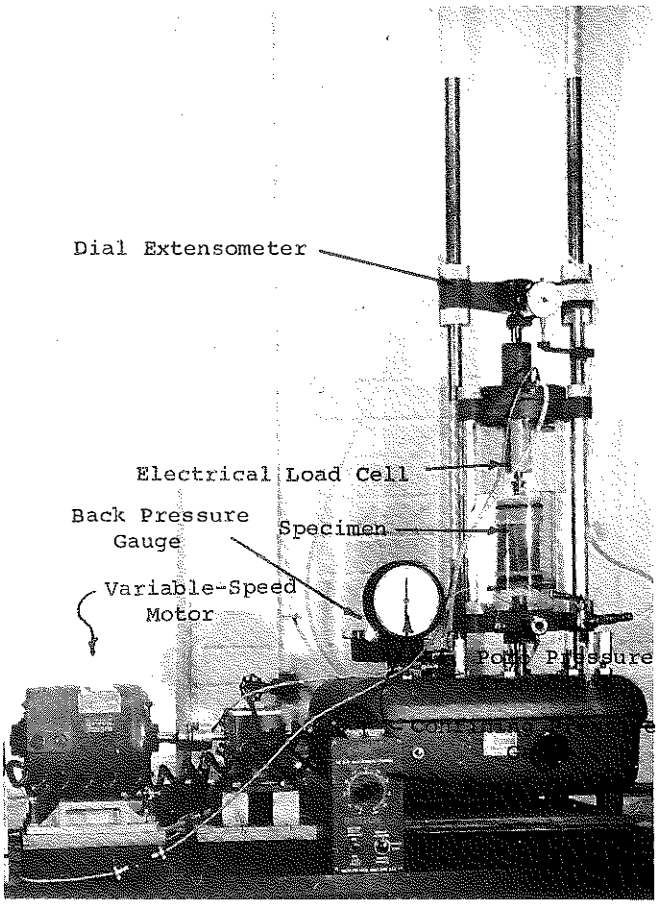

Figure 2. Triaxial Testing Equipment.

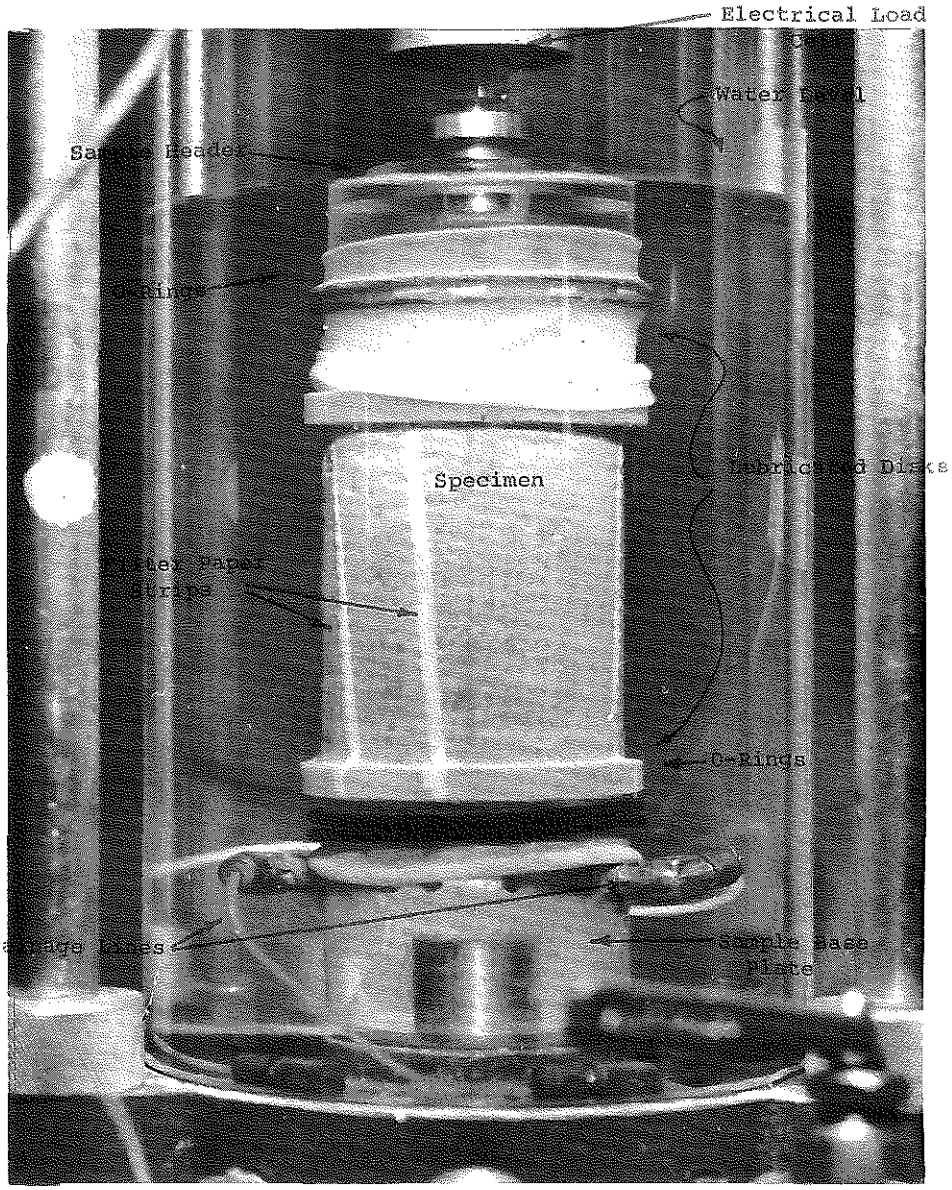

Figure 3. Triaxial Test Chamber.

desired position by loosening wing nuts. After positioning, the cutter was slowly pushed down into the sample. Concurrently, the excess soil was trimmed away by using carving knives, etc. When the frame was lowered to its final position and the cutter was filled with the specimen, the cutter was removed and the specimen extruded with the extrusion block. To insure the least possible disturbance, the cutter was lubricated with a lightweight oil. If the surface of the extruded specimen was not smooth, bits of the soil trimmings were used to fill any voids. After this, the cutter was again gently pushed over the specimen to insure a proper-sized specimen.

The specimen was then placed in the end-trimming device and trimmed so that the ends were perpendicular to the longitudinal axis. Specimens were trimmed to be three inches long.

Several measurements of the diameter and height of each specimen were made and the weight of the test specimen was determined. The specimen was then ready to be placed in the triaxial chamber on the pedestal which had been prepared as follows: 1) a saturated porous stone was placed in the indentation of the pedestal, 2) strips of filter paper were placed over the porous stone, and 3) a polished plexiglass or teflon disk, slightly larger in diameter than the specimen, was placed over the porous stone on the pedestal. The disk was coated with a thin film of silicone grease to reduce end friction between the specimen and the end cap and thus allow for more uniform deformation. The specimen was then placed on the coated disk, and the strips of filter paper folded up along the sides of the specimen to the top of the specimen in order to provide drainage paths around the polished disk.

Using a vacuum membrane-expander, a thin leak-proof membrane was placed over the specimen. Two rubber O-rings were placed around the membrane at the pedestal to provide a seal. A coated, polished disk was placed on the specimen and then a header or top cap was placed over this. Two rubber O-rings were then placed around the membrane at the header to provide a seal at the top of the specimen.

The hollow plexiglass cylinder was placed on the base, and the top cover was secured by means of the three vertical rods and nuts. Large O-rings were used to form a pressure seal between the cylindrical chamber and the base and the top cover. The loading piston was then lowered until it entered, but not contact, the indentation in the top end cap.

The test chamber containing the specimen was placed in the loading machine and filled with water to an elevation approximately one inch above the O-rings around the top header cap. To deair the drainage lines prior to beginning the test, a vacuum was applied to one drainage line while the end of the other was submerged in a beaker of water. This removed air from between the sample and membrane and drew water

from the beaker into the drainage lines. The vacuum line was then disconnected and a burette attached to the line. Water was allowed to flow back from the burette through the drainage lines until it was apparent that all air bubbles had been removed. A small pressure (approximately two pounds per square inch) was applied to the test chamber during this process to prevent water from entering the space between the sample and membrane. The pore- pressure line was then connected to the pore-pressure measuring device while water was running to prevent the trapping of air in the system.

The confining pressure was applied to the specimen by means of the pressure regulator. Concurrently, a back pressure was applied to the top of the burette by means of another pressure regulator. The consolidation pressure achieved was the difference between these two pressures. A back pressure (usually 30 pounds per square inch) was applied overnight to insure that the specimen was saturated.

All of the testing performed in this research consisted of consolidated undrained triaxial tests preceded by one or more stress relaxation tests, all with pore pressure measurements. Two types of tests were performed on each series of remolded specimens. First, a large number of "routine" relaxation-triaxial tests were performed at various consolidation pressures to precisely define the Mohr's failure envelope and to develop relations between relaxation modulus and ultimate strength, relaxation pore pressure and pore pressure at failure, etc. Second, special relaxation-triaxial tests were performed in which relaxation data were obtained at two or three consolidation pressures prior to testing the specimen to failure. Only the routine relaxation-triaxial tests were performed on the undisturbed specimens.

After allowing the specimen to consolidate under a back pressure overnight, the valve between the specimen and back pressure system was closed and a check for leakage and completion of the consolidation process was made. If the consolidation process was completed and there was no leakage through or around the membrane, the pore pressure transducer would continue to read zero. If there were no leaks but the degree of consolidation was less than 100 percent, the pore pressure would rise slightly and approach a value considerably less than the consolidation pressure. If there was a leak, the pore pressure would rise slowly or rapidly, depending upon the leakage rate, and approach the consolidation pressure. In the case of incomplete consolidation, either more time was allowed or the slightly lower consolidation pressure was accepted and the test completed. In this case the consolidation pressure (σ_3) was the chamber pressure minus the sum of the back pressure and the pore pressure rise. In the case of a leak, the test was aborted and the specimen discarded.

After determining that consolidation was complete and there was no leakage, a final reading of the

was sheared in an undrained condition.

In the triaxial test, the strain rate used in applying the axial load was two percent per hour. This insured a failure time of not less than four hours and in most cases approximately eight hours. This was sufficient time to permit equilization of pore pressures within the specimen. Readings of the deformation, applied load and pore pressure were taken at approximately five-minute intervals at the beginning of the test and at 30-minute intervals thereafter.

The test was continued until the stress decreased or remained essentially constant. Some specimens yielded under nearly constant stress while the load continued to increase slightly due to the increasing cross-sectional area. An examination of a few readings indicated whether or not the maximum stress had actually been reached.

After failure, all pressures were released and the confining fluid drained from the test chamber. The testing apparatus was disassembled -- being careful not to disturb the failed specimen. The specimen was examined and the mode of failure sketched for future reference. The specimen was weighed and placed in an oven to dry in order to obtain data to calculate the moisture content and unit weight.

The special relaxation-triaxial tests differed from regular or routine tests only in that more than one stress relaxation test was performed upon each specimen at various consolidation pressures. For most special tests, a specimen was consolidated to 10 psi overnight and a relaxation test performed the following morning. The specimen was then consolidated to 30 psi until late afternoon or the following morning when another relaxation test was performed. The specimen was again consolidated overnight under 50 psi and a third relaxation test performed the following morning. In most cases, overnight consoliation was required to approach 100 percent consolidation. The mechanics of testing were exactly as described for the routine tests. Immediately after the third relaxation test, the specimen was tested to failure in triaxial shear. In some cases the 30 psi consolidation was omitted and only two relaxation tests were performed on the special specimens.

Computations

Failure Envelopes -- The Mohr-Coulomb failure theory states that failure occurs if the shear stress on any plane equals the shear strength of the material, and that the shear strength, s, is a function of the normal stress, σ. This function is usually assumed to be of the form

$$s = c + \sigma \tan \phi \qquad 1$$

and is shown as a straight line in Figure 4. The slope of the line is equal to tan ϕ and the τ - (shear stress) axis intercept is equal to c. The quantities ϕ and c are material parameters called angle of internal friction and cohesion, respectively, and σ is the normal stress. Equation 1 represents the maximum shear stress that may be sustained in a material. Any combination of normal and shear stresses that plot below the line represents a safe state of stress, whereas stresses that plot above the strength function cannot exist because failure would have occurred before such stresses could be reached. A point on the line represents stresses that will cause failure.

If a specimen of material is acted on by major and minor principal stresses, σ_1 and σ_3, the normal and shear stresses on any plane may be calculated graphically by plotting a Mohr's circle of stress. Since the stress in a material can never exceed its strength, no part of a Mohr's circle can project above the envelope; and all circles representing failure are tangent to the envelope. Thus, a convenient means for determining the failure envelope is to plot a series of Mohr's circles representing failure stresses for various applied combinations of major and minor stresses. The line which is tangent to the circles, or envelops them, is the failure envelope.

Different failure envelopes are obtained from the various types of triaxial tests when total stresses are used, since different pore water pressures are developed in these tests. However, irrespective of the type of test, there exists a unique failure envelope for the material in terms of effective stresses, $\bar{\sigma}$. The effective stress envelope then is

$$s = \bar{c} + \bar{\sigma} \tan \bar{\phi} = \bar{c} + (\sigma - u) \tan \bar{\phi} \qquad 2$$

where u is the pore water pressure and $\bar{c}$ and $\bar{\phi}$ are the effective stress strength parameters of the material. The center of the effective stress Mohr's circles is $(\bar{\sigma}_1 + \bar{\sigma}_3)/2$, 0 and the radius is $(\sigma_1 - \sigma_3)/2 = (\bar{\sigma}_1 - \bar{\sigma}_3)/2$. $\bar{\sigma}_1$ and $\bar{\sigma}_3$ can be determined as follows:

$$\bar{\sigma}_3 = \sigma_3 - u$$

$$\bar{\sigma}_1 = \sigma_1 - u = \sigma_a + \sigma_3 - u$$

where

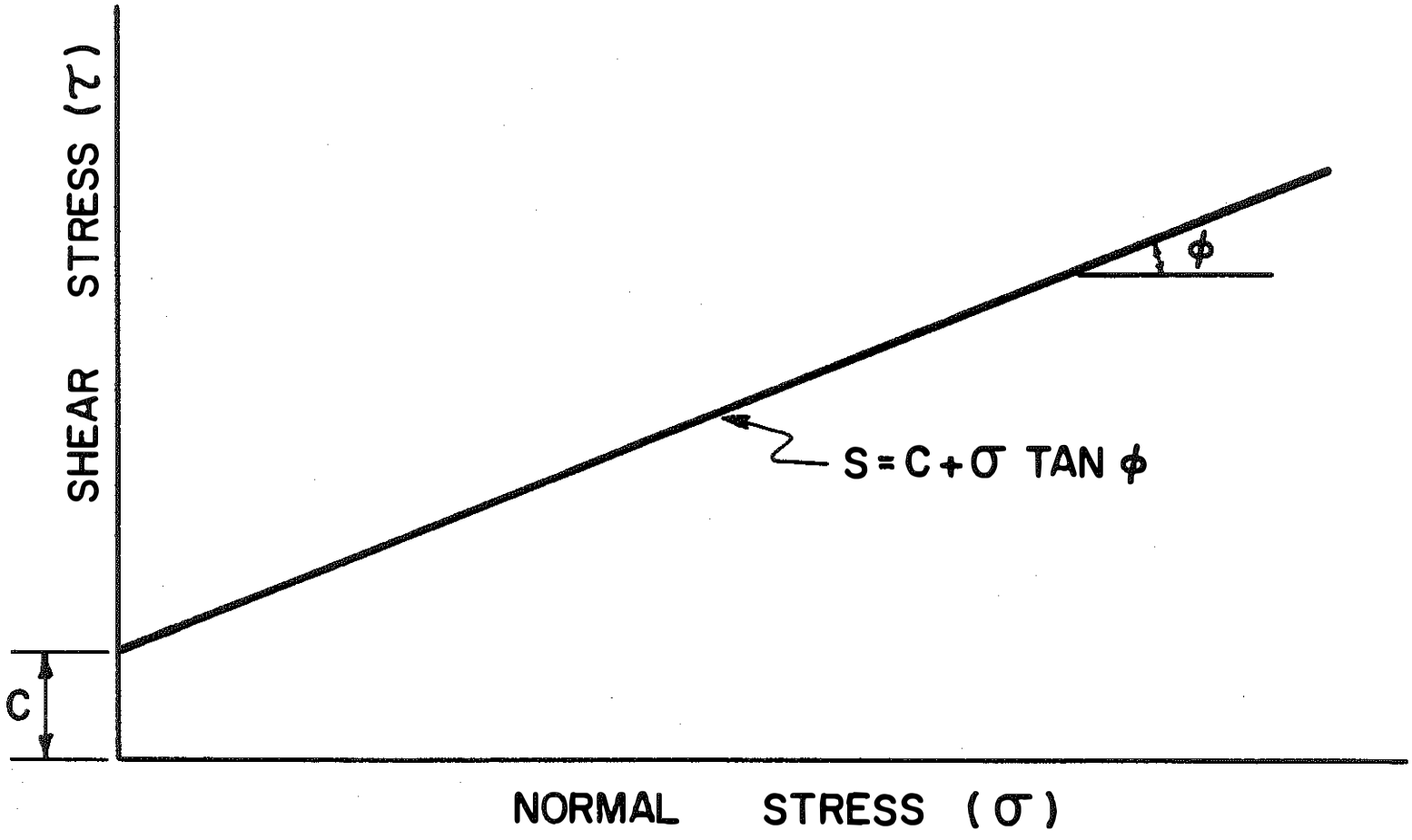

Figure 4. Illustration of the Mohr-Coulomb Failure Theory.

$\sigma_1 = \sigma_a + \sigma_3$,

$\sigma_a = \sigma_1 - \sigma_3$ = P/A = the applied stress difference,

P = applied axial load, and

A = cross sectional area of specimen.

A method of obtaining the Mohr's failure envelope, illustrated in Figure 5, avoids the confusion of a large number of superimposed Mohr's circles. One half of the stress difference, $(\bar{\sigma}_1 - \bar{\sigma}_3)/2 = q$, is plotted against the mean effective stress, $(\bar{\sigma}_1 + \bar{\sigma}_3)/2 = p$. The line through these points intersects the Mohr's envelope on the normal stress axis since, in the limit, a Mohr's circle would become a point somewhere on the axis. The slope, tan ψ, of the line through these points is related to the slope of the Mohr's envelope by

$$a/b = \tan \psi = \sin \bar{\phi}. \qquad 3$$

The intercept $\bar{c}$ can be calculated from

$$e = \bar{c}/\tan \bar{\phi} = d/\tan \psi, \qquad 4$$

and substituting Equation 3 into 4 yields

$$\bar{c} = d/\cos \bar{\phi} \qquad 5$$

where d = the intercept on the shear stress axis of the line through the p - q points.

Pore Pressure Parameters -- For a change in stress under undrained conditions, the change in pore water pressure may be expressed as

$$\Delta u = B[\Delta\sigma_3 + A(\Delta\sigma_1 - \Delta\sigma_3)] \qquad 6$$

where A and B are Skempton's pore pressure parameters. B can be measured in the triaxial test by applying a stress change $\Delta\sigma_3 = \Delta\sigma_1$. Equation 6 reduces to $\Delta u = B\Delta\sigma_3$ and thus

$$B = \Delta u/\Delta\sigma_3. \qquad 7$$

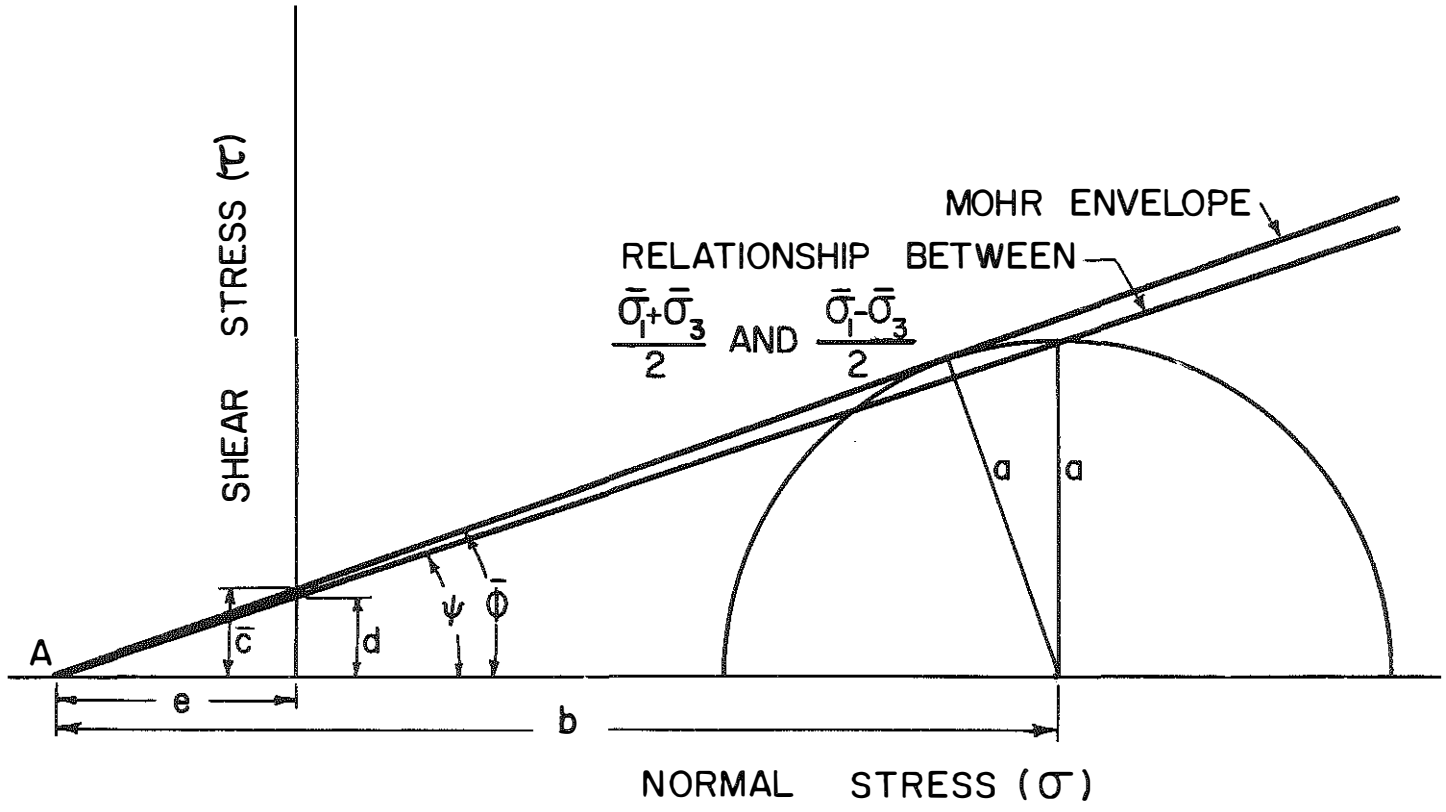

Figure 5. Relationship of Mohr's Envelope to $(\bar{\sigma}_1 + \bar{\sigma}_3)/2$ vs $(\bar{\sigma}_1 - \bar{\sigma}_3)/2$.

Since σ_3 is constant in a triaxial test, the parameter A can be obtained from Equation 6 as

$$A = \triangle u/B\triangle\sigma_1. \qquad 8$$

Triaxial Test Stresses and Strains-- Assuming that the specimen strains equally in all directions under the confining pressure, the length of the specimen after consolidation may be determined by means of a trial-and-error method using the following equation:

$$AL - \triangle V = \pi(R - R\triangle L/L)^2(L - \triangle L) \qquad 9$$

where

A = initial cross-sectional area of specimen as determined by physical measurements,
L = initial length of specimen as determined by physical measurements,
$\triangle V$ = volume change as measured by the burette,
R = initial radius of the specimen as determined by physical measurements, and
$\triangle L$ = change in length of specimen during consolidation.

Alternatively, the axial strain, ϵ_1, resulting from consolidation can be approximated quite accurately from

$$\epsilon_1 = \triangle V/3V. \qquad 10$$

The axial strain, ϵ_1, for a given applied load is calculated as

$$\epsilon_1 = \triangle l/l_o \qquad 11$$

where

$\triangle l$ = change in length of specimen as determined from the deformation indicator, and
l_o = length of specimen after consolidation.

The average cross-sectional area, A_f, for a given applied strain is calculated as follows:

$$A_f = V_o/(l_o - \triangle l)$$

$$\epsilon = [\epsilon_1 + 2(-0.5\epsilon_1)]/3 = 0.$$

The deviator strain for the undrained test is then defined as

$$e_d = \epsilon_1 - \epsilon = \epsilon_1. \qquad 19$$

Substituting Equations 17 and 19 into Equation 13,

$$G = P/3A_f\epsilon_1 = KP, \qquad 20$$

where

$$K = 1/3\ A_f\epsilon_1$$

TEST RESULTS AND FINDINGS

Undisturbed Soils

Regular relaxation-triaxial tests were performed on five undisturbed specimens from the Lyon County project, ten from the Jefferson County project, and sixteen from the Webster-McLean Counties project. Plots were prepared of the peak relaxation modulus vs failure stress, the relaxation modulus at 1/2-hour relaxation time vs failure stress, and pore pressure from the relaxation test vs pore pressure at failure in the triaxial test. Correlation curves so obtained are shown in Figure 6. While considerable scatter was evidenced, the correlation was considered sufficiently good to warrant further study. It was expected that much of the scatter was due to sample differences.

Remolded Soils

Six series of relaxation-triaxial tests were performed on the remolded specimens. Each series consisted of from 11 to 14 relaxation-triaxial tests at various consolidation pressures, and three special relaxation-triaxial tests. The six series consisted of one each for the four Kentucky soils and two for the kaolinite. One series of tests on the kaolinite was performed at a relaxation strain (nominal) of 0.6 percent; the other five series were performed at a 0.3 percent strain. Specimen conditions at failure are shown in Table 4.

Regular Relaxation-Triaxial Tests

From the regular relaxation-triaxial tests, the following curves were plotted:

1. Stress vs strain,
2. Pore pressure vs strain,
3. Pore pressure parameter AB vs strain,
4. Mohr's circles and failure envelopes for failure defined as the maximum stress difference ($\sigma_1 - \sigma_3$),
5. p vs q and failure envelopes for failure defined as the maximum stress difference,
6. p vs q and failure envelopes for failure defined as the maximum effective stress ratio ($\bar{\sigma}_1/\bar{\sigma}_3$),

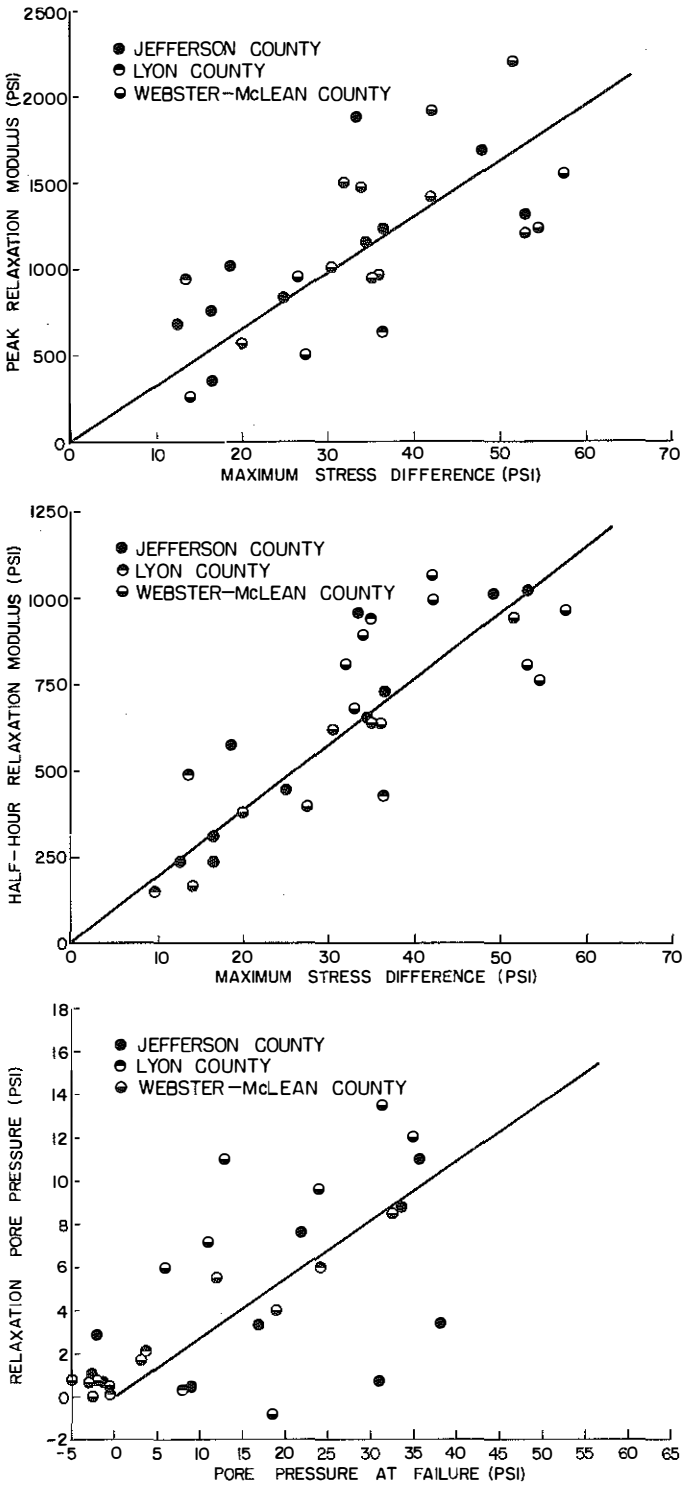

Figure 6. Correlation of Relaxation Modulus with Failure Stress and Relaxation Pore Pressure with Pore Pressure at Failure for Undisturbed Soils.

Table 4. Conditions of Remolded Specimens at Failure.

Soil	Confining Pressure (psi)	Degree of Saturation (%)	Void Ratio	Moisture Content (%)	Dry Unit Weight (lb/ft3)
Kaolinite 0.3% Strain	10	100	0.95	37.3	83.2
	10	100	0.96	36.8	83.0
	15	99	0.98	37.3	82.2
	25	99	0.96	36.3	83.0
	35	100	0.93	36.1	84.1
	45	98	0.94	35.5	83.6
	55	91	0.97	33.7	82.7
	65	97	0.90	33.5	85.7
	50	98	0.93	34.7	84.4
Kaolinite 0.6% Strain	5	95	1.03	37.4	80.3
	10	99	0.99	37.7	81.8
	15	100	0.95	37.2	83.4
	20	100	0.94	36.6	84.0
	25	100	0.94	36.5	83.6
	30	99	0.96	36.5	83.0
	45	100	0.87	34.7	87.2
	55	91	1.00	34.9	81.5
	60	99	0.91	34.6	85.2
	65	96	0.94	34.6	83.9
	50	100	0.88	34.6	86.7
	50	99	0.92	34.6	84.8
Baxter Series	5	99	1.11	39.7	81.8
	10	97	1.13	39.3	81.2
	15	100	1.08	38.7	83.0
	25	97	1.09	38.1	82.5
	30	97	1.06	37.0	83.8
	35	99	1.02	36.2	85.6
	40	98	1.01	35.6	85.3
	45	98	0.99	35.0	86.9
	50	100	0.96	35.3	87.9
	55	100	0.96	35.1	88.0
	58	100	0.94	34.1	88.8
	65	100	0.95	34.4	88.5
	67	99	0.96	34.4	88.0
	50	100	0.99	37.7	86.6
Calloway Series	5	98	0.64	23.7	101.0
	10	98	0.64	23.6	101.0
	15	99	0.63	23.4	101.6
	20	98	0.63	23.1	101.9
	25	100	0.60	22.5	103.6
	50	97	0.59	21.5	104.4
	55	99	0.58	21.3	105.2
	60	100	0.56	21.4	106.0
	65	97	0.57	20.9	105.6
	69	99	0.57	21.0	105.8
Eden Series	5	91	0.92	31.0	87.6
	10	94	0.88	30.4	89.6
	15	92	0.88	29.8	89.6
	20	90	0.87	29.1	89.7
	25	89	0.91	29.9	88.1
	25	92	0.85	29.1	90.8
	30	93	0.85	29.0	91.2
	35	95	0.83	29.2	91.9
	40	90	0.86	28.6	90.7
	45	90	0.84	28.1	91.5
	50	93	0.84	29.0	91.2
	55	96	0.78	27.7	94.4
	60	92	0.86	29.2	90.5
	65	88	0.82	26.9	92.4
	70	92	0.82	27.8	92.6
	50	91	0.88	29.4	89.6
	50	88	0.84	27.3	91.4
	50	93	0.81	27.7	93.1
Maury Series	5	100	0.78	29.7	94.0
	10	99	0.77	28.4	94.4
	15	100	0.75	28.9	95.4
	20	100	0.75	28.0	95.6
	25	100	0.75	28.0	95.6
	30	100	0.74	27.5	96.2
	35	100	0.71	27.0	97.6
	40	99	0.75	27.7	95.6
	45	100	0.73	27.2	96.8
	50	99	0.72	26.3	97.3
	55	98	0.73	26.8	96.5
	60	96	0.74	26.3	96.2
	65	99	0.71	26.3	97.4
	70	97	0.66	23.9	100.6
	50	99	0.69	25.2	99.0
	50	97	0.70	25.5	98.0

7. Relaxation modulus vs time,

8. Pore pressure from relaxation tests vs time,

9. Peak relaxation modulus vs failure stress,

10. 1/2-hour modulus vs failure stress,

11. Peak modulus/1/2-hour modulus vs failure stress,

12. Peak modulus/1-minute modulus vs failure stress,

13. Relaxation pore pressure vs pore pressure at failure,

14. Consolidation pressure vs AB at failure,

15. Consolidation pressure times pore pressure parameter B vs AB at failure, and

16. Consolidation pressure vs failure stress.

The plots of stress vs strain, pore pressure vs strain, and AB vs strain are shown in Appendix A. Shown in Appendix B are plots of relaxation modulus vs time and relaxation pore pressure vs time. A comparison of relaxation and triaxial test stresses and strains is contained in Table 5.

Relaxation tests preconditioned the specimens to the extent that stress buildup in triaxial tests was very rapid at the beginning with the stress reaching approximately the peak relaxation value between 0.1 and 1.0 percent strain. The stress-strain curves exhibited a proportional limit, near the peak relaxation stress, contrary to the usual behavior of non-prestressed soil (see figures in Appendix A). The proportional limit was almost always slightly less than the peak relaxation stress. The peak stress in relaxation tests generally varied between 92 and 46 percent of the failure stress. Peak relaxation stresses in all but 13 tests were between 80 and 50 percent of failure stress (see figures in appendix). There were three tests in which the peak stress actually exceeded the failure stress. Pore pressure parameter AB at failure varied from near zero for low consolidation pressures to between one and slightly greater than two for higher consolidation pressures (see figures in Appendix A).

Effective stress failure envelopes were obtained using two methods of determining the failure stress, that is, the maximum stress difference, $\sigma_1 - \sigma_3$, and the maximum effective stress ratio, $\bar{\sigma}_1/\bar{\sigma}_3$. In Figures 7 through 12 are plots of p vs q for each definition of failure and Mohr's circles for failure defined as the maximum stress difference.

To establish correlations between relaxation test data and ultimate strength, various curves were plotted. Curves of peak relaxation modulus vs failure stress are shown in Figure 13, and the 1/2-hour relaxation modulus vs failure stress curves are shown in Figure 14. Relaxation pore pressure vs pore pressure at failure

Table 5. Comparison of Relaxation and Triaxial Test Stresses and Strains.

Soil	Consolidation Pressure (psi)	Failure Stress Triaxial Test $(\sigma_1-\sigma_3)$	Peak Stress Relaxation Test $(\sigma_1-\sigma_3)$	Proportional Limit $(\epsilon_1-\epsilon_3)$	Proportional Limit Percent Strain	Proportional Limit / Failure Stress	Peak Stress / Failure Stress
Kaolinite, 0.3% Strain	5	12.6	8.2	6.3	0.1	0.50	0.65
	10	18.3	9.5	6.8	0.2	0.37	0.52
	10	18.0	9.3	7.5	0.1	0.42	0.52
	15	14.0	9.4	7.5	0.1	0.54	0.67
	20	17.4	10.4	8.2	0.4	0.47	0.60
	25	17.0	10.2	8.5	0.3	0.50	0.60
	30	21.0	9.7	9.3	0.5	0.44	0.46
	35	15.0	10.3	7.8	0.2	0.41	0.54
	40	24.0	12.6	10.0	0.2	0.42	0.53
	45	39.7		17.5	0.1	0.44	
	50	28.5	14.2	12.5	0.2	0.44	0.50
	55	46.3	20.9	16.0	0.2	0.34	0.45
	50	30.7	19.0	14.0	0.2	0.46	0.62
	50	33.3	15.3	14.4	0.5	0.43	0.46
	50	28.5	14.8	12.4	0.3	0.44	0.52
Kaolinite, 0.6% Strain	5	11.0	7.8	6.0	0.1	0.54	0.71
	10	12.5	8.1	6.8	0.3	0.54	0.66
	15	15.0	8.3	7.0	0.3	0.47	0.56
	20	17.5	10.2	8.5	0.3	0.49	0.58
	25	19.0	10.4	8.8	0.3	0.46	0.55
	30	20.0	13.4	11.5	0.2	0.58	0.67
	35	12.6	13.0	5.5	0.3	0.44	1.03
	40	16.4	9.2	10.5	0.6	0.64	0.56
	45	20.8	11.3	10.0	0.2	0.48	0.55
	50	22.0	12.2	10.3	0.4	0.46	0.55
	55	16.4	10.9	9.0	0.2	0.55	0.66
	50	31.5	20.6	17.0	0.3	0.54	0.65
	50	33.0	22.3	18.0	0.3	0.54	0.68
	50	29.5	18.4	17.0	0.3	0.58	0.62
Baxter Series	5	9.2	6.4	6.5	0.4	0.70	0.69
	10	9.5	10.2	6.5	0.4	0.68	1.06
	15	12.5	8.4	8.5	0.2	0.68	0.67
	25	15.3	8.4	8.3	0.4	0.53	0.55
	30	19.3	12.4	8.8	0.4	0.45	0.64
	35	16.1	15.8	6.0	0.5	0.37	0.98
	40	24.0	16.0	14.5	0.6	0.60	0.66
	45	30.4	15.6	14.5	0.6	0.47	0.57
	50	29.5	19.8	15.0	0.2	0.50	0.67
	55	29.8	19.5	15.0	0.2	0.50	0.66
	60	34.7	21.0	24.0	0.5	0.69	0.61
	65	31.5	19.5	14.3	0.2	0.45	0.62
	70	35.5	21.9	18.3	0.4	0.51	0.62
	50	27.8	18.5	11.5	0.2	0.42	0.67
	50	27.9	18.0	11.5	0.2	0.41	0.65
Calloway Series	5	14.0	9.0	8.8	0.3	0.63	0.64
	10	15.5	11.6	10.3	0.5	0.66	0.75
	15	15.6	10.6	10.3	0.3	0.66	0.64
	20	19.8	12.3	12.0	0.4	0.61	0.62
	25	22.0	12.3	15.8	0.8	0.72	0.56
	30	23.8	13.7	11.5	0.2	0.49	0.58
	35	26.0	16.2	15.8	0.5	0.61	0.62
	40	27.6	19.5	16.8	0.2	0.61	0.71
	45	26.8	22.1	18.3	0.4	0.68	0.82
	50	33.0	28.5	18.3	0.3	0.55	0.87
	55	39.0	24.7	24.3	0.6	0.62	0.63
	60	45.7	23.0	22.8	0.5	0.52	0.52
	65	38.3	29.0	24.8	0.3	0.65	0.76
	70	39.8	13.9	25.5	0.6	0.64	0.35
	50	31.2	25.5	21.5	0.5	0.69	0.82
	50	32.6	23.9	21.8	0.5	0.67	0.73
Eden Series	5	10.5	8.5	5.0	0.2	0.48	0.81
	10	12.8	7.0	5.0	0.2	0.39	0.55
	15	15.3	9.9	6.0	0.2	0.39	0.64
	20	19.0	11.8	10.0	0.6	0.53	0.62
	25	21.2	16.3	10.0	0.2	0.47	0.77
	25	19.0	14.7	11.0	0.6	0.58	0.77
	30	19.7	14.0	14.0	1.0	0.71	0.71
	35	19.0	15.3	11.0	0.6	0.58	0.80
	40	18.0	14.0	11.0	0.4	0.61	0.78
	45	22.5	15.3	14.0	2.0	0.62	0.68
	50	20.0	15.4	10.0	0.2	0.50	0.77
	55	31.0	17.7	14.0	0.2	0.45	0.57
	60	20.0	13.0	10.5	0.2	0.53	0.65
	65	33.0	25.9	20.0	0.2	0.61	0.78
	70	29.0	19.3	16.0	0.3	0.55	0.66
	50	19.0	15.8	5.3	0.2	0.28	0.79
	50	28.8	22.6	17.0	0.2	0.61	0.83
Muery Series	5	13.4	11.2	10.1	0.4	0.76	0.84
	10	14.8	10.8	11.3	0.4	0.76	0.70
	15	15.5	12.8	10.0	0.3	0.63	0.80
	20	18.8	17.3	11.0	0.2	0.59	0.92
	25	19.8	17.5	12.3	0.2	0.62	0.89
	30	19.5	15.3	11.0	0.3	0.56	0.78
	35	22.4	18.2	13.5	0.5	0.60	0.81
	40	20.6	28.3	11.3	0.3	0.55	1.38
	45	22.0	17.2	12.3	0.2	0.56	0.78
	50	23.0	16.9	13.5	0.6	0.60	0.74
	55	23.2	19.4	12.5	0.2	0.54	0.84
	60	27.0	16.7	17.0	0.4	0.63	0.62
	65	27.7	18.2	17.0	0.3	0.61	0.66
	70	42.2	15.9	27.7	0.4	0.66	0.38
	50	32.5	25.7	20.0	0.3	0.62	0.79
	50	35.5	23.5	19.0	0.5	0.54	0.66
	50	31.9	27.3	20.0	0.2	0.63	0.86

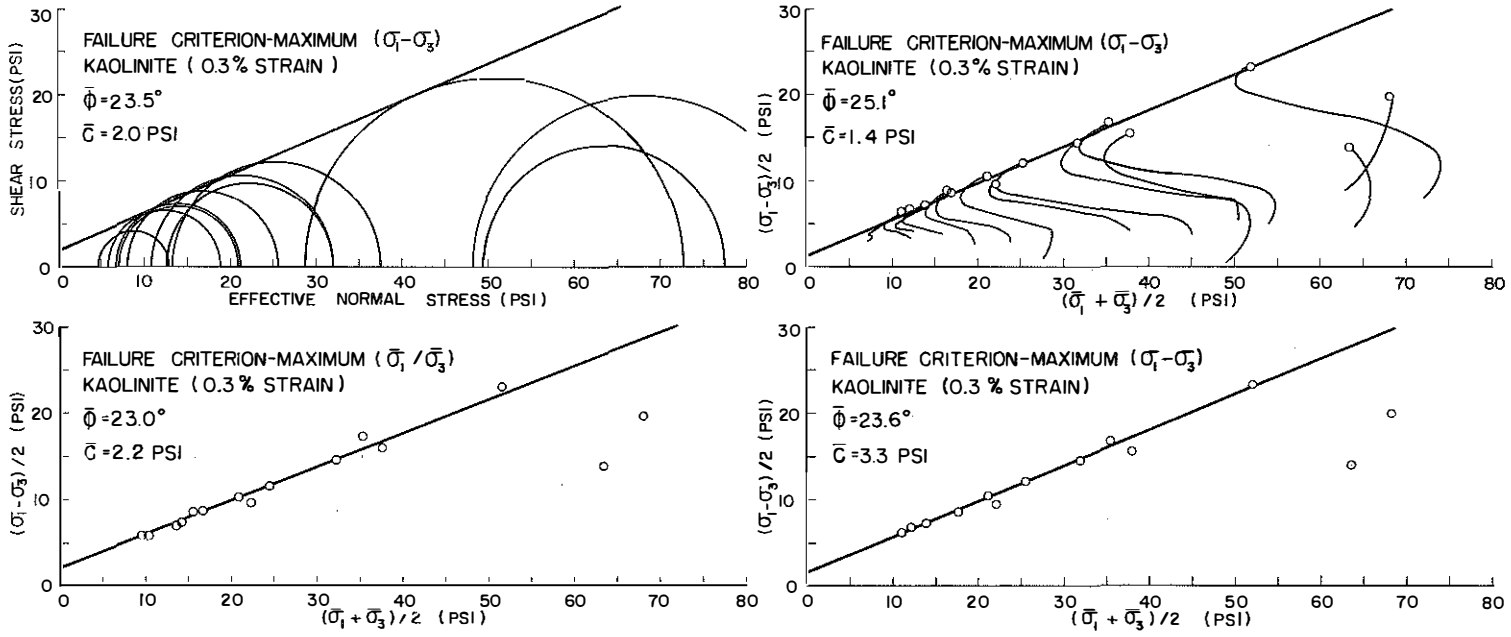

Figure 7. Conventional Failure Envelopes – Kaolinite (0.3 Percent Relaxation Strain).

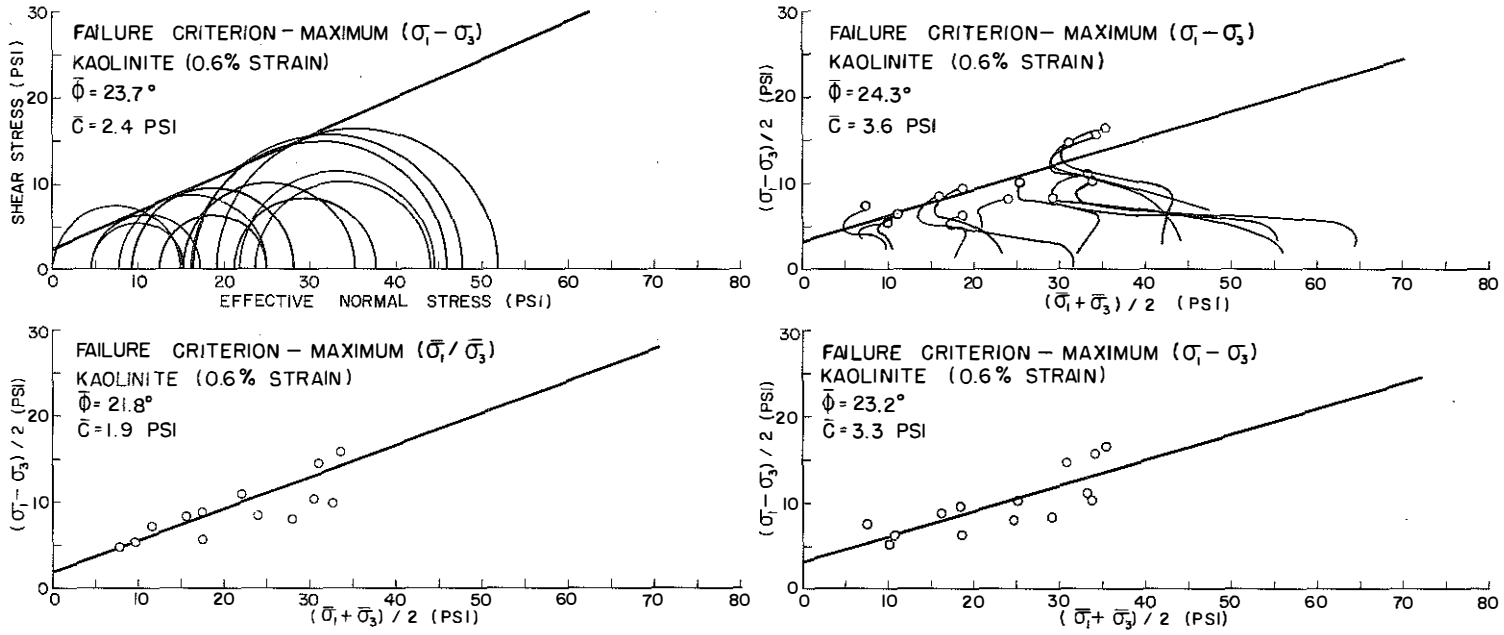

Figure 8. Conventional Failure Envelopes -- Kaolinite (0.6 Percent Relaxation Strain).

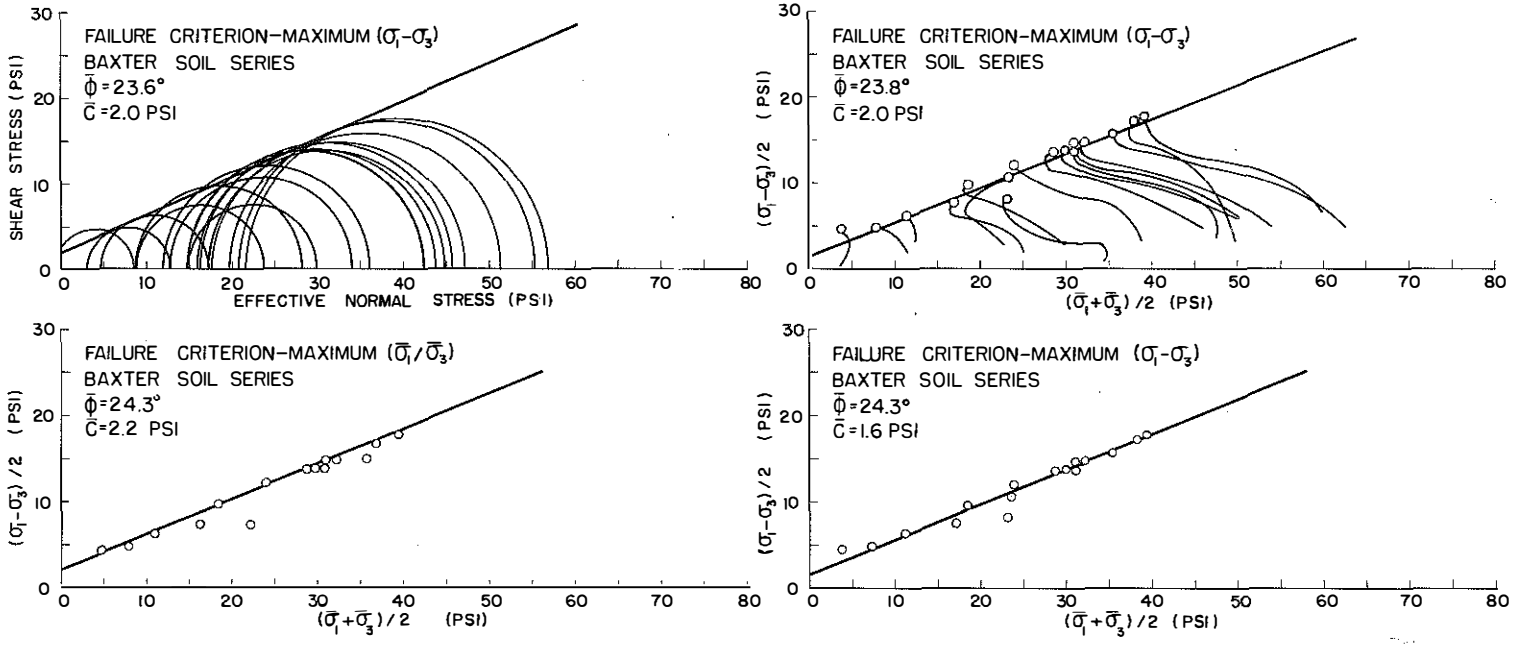

Figure 9. Conventional Failure Envelopes -- Baxter Soil Series.

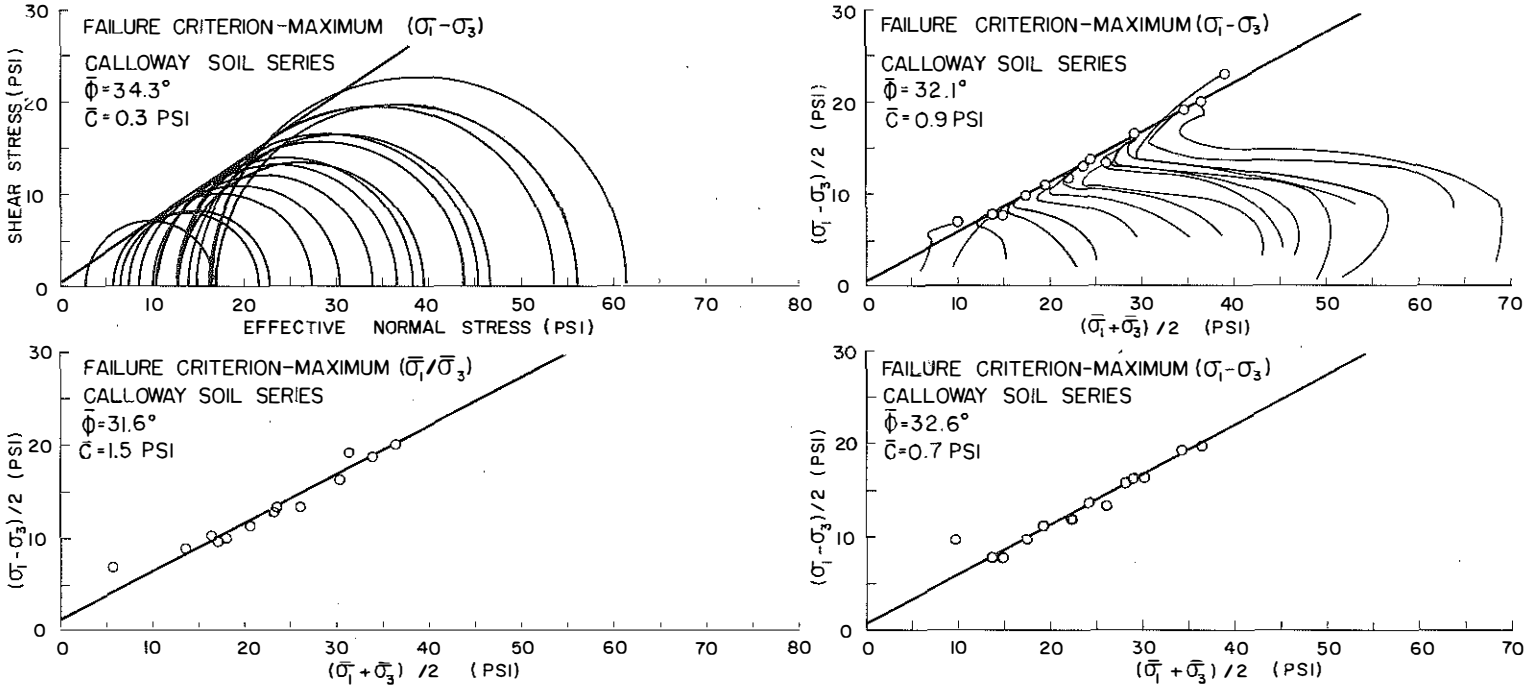

Figure 10. Conventional Failure Envelopes – Calloway Soil Series.

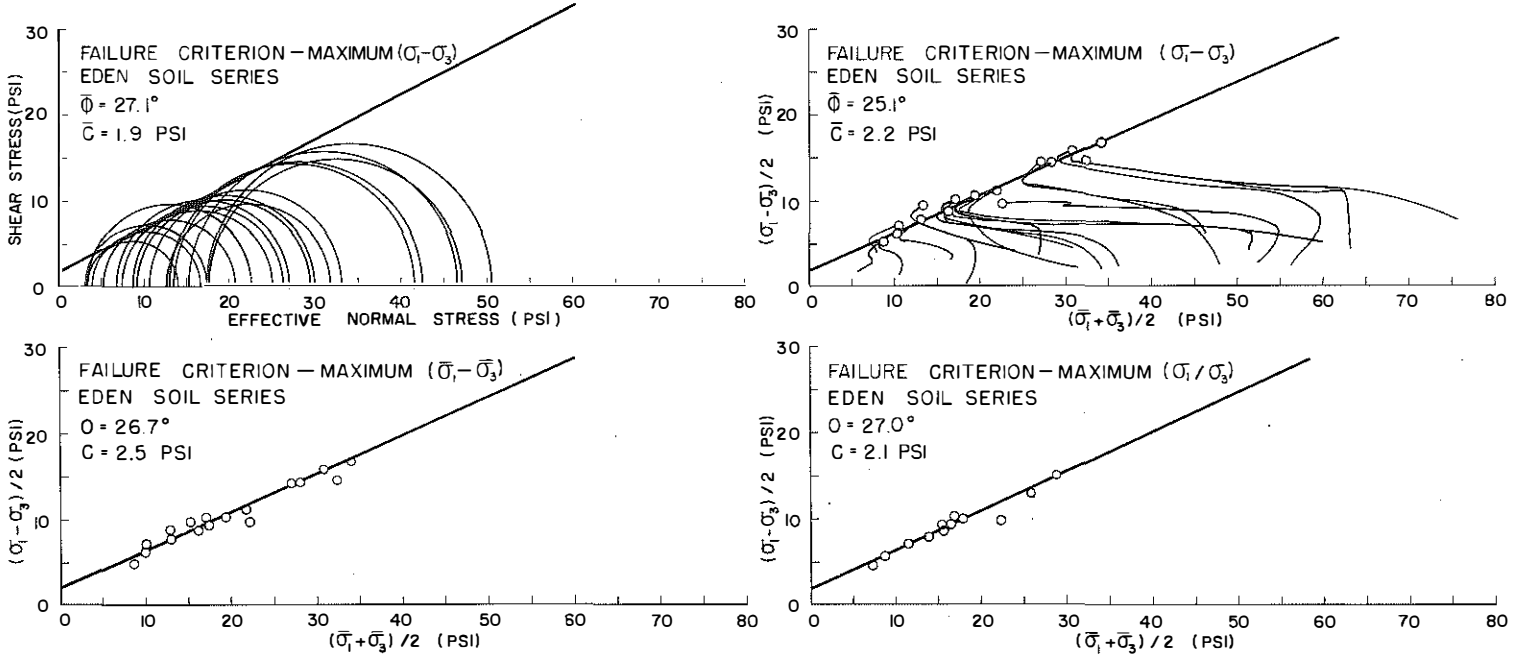

Figure 11. Conventional Failure Envelopes-- Eden Soil Series.

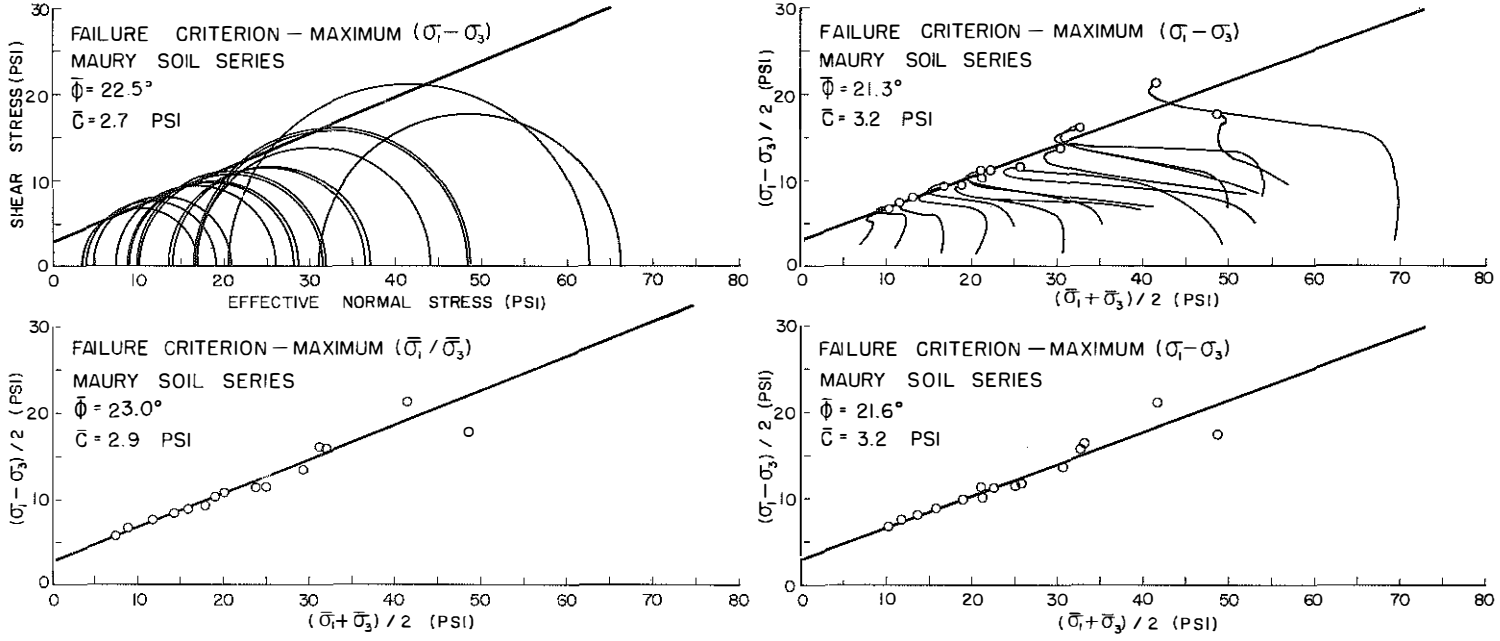

Figure 12. Conventional Failure Envelopes – Maury Soil Series.

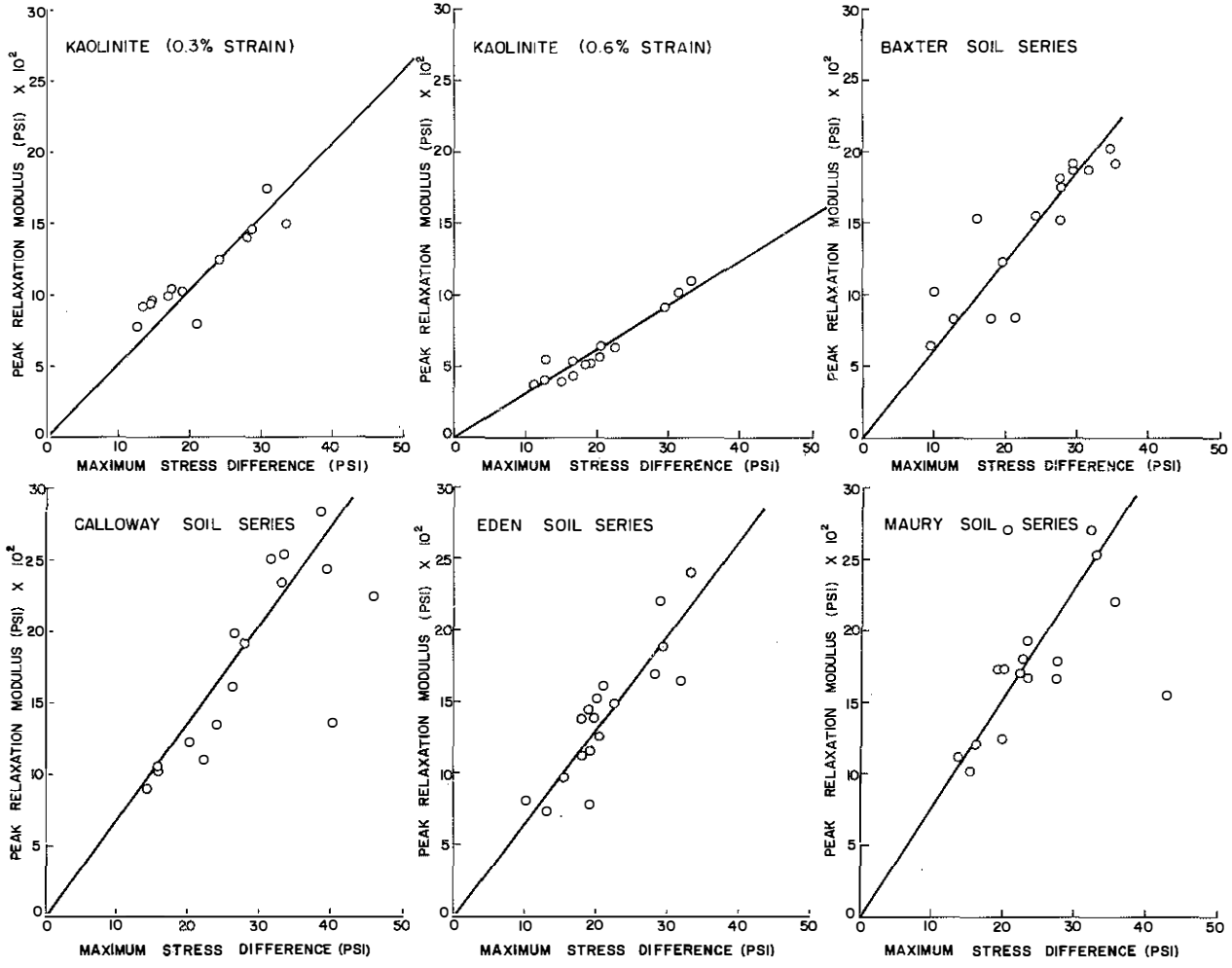

Figure 13. Correlation of Peak Relaxation Modulus with Failure Stress.

curves are shown in Figure 15. Ratios of peak relaxation modulus to the modulus after one minute vs failure stress and ratios of peak modulus to 1/2-hour modulus vs failure stress were plotted to aid in evaluating test results and are shown in Figures 16 and 17. Ideally, these ratios should be constants for identical specimens, and the amount of divergence is an indication of the reliability of each test. Failure stress as used in the above correlation curves is defined as the maximum stress differences, $\sigma_1 - \sigma_3$.

These curves indicate very strong correlation between the relaxation modulus and failure stress. However, the correlation between pore pressures was less satisfactory and generally not reliable or useable. Therefore, various other curves were prepared relating a pore pressure parameter to the consolidation pressure. Curves of consolidation pressure vs AB at failure are shown in Figure 18 and consolidation pressure times pore pressure parameter B vs AB at failure in Figure 19. Plots of consolidation pressure vs failure stress are shown in Figure 20. The curves of consolidation pressure vs AB at failure and consolidation pressure times pore pressure parameter B vs AB at failure proved to be more useful.

Special Relaxation-Triaxial Tests

Either two or three special relaxation-triaxial tests were performed as part of each of the six series of tests In most cases, relaxation data were obtained at three consolidation pressures -- 10, 30, and 50 psi -- for each test. In some cases, the 30- psi relaxation test was omitted. Ultimate strength data were obtained for each special specimen consolidated to 50 psi. Plots of stress vs strain, pore pressure vs strain, and pore pressure parameter AB vs strain for each special triaxial test are shown in Appendix A. Shown in Appendix B are plots of relaxation modulus vs time and relaxation pore pressure vs time for each special relaxation test.

Six Mohr's failure envelopes were prepared for each special test. The Mohr's circle obtained from the special triaxial test, consolidated to 50 psi, was incorporated into each failure envelope. The other circles used in constructing failure envelopes were obtained from different combinations of correlation curves already established and presented previously. Two correlation curves were required to determine each circle. Failure stress was determined from curves of peak modulus vs failure stress or 1/2-hour modulus vs failure stress, and in one case, from the consolidation pressure vs failure stress. Pore pressure was determined from curves of relaxation pore pressure vs pore pressure at failure, consolidation pressure vs AB at failure, and in one case, B times consolidation pressure vs AB at failure. Pore pressure parameter AB

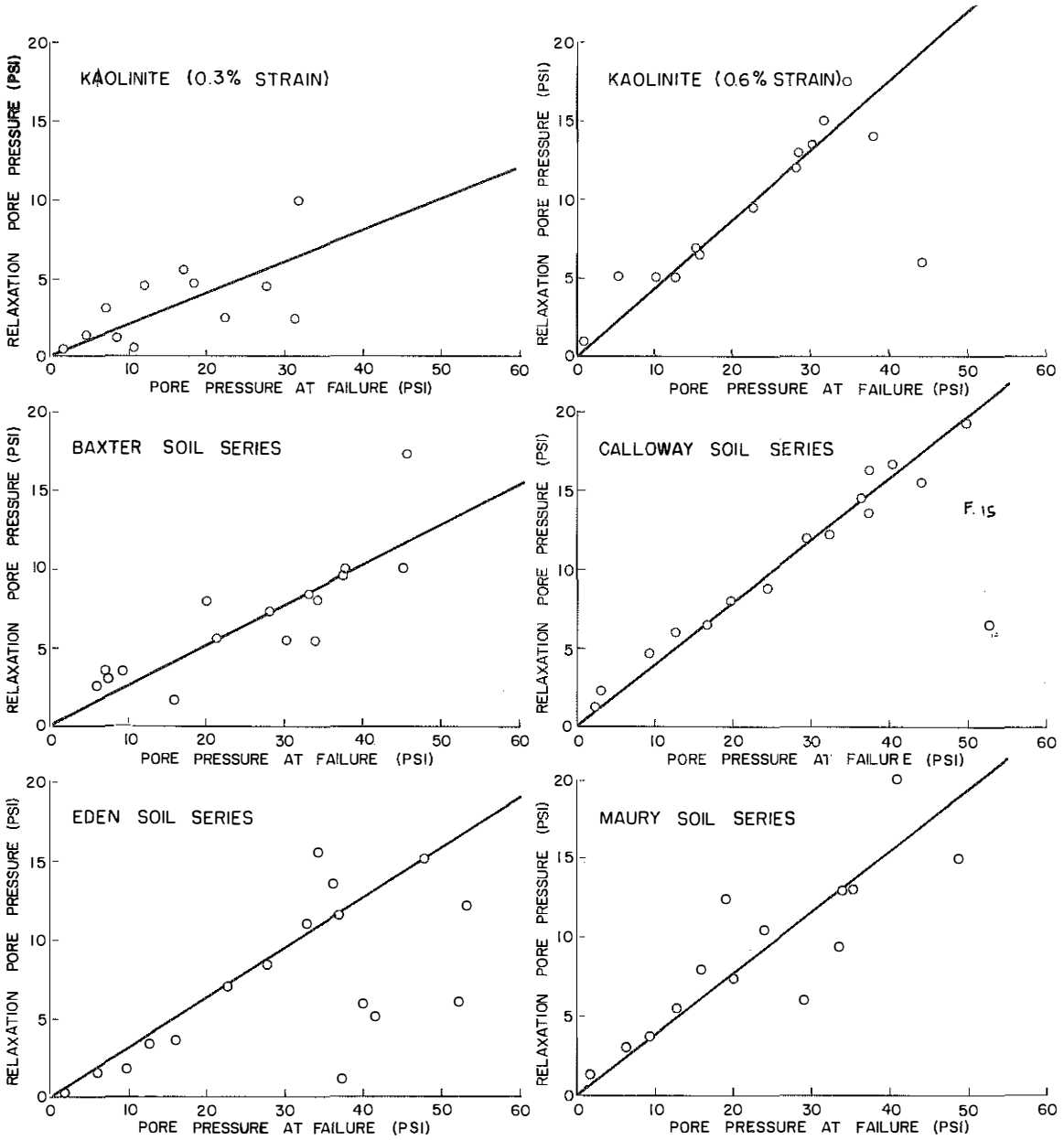

Figure 15. Correlation of Relaxation Pore Pressure with Pore Pressure at Failure.

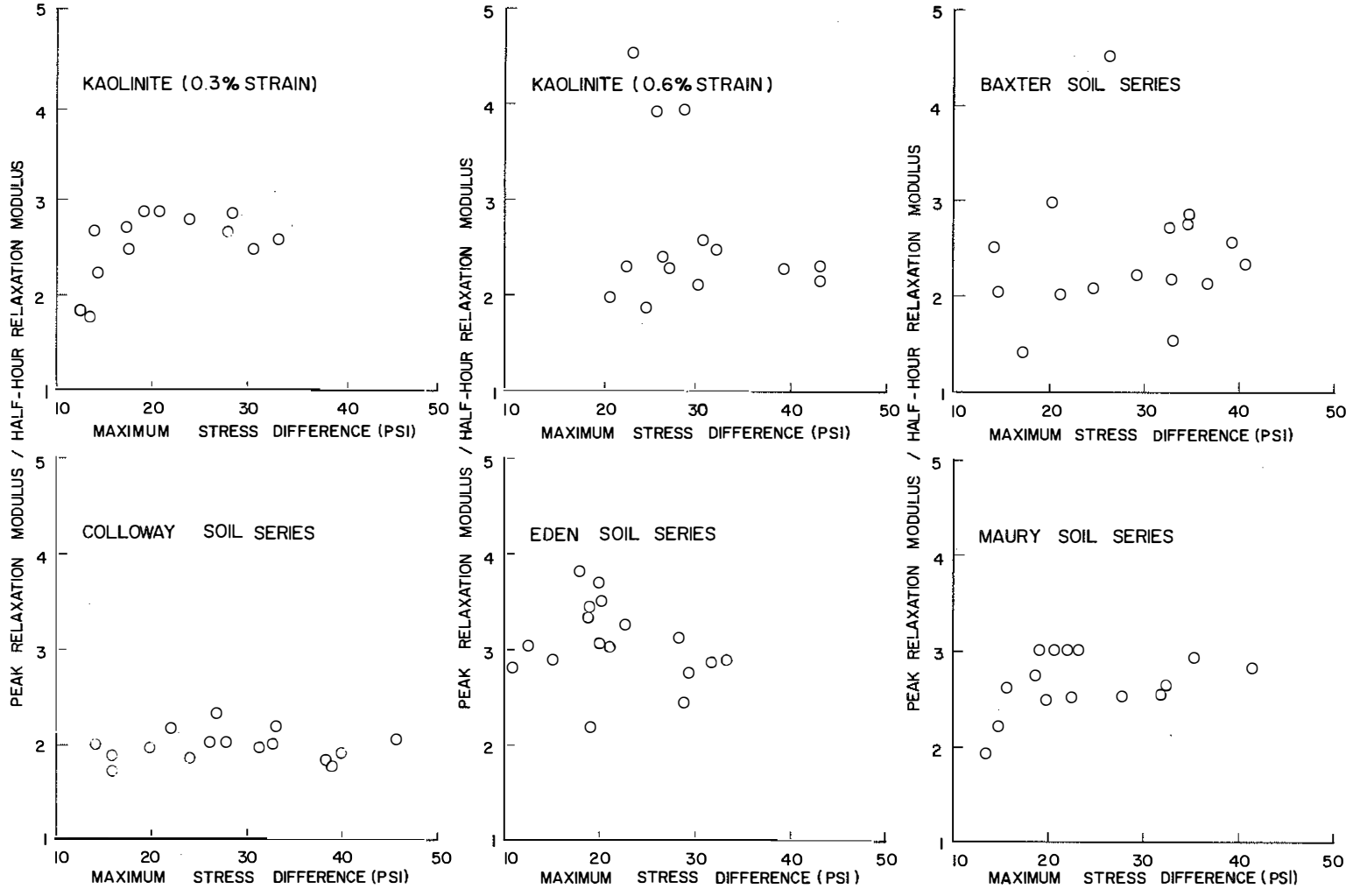

Figure 17. Ratio of Peak Relaxation Modulus to ½ - hour Relaxation Modulus vs Failure Stress.

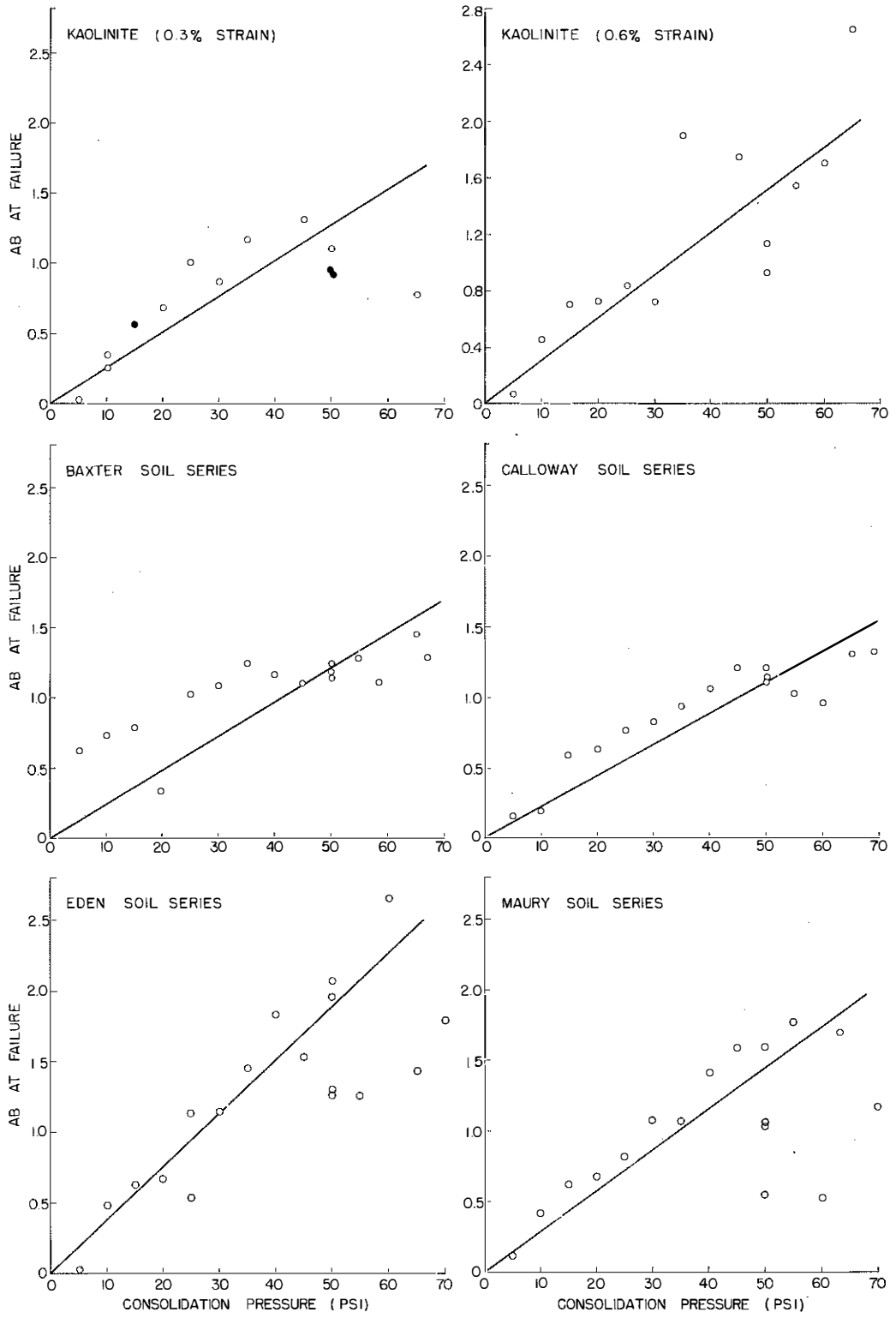

Figure 18. Correlation of Consolidation Pressure with Pore Pressure Parameter AB at Failure.

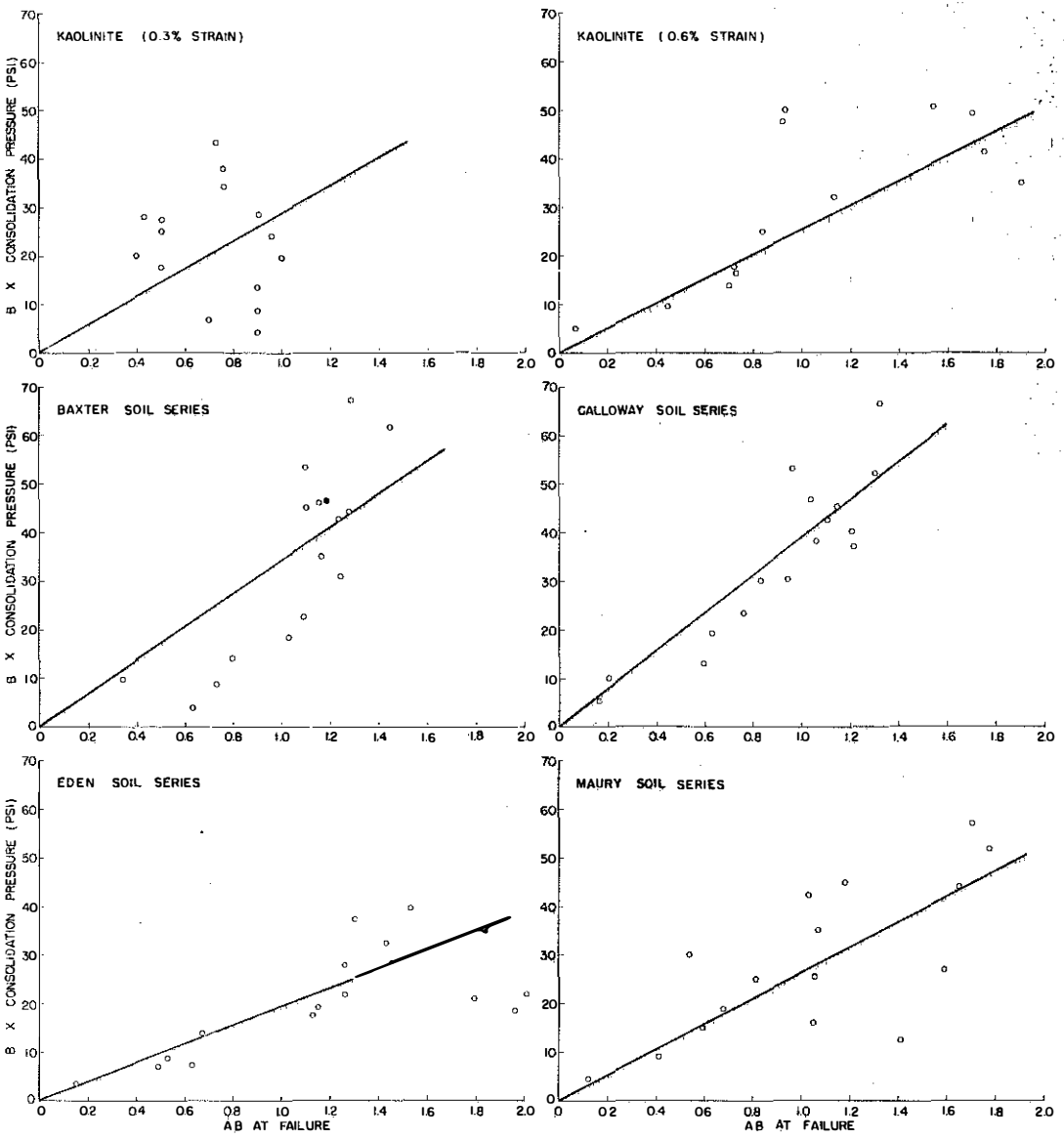

Figure 19. Correlation of Pore Pressure Parameter B times Consolidation Pressure with Pore Pressure Parameter AB at Failure.

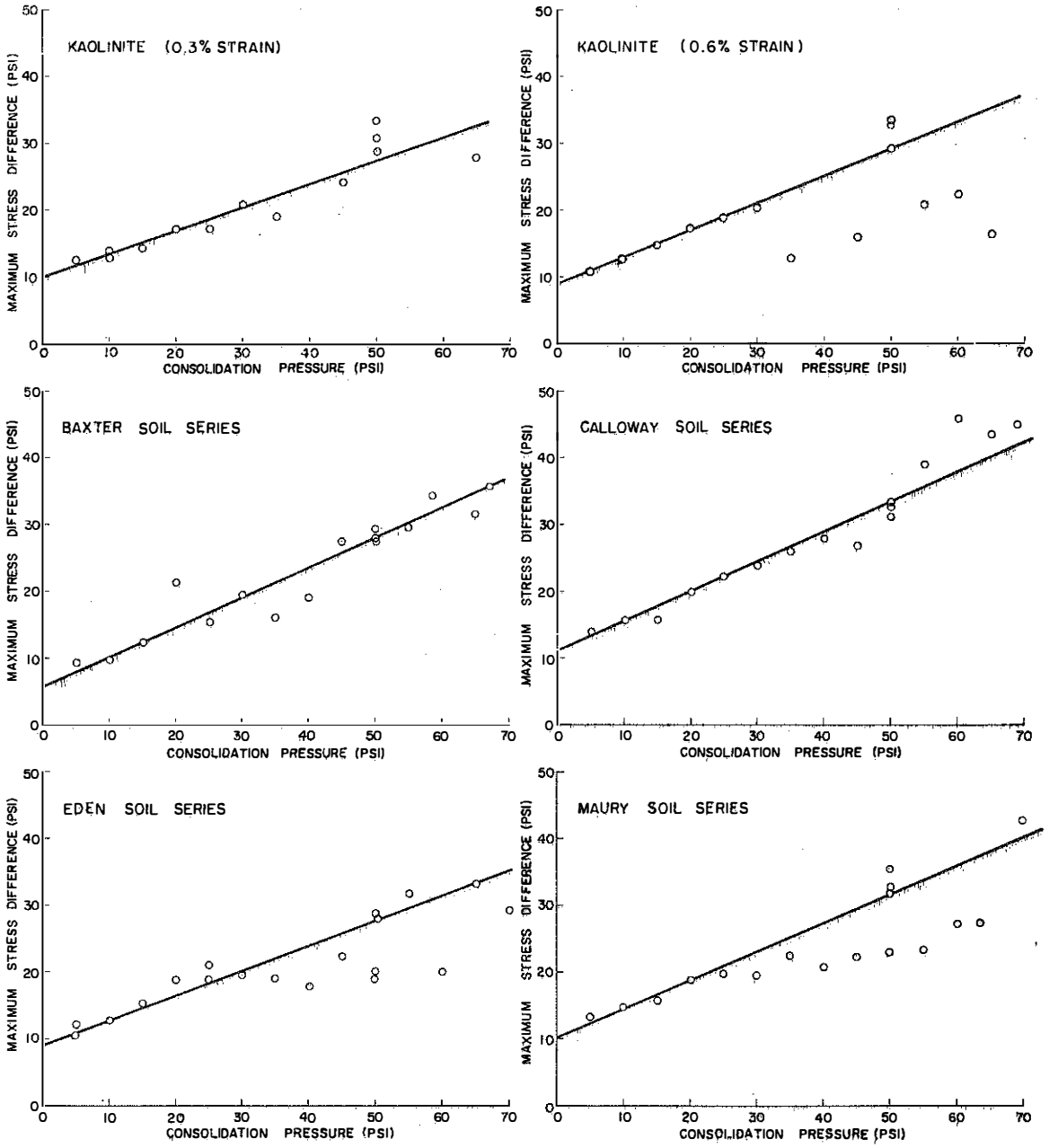

Figure 20. Correlation of Consolidation Pressure with Failure Stress.

determined from correlation curves was multiplied by the failure stress previously determined from other curves to determine the pore pressure. Mohr's circles for each special relaxation test were prepared from sets of failure stress and pore pressure as follows:

1. $\sigma_1 - \sigma_3$ from peak modulus (G_{max}) vs failure stress

   Pore pressure from consolidation pressure vs AB at failure (AB_f)

2. $\sigma_1 - \sigma_3$ from 1/2-hour modulus ($G_{½\text{-hr}}$) vs failure stress

   Pore pressure from consolidation pressure vs AB at failure

3. $\sigma_1 - \sigma_3$ from peak modulus vs failure stress

   Pore pressure from relaxation pore pressure (u_r) vs pore pressure at failure (u_f)

4. $\sigma_1 - \sigma_3$ from 1/2-hour modulus vs failure stress

   Pore pressure from relaxation pore pressure vs pore pressure at failure

5. $\sigma_1 - \sigma_3$ from peak modulus vs failure stress

   Pore pressure from B times consolidation pressure vs AB at failure

6. $\sigma_1 - \sigma_3$ from consolidation pressure vs failure stress

   Pore pressure from consolidation pressure vs AB at failure.

These Mohr's circles, used in conjunction with cricles determined directly from the special triaxial tests, permitted failure envelopes to be constructed for comparison with envelopes obtained from the regular tests presented previously.

The procedure used to determine failure stress, $\sigma_1 - \sigma_3$, and pore pressure to be used in constructing additional Mohr's circles or locating additional points on the failure envelope will be illustrated by an example. All of the correlation curves, with the exception of consolidation pressure vs failure stress, indicated a straight line through the origin. Thus the peak modulus from the special relaxation test at 50-psi consolidation pressure was plotted vs the failure stress from the triaxial test, and a line was drawn through this point and the origin. An effective stress Mohr's circle was calculated and plotted from the special triaxial data. Then, for each relaxation test at lower consolidation pressures on the same special specimen, the peak modulus was determined. This value was used to enter the peak modulus vs failure stress curve to determine a value of failure stress. Another correlation curve was prepared by plotting the consolidation pressure, 50 psi, vs the pore pressure parameter AB, from the special triaxial test data. Then the value of consolidation pressure, 10 psi or 30 psi, for the particular relaxation test on the same specimen was used to enter this curve, and a value of AB thus determined. This value of AB was multiplied by the value for

failure stress determined from the peak modulus vs failure stress curve to obtain the pore pressure. These values of failure stress and pore pressure were used to obtain another Mohr's circle or point on the failure envelope.

Failure envelopes calculated by the method thus described are shown in Figures 21 through 31. These figures -- when compared with the conventional failure envelopes, Figures 7 through 12 -- show that failure stress and pore pressure from Sets 1 and 5 above give the best and most consistent agreement. Therefore, Table 6 was prepared which compare the effective friction angle, $\bar{\phi}$, and effective cohesion, $\bar{c}$, from the special tests with those of the convention triaxial tests. The average of tan $\bar{\phi}$ calculated by either of the two best methods for each series agrees, with one exception, to within 15 percent or better with tan $\bar{\phi}$ obtained by conventional methods. The values of cohesion determined from special tests differs from values obtained from conventional tests by from 0.7 psi to 2.2 psi.

Discussion of Findings

A comparison of relaxation test results obtained from the two kaolinite series, one strained 0.3 percent and the other 0.6 percent, is informative. Strength parameters from the relaxation tests compare favorably with values oobtained from conventional failure envelopes (see Figures 7 and 8). However, the series strained 0.6 percent, Figure 8, exhibited considerably more scatter of points. Since the specimens used for both series were made at the same time and from the same batch, they were very nearly identical. They were tested concurrently so the effect of aging was the same for both series. Furthermore, the only difference in the two series was the value of relaxation strain. If follows then that the higher relaxation strain influenced the failure stress in an inconsistent manner, thus causing the scatter of points on the failure envelope.

Small differences in the time required to apply the strain probably influenced results. The 0.6 percent strains were applied to the specimens in approximately 1/2 to 1 second. Strains of the same order of magnitude applied to similar specimens, not shown, at a much higher rate (almost instantaneously) actually caused failure as evidenced by vertical cracks and stress relaxation to zero at a pronounced rate.

Correlation curves of relaxation modulus vs failure stress show the same trend, that is, better agreement for the series strained only 0.3 percent. On the other hand, the correlation of relaxation pore pressure vs pore pressure at failure for the series strained 0.6 percent is decidedly better. This is as would be expected

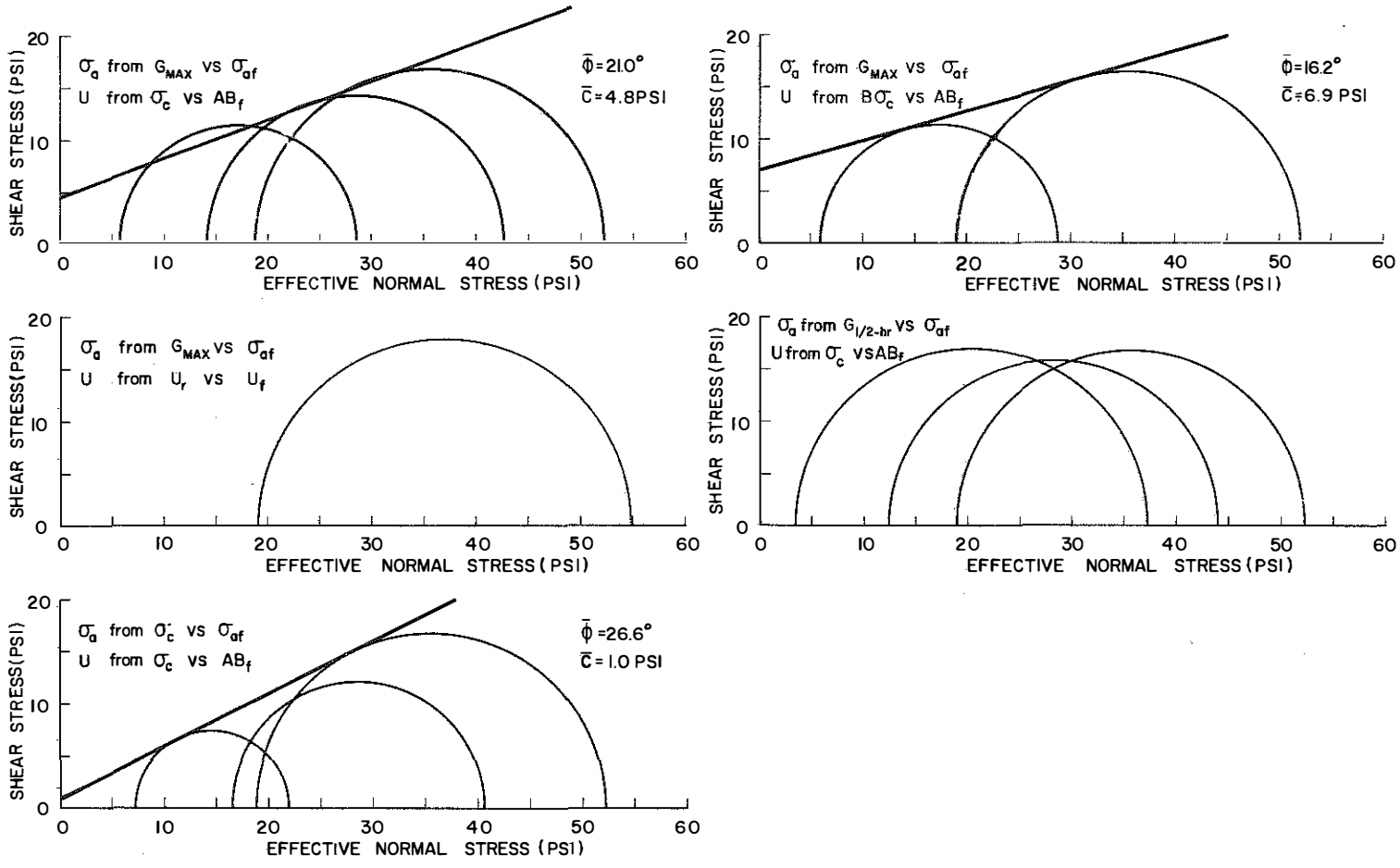

Figure 21. Failure Envelopes from Special One - Specimen Test No. 1 -- Kaolinite (0.3 Percent Relaxation Strain).

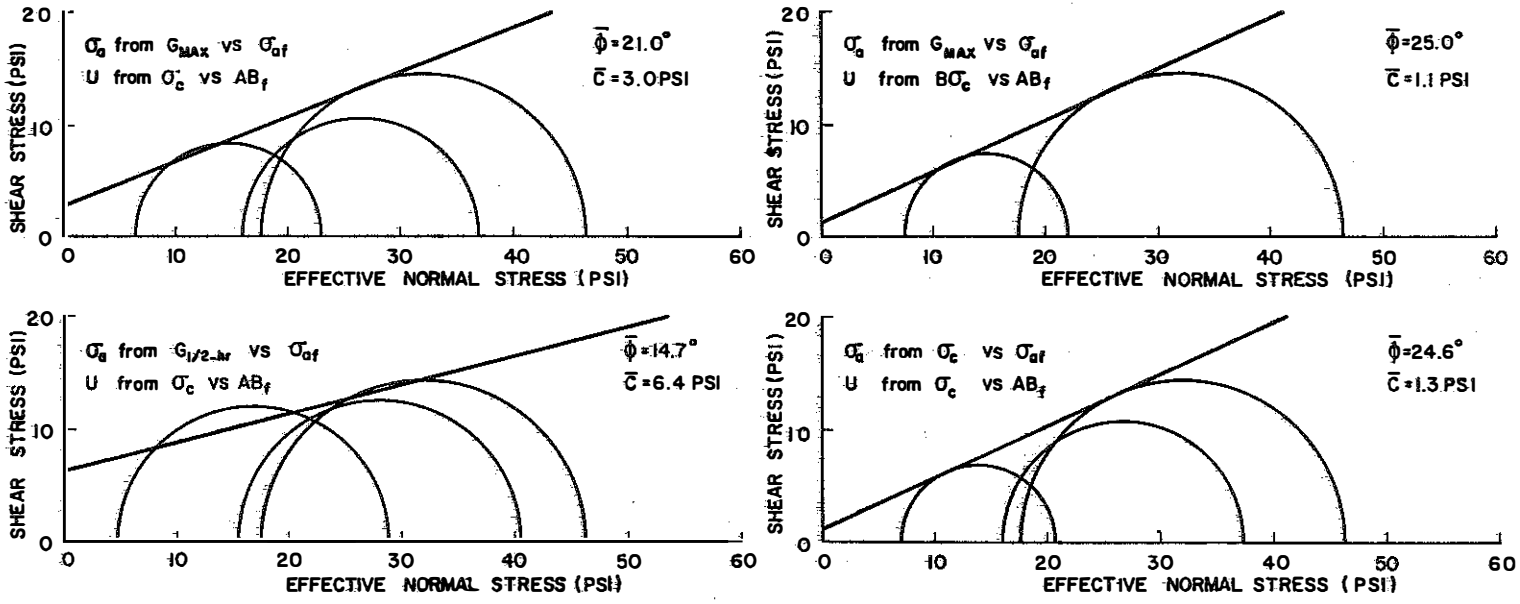

Figure 22. Failure Envelopes from Special One - Specimen Test No. 2 -- Kaolinite (0.3 Percent Relaxation Strain).

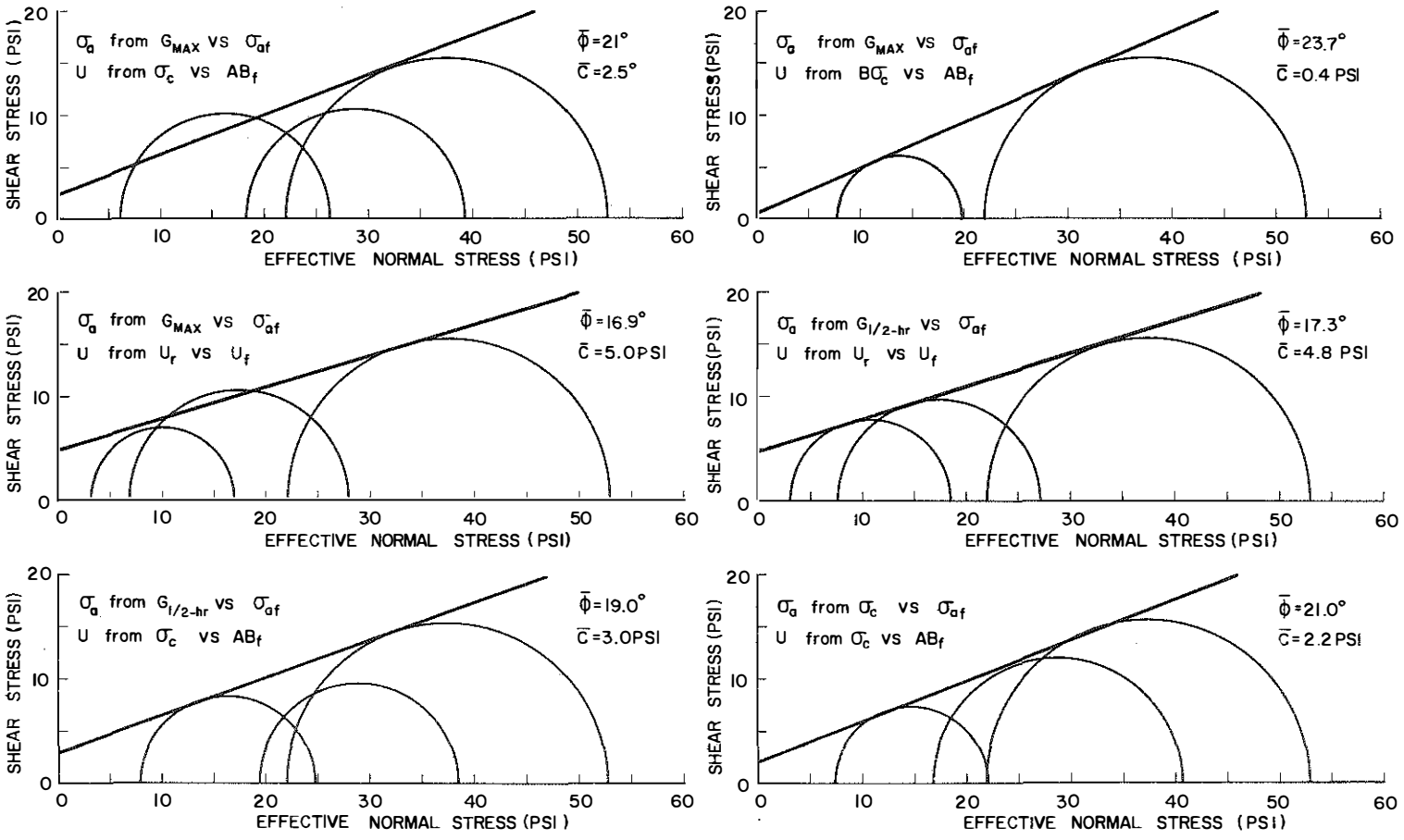

Figure 23. Failure Envelopes from Special One - Specimen Test No. 1 – Kaolinite (0.6 Percent Relaxation Strain).

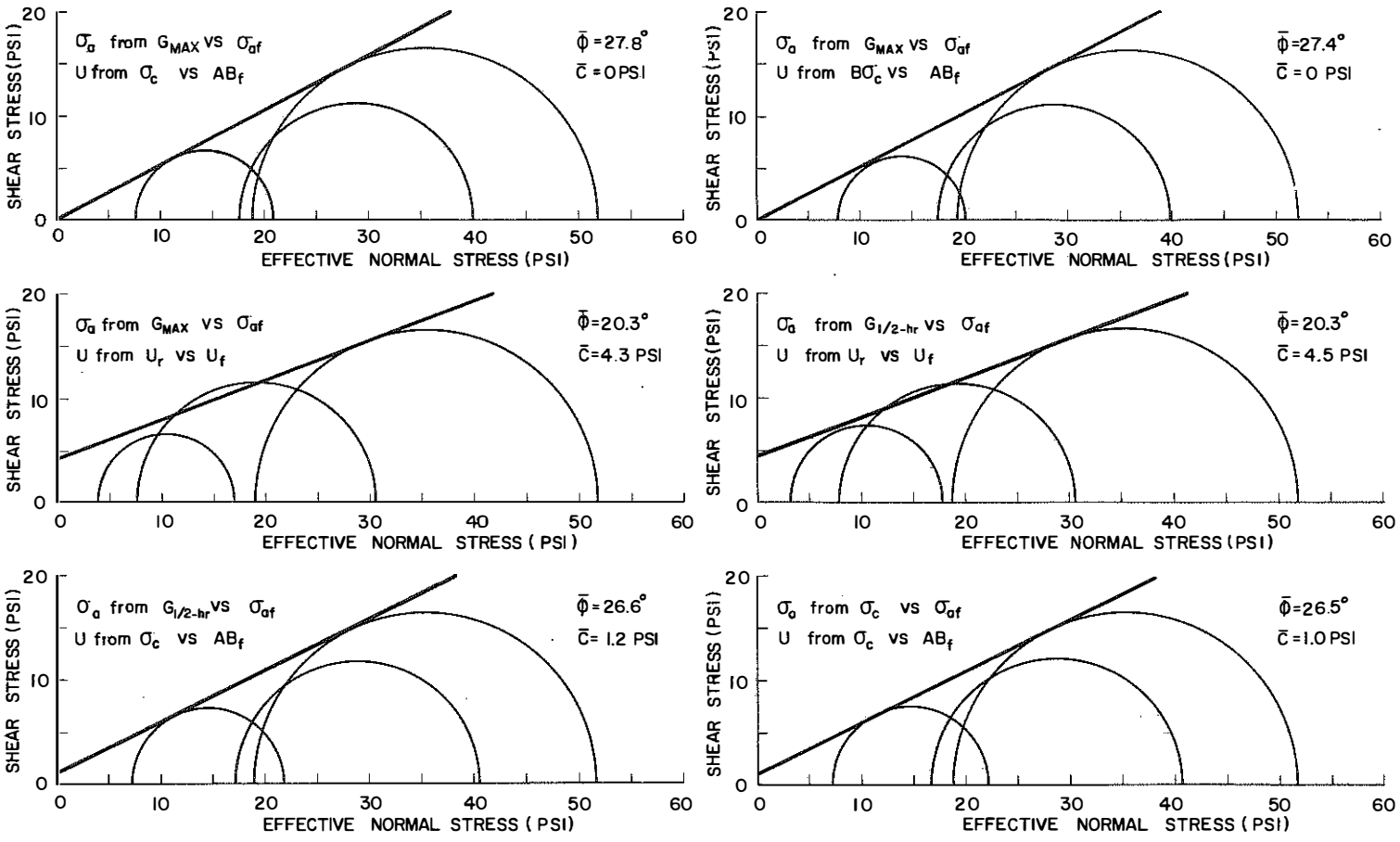

Figure 24. Failure Envelopes from Special One - Specimen Test No. 2 – Kaolinite (0.6 Percent Relaxation Strain).

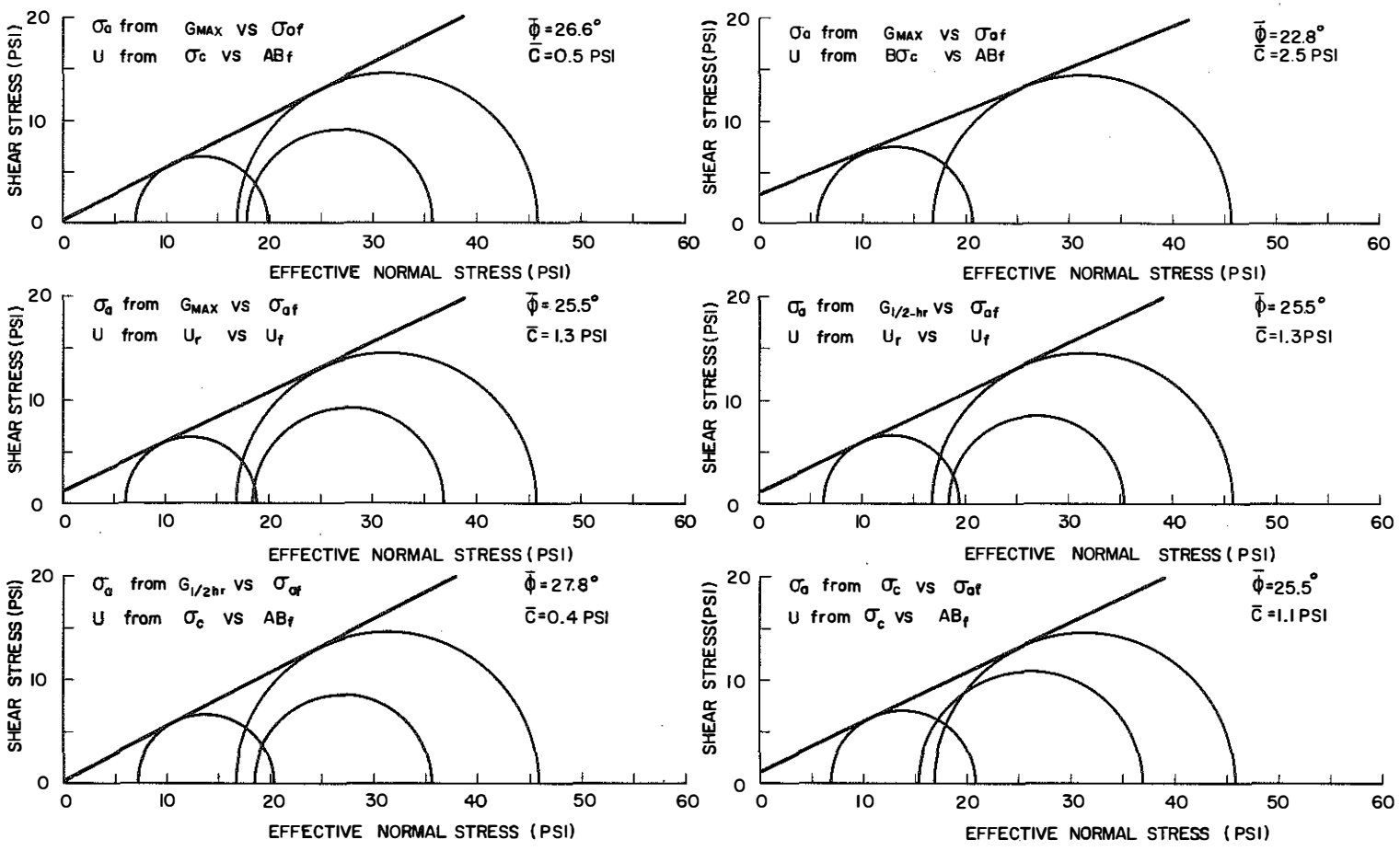

Figure 25. Failure Envelopes from Special One - Specimen Test No. 3 – Kaolinite (0.6 Percent Relaxation Strain).

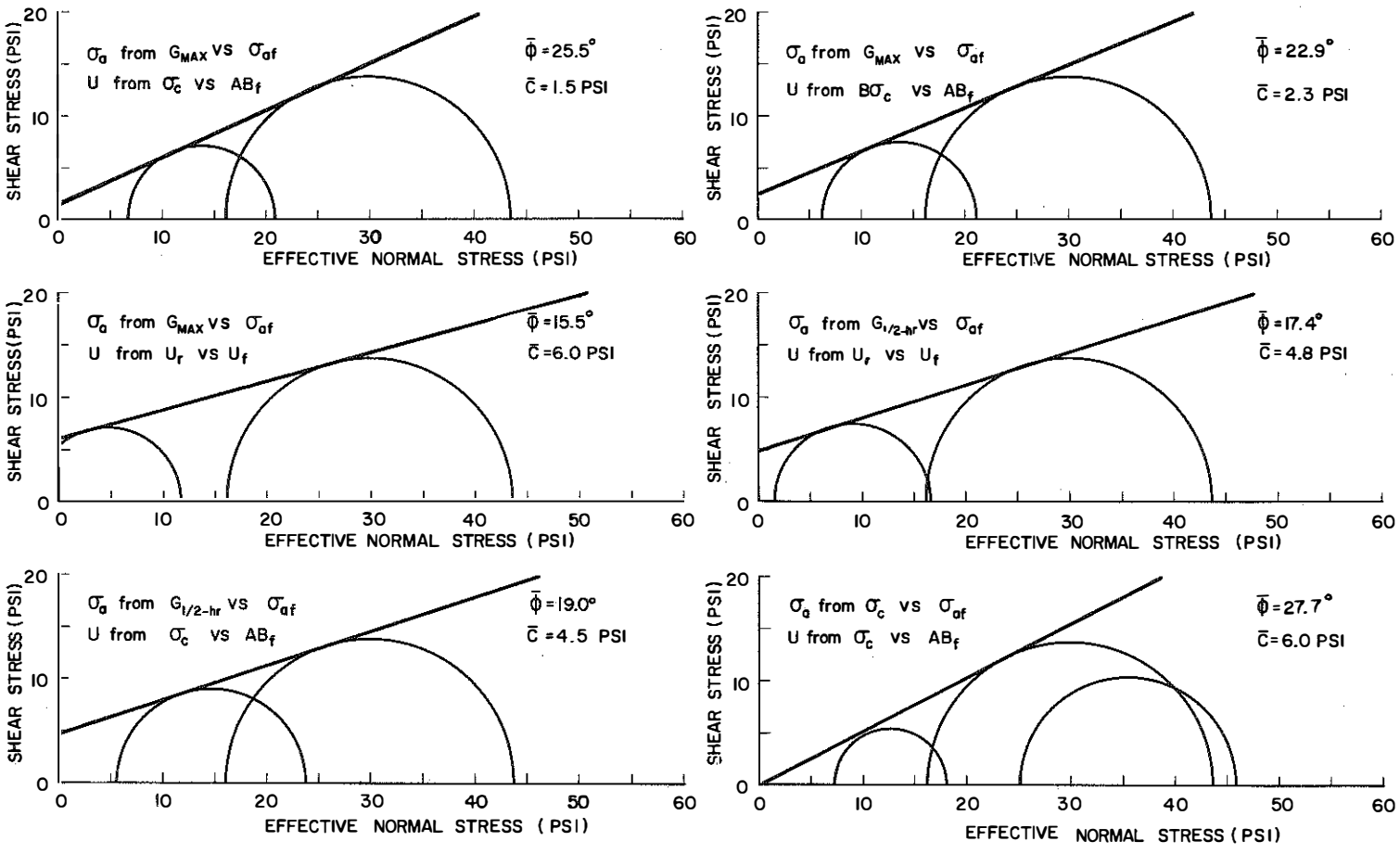

Figure 26. Failure Envelopes from Special One - Specimen Test No. 1 -- Baxter Soil Series.

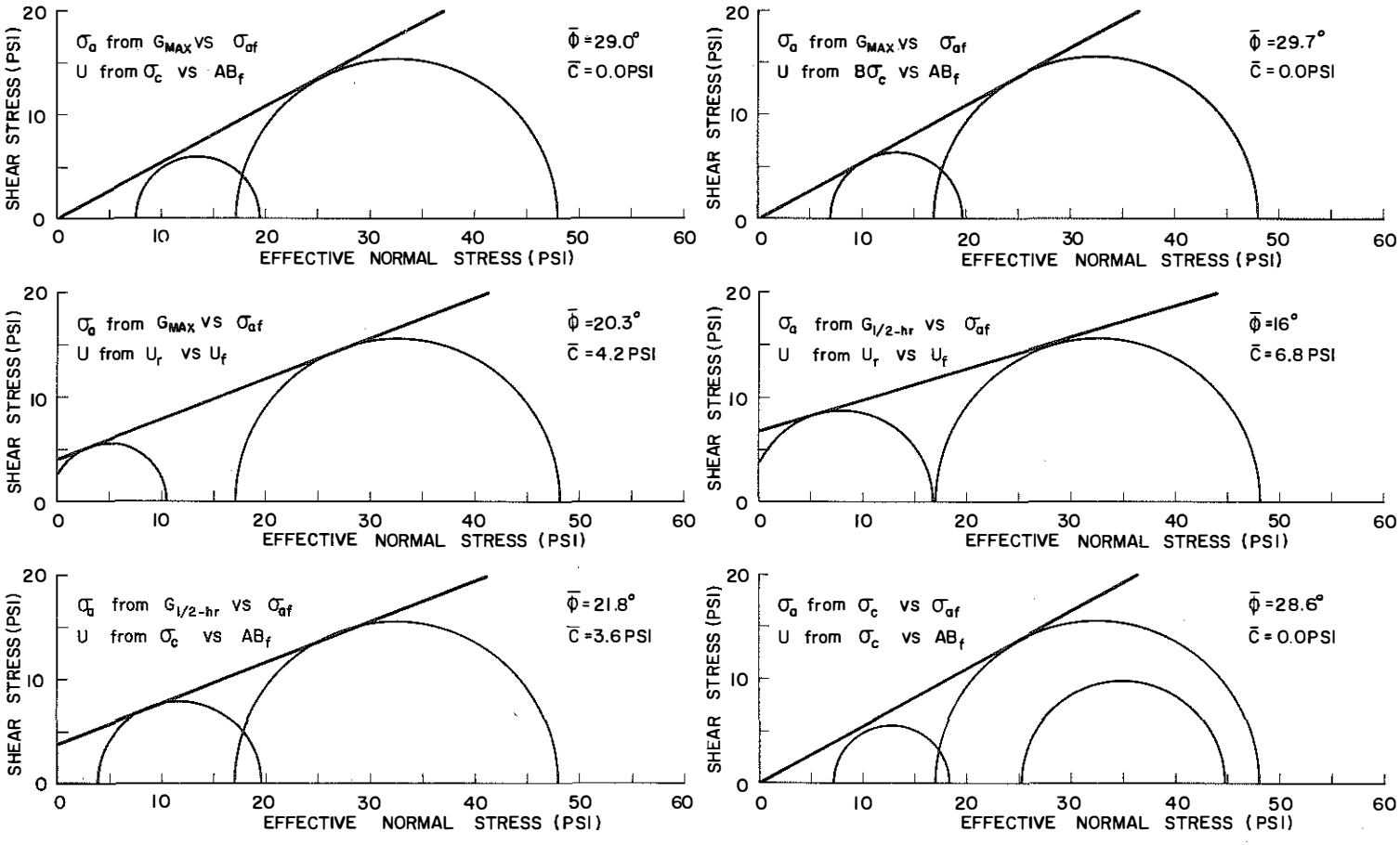

Figure 27. Failure Envelopes from Special One - Specimen Test No. 2 -- Baxter Soil Series.

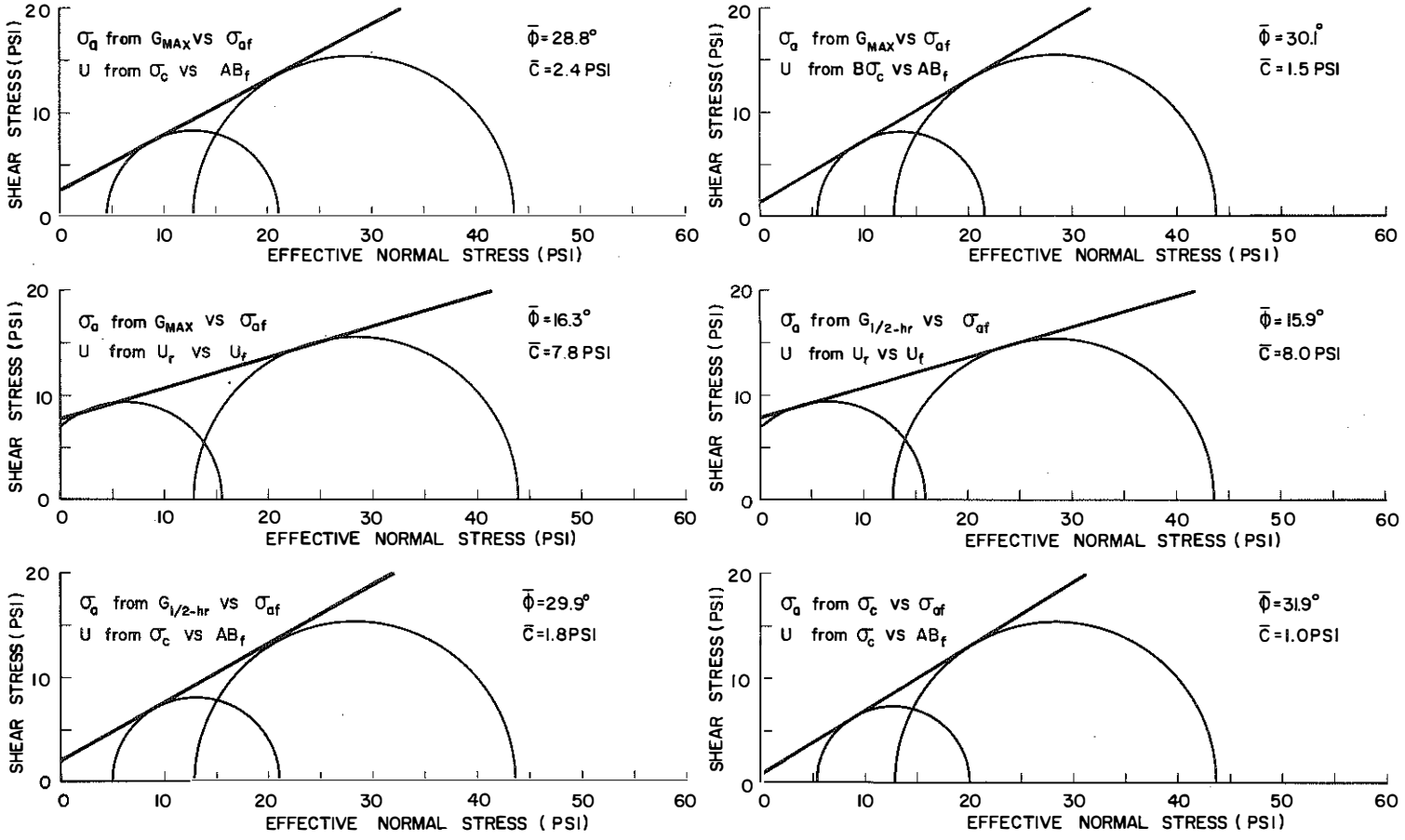

Figure 28. Failure Envelopes from Special One - Specimen Test -- Calloway Soil Series.

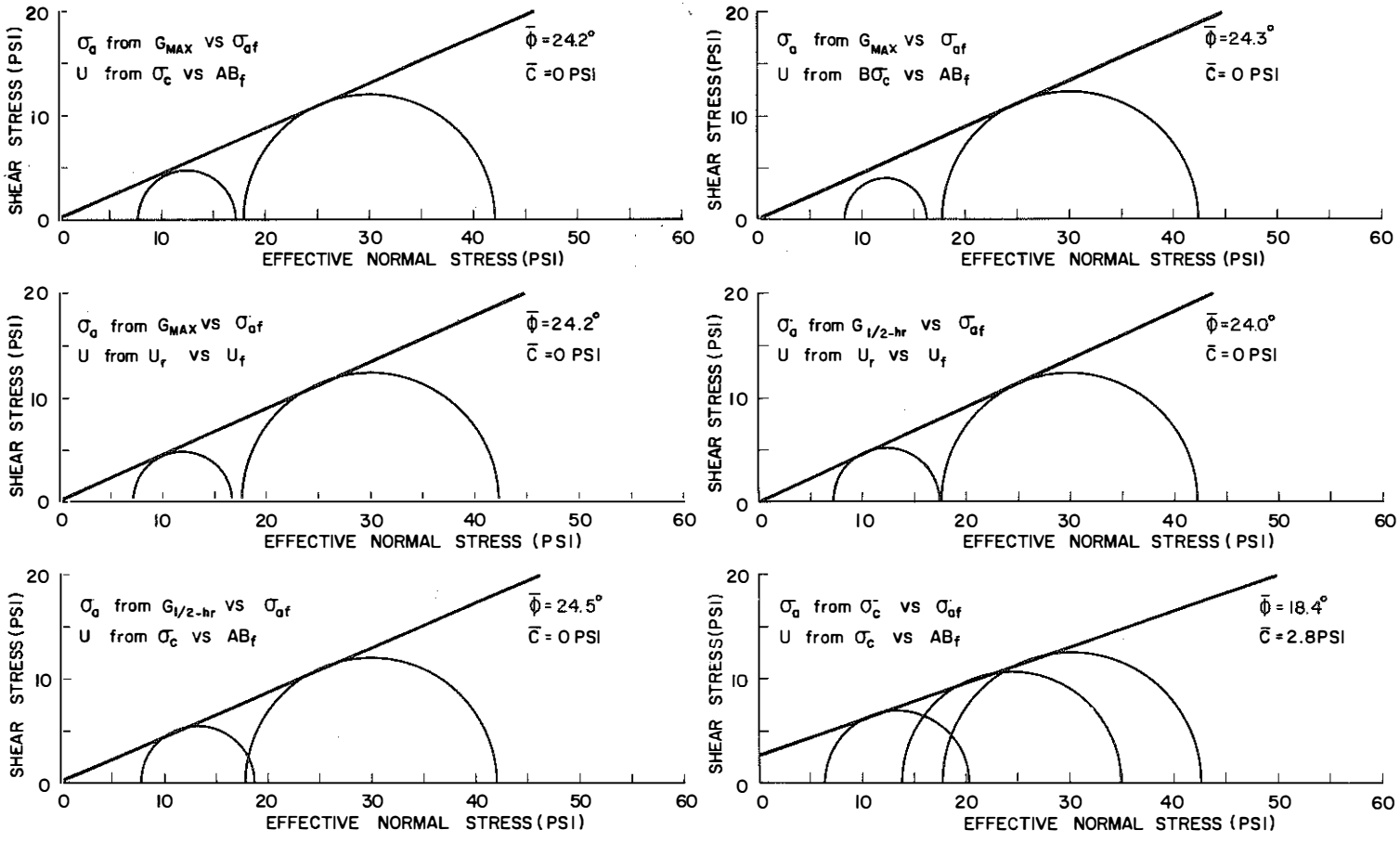

Figure 29. Failure Envelopes from Special One - Specimen Test – Eden Soil Series.

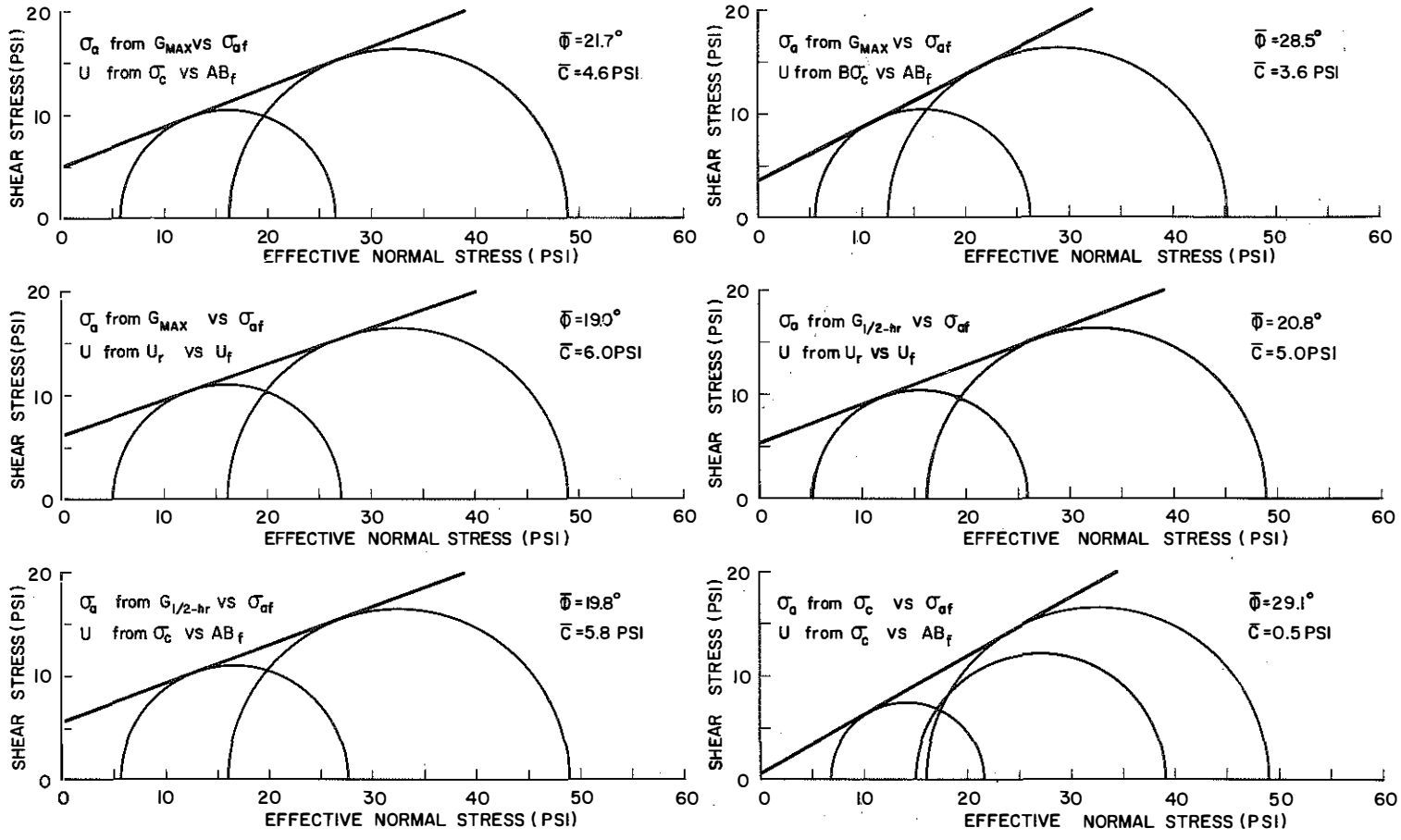

Figure 30. Failure Envelopes from Special One - Specimen Test No. 1 – Maury Soil Series.

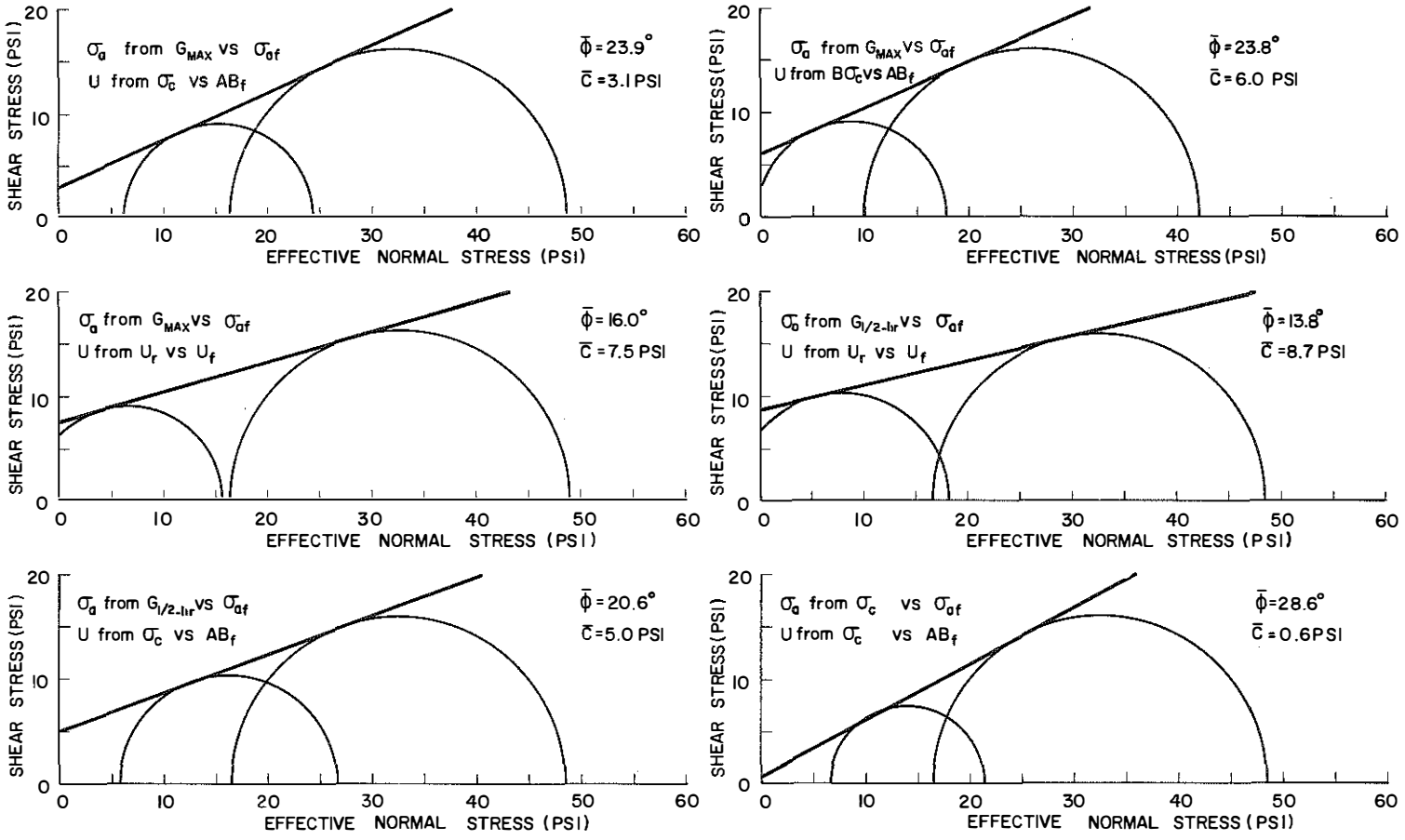

Figure 31. Failure Envelopes from Special One - Specimen Test No. 2 -- Maury Soil Series.

since the buildup of pore pressure is a function of the tendency for volume change which, in turn, is a function of strain. The smaller strains, evidently, were just not sufficient to produce good, repeatable pore pressure responses.

The failure envelopes, Figures 7 through 12, indicate that different definitions of failure and different methods of constructing envelopes have very little effect on the values of $\bar{\phi}$ and $\bar{c}$. However, failure envelopes consisting of more than three or four points constructed by plotting p vs q are apparently more accurate than those based on Mohr's circles, as many of the latter can be confusing.

An unexpected result was the better correlation of peak modulus vs failure strength than the 1/2-hour modulus vs failure strength -- compare Figure 13 and Figure 14. Although the relaxation test deformation, with the exception of the specimens strained 0.6 percent, was applied in about 1/2 second with very little variation, it was expected that small variations in strain application times might effect the value of the peak relaxation modulus to a greater extent than the 1/2-hour modulus. There is only a weak correlation of the divergent points in Figure 17, the ratio of peak to 1/2-hour modulus, with divergent points in Figures 13 and 14, relaxation modulus vs failure strength. Thus Figure 17 was not used to access the reliability of test results.

Most of the pore pressure correlation curves, Figures 15, 18 and 19, were disappointing. However, the curves of consolidation pressure vs pore pressure parameter AB and B times consolidation pressure vs AB, Figures 18 and 19, yielded good results.

The curves relating consolidation pressure and failure stress, Figure 20, indicate acceptable correlations. They do not go through the origin, however, and thus cannot be established from tests on a single specimen as can the curves of relaxation modulus vs failure stress and consolidation pressure vs AB at failure. It is interesting that all except one of the consolidation pressure vs failure stress curves intercept the stress axis at approximately 10 psi. The extrusion process of preparing specimens may have contributed to this result.

Figures 21 through 31, failure envelopes constructed from special relaxation-triaxial tests on one specimen, are the final results of this research. They show that the type of special relaxation-triaxial tests described herein yield failure envelopes which correlate favorably with envelopes obtained by the most rigorous and painstaking efforts of conventional methods. Not all of the graphical methods used for obtaining values of maximum stress difference, $\sigma_1 - \sigma_3$, and pore pressure were equally successful; but all failure envelopes are included for completeness. The envelopes calculated using pore pressure from relaxation pore pressure vs pore pressure at failure curves were the least satisfactory; those calculated using failure stress from the 1/2-hour modulus vs failure stress curves also were inadequate. The failure envelopes

that depend upon plots of consolidation pressure vs failure stress were consistent and generally good, but are of little interest here since at this time it appears that this type of correlation curve cannot be established from tests on a single specimen.

The two other procedures, in which the failure stress difference was obtained from curves of peak modulus vs failure stress and pore pressure was determined from curves of consolidation pressure or B times consolidation pressure vs AB at failure, gave very satisfactory results. Table 6 summarizes and compares the values of $\bar{\phi}$ and $\bar{c}$ so obtained with values of the same parameters from conventional tests. The agreement between effective friction angles varied between 0.4 degrees and 4.0 degrees, and the agreement between effective cohesion values varied between 0.7 psi and 2.2 psi.

Since nonuniformity is inherent in soils, especially for those soils sampled in situ, there is a need to gain an insight into the variation which actually exists. This can be accomplished by conventional methods only by testing a large number of specimens. The conventional failure envelopes presented herein were determined from a large number of tests minimum of 11. With this large number of points, accurate failure envelopes could be constructed by giving less weight to those points which appeared to be influenced by some error. An absolute minimum of two points are required to define a failure envelope. It is common practice in many laboratories to use three points. If three points plot reasonably close to a straight line, the envelope can be considered correct and accurate. However, if they do not, at least one point is erroneous; and, furthermore, it is usually not possible to determine positively which is the maverick. In such cases, equal weight is given to all three points; and the line which fits best is considered to be the failure envelope, thus accepting some error and minimizing the possible error. Either the testing of non-identical specimens or faulty tests on identical specimens will result in scattered points on failure envelopes. Envelopes constructed on the basis of only three tests can be very misleading if the specimens are not identical. Figure 32 illustrates the effect of non-identical specimens on the failure envelope. With test results such as these, it is not possible to construct an accurate failure envelope. If special relaxation-triaxial tests were performed on the specimens of Figure 32, three failure envelopes would result, and the sample variation would be apparent.

The special relaxation-triaxial test procedure used in this research was developed to eliminate the effect of non-identical specimens and certain test errors and thereby increase the accuracy of results for a given number of specimens tested. Several identical specimens are not necessary since an adequate failure envelope can be determined from the special test on a single specimen. However, if only one test is performed, it may not be possible to detect or assess the seriousness of testing error. Thus, it is desirable

The following recommendations are offered concerning the use and further study of the special testing and analysis procedures described herein:

1. Special relaxation-triaxial tests should be performed on a wide range of soil types to see if the special testing procedure is valid for other soil types.

2. A study should be made to determine if there is a better correlation between the modulus obtained from repeated load tests and maximum stress difference than between the peak relaxation modulus and maximum stress difference.

3. Very rigid supports should be used to mount the axial deformation gauges, and special care should be taken to ensure that the loading piston is properly seated in the top sample cap.

4. Special precautions, such as the use of double, coated membranes or a method of applying confining pressures in which air does not come in contact with the confining fluid, should be used to minimize the diffusion of air through membranes.

The stress relaxation data are currently being analyzed to develop suitable mathematical representations of rheological behavior. The general procedure for analysis is to transform the experimental curves to mechanical models and distributions of relaxation times. The extent of linearity and the possible applicability of the superposition principle is to be assessed.

Constant stress test data are also being obtained for the same five remolded soils for which extensive relaxation and ultimate strength data are available. All of these data are being utilized in an attempt to develop improved design procedures which include the parameter time. A possible rheological criterion for stability analysis -- the upper yield limit obtained from the constant stress tests -- is being investigated. Comparisons are to be made between conventional shear strength parameters using the ultimate strength data and the rheological parameters.

APPENDIX A

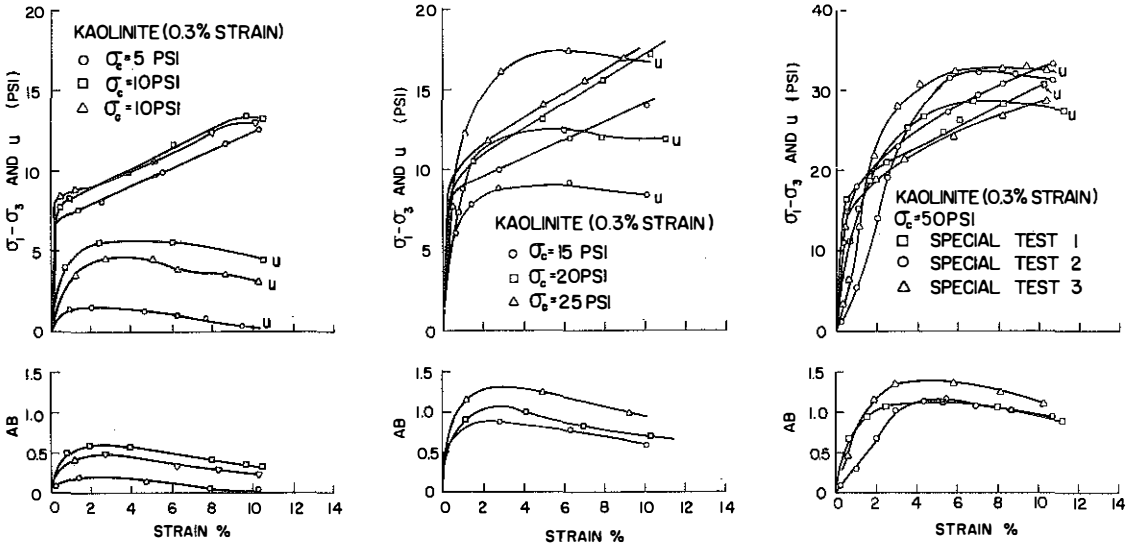
KAOLINITE (0.3% STRAIN)
o σc=5 PSI
□ σc=10PSI
△ σc=10PSI
σ1-σ3 AND u (PSI)
AB
STRAIN %
KAOLINITE (0.3% STRAIN)
o σc=15 PSI
□ σc=20PSI
△ σc=25PSI
σ1-σ3 AND u (PSI)
AB
STRAIN %
KAOLINITE (0.3% STRAIN)
σc=50PSI
□ SPECIAL TEST 1
○ SPECIAL TEST 2
△ SPECIAL TEST 3
σ1-σ3 AND u (PSI)
AB
STRAIN %

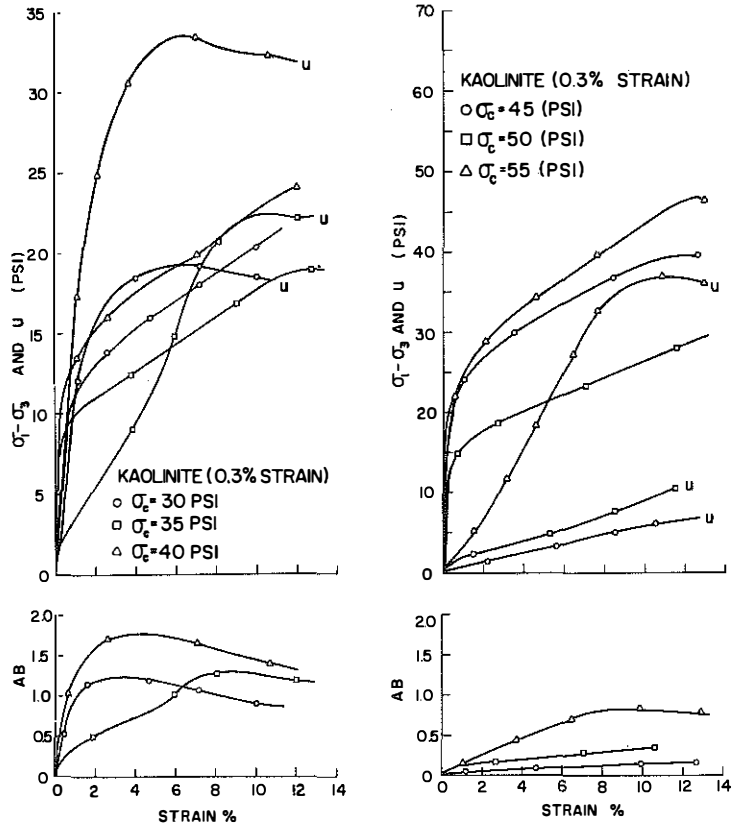
KAOLINITE (0.3% STRAIN)
o σc= 30 PSI
□ σc= 35 PSI
△ σc=40 PSI
σ1-σ3 AND u (PSI)
AB
STRAIN %
KAOLINITE (0.3% STRAIN)
o σc=45 (PSI)
□ σc=50 (PSI)
△ σc=55 (PSI)
σ1-σ3 AND u (PSI)
AB
STRAIN %

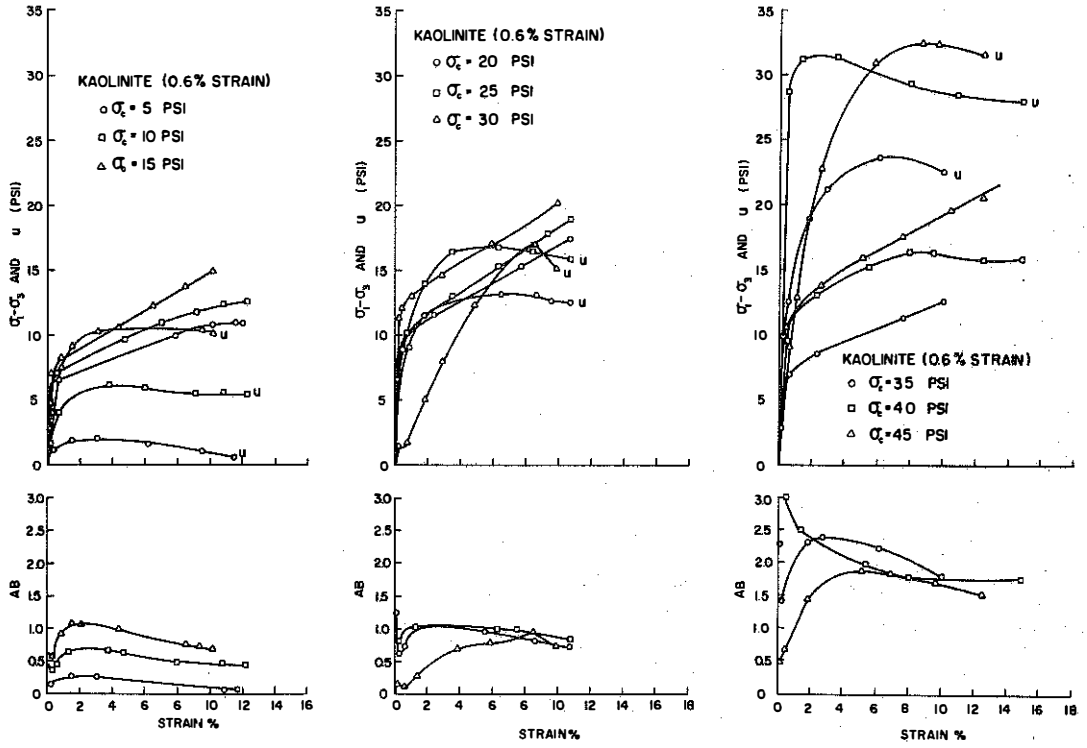
KAOLINITE (0.6% STRAIN)
σc = 5 PSI
σc = 10 PSI
σc = 15 PSI
σ1-σ3 AND u (PSI)
AB
STRAIN %

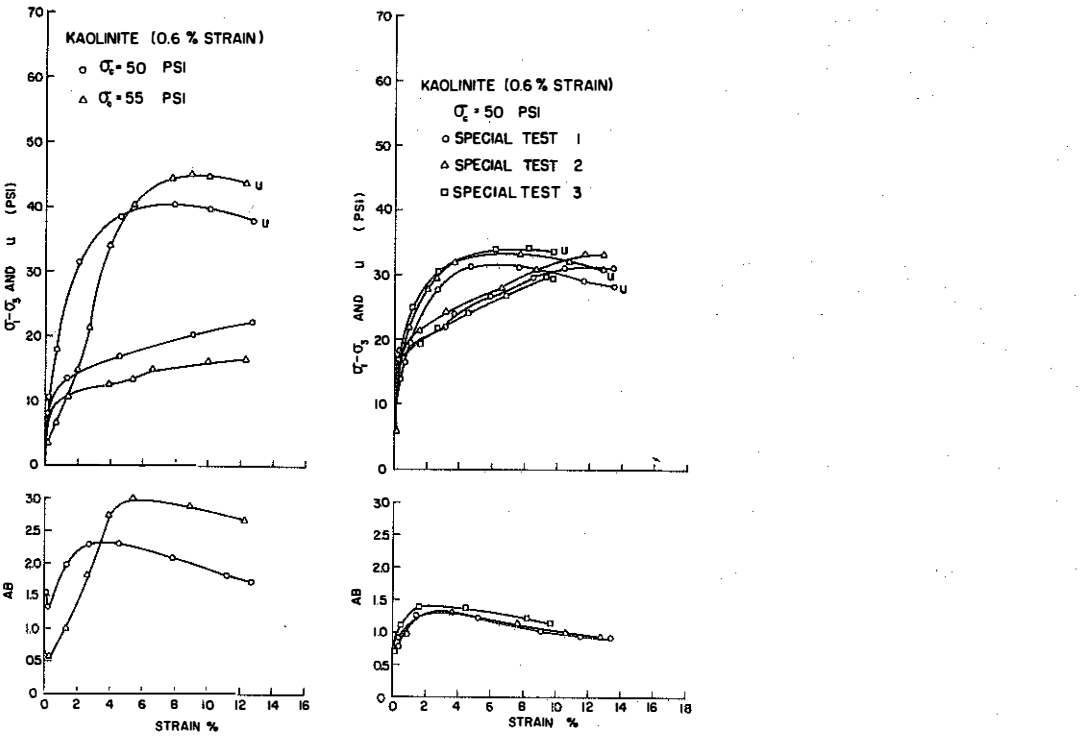
KAOLINITE (0.6% STRAIN)
σc = 20 PSI
σc = 25 PSI
σc = 30 PSI
σc = 35 PSI
σc = 40 PSI
σc = 45 PSI
σ1-σ3 AND u (PSI)
AB
STRAIN %

KAOLINITE (0.6 % STRAIN)
σc = 50 PSI
σc = 55 PSI
KAOLINITE (0.6 % STRAIN)
σc = 50 PSI
SPECIAL TEST 1
SPECIAL TEST 2
SPECIAL TEST 3
σ1-σ3 AND u (PSI)
AB
STRAIN %

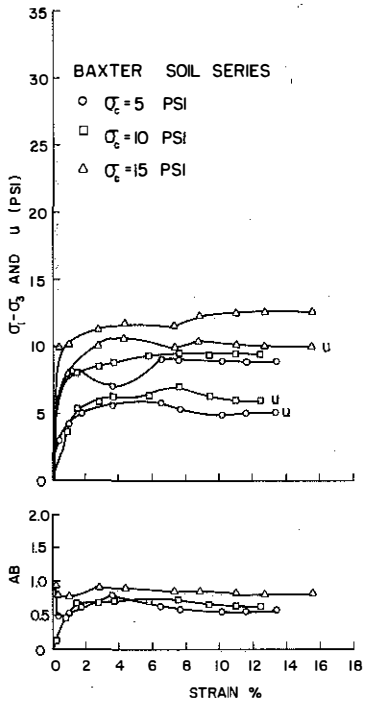
BAXTER SOIL SERIES
○ σc = 5 PSI
□ σc = 10 PSI
△ σc = 15 PSI
σ1-σ3 AND u (PSI)
AB
STRAIN %

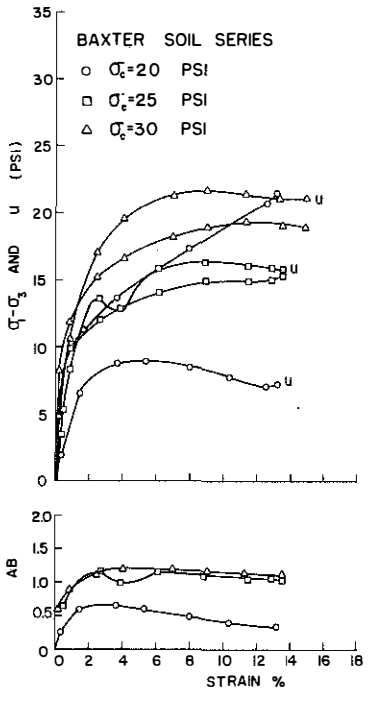
BAXTER SOIL SERIES
○ σc = 20 PSI
□ σc = 25 PSI
△ σc = 30 PSI
σ1-σ3 AND u (PSI)
AB
STRAIN %

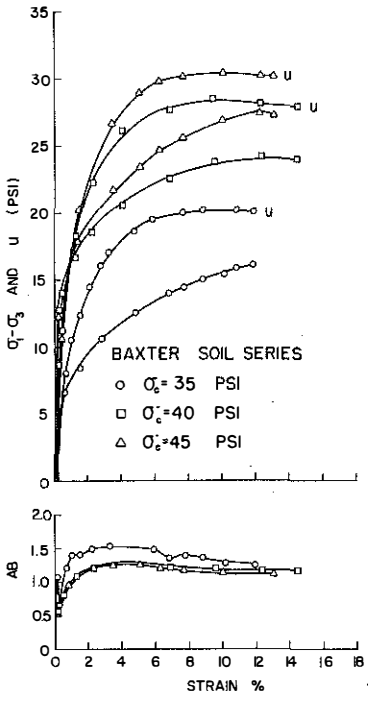
BAXTER SOIL SERIES
○ σc = 35 PSI
□ σc = 40 PSI
△ σc = 45 PSI
σ1-σ3 AND u (PSI)
AB
STRAIN %

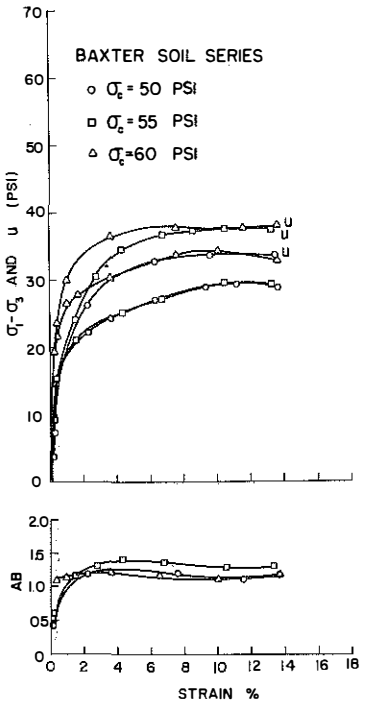
BAXTER SOIL SERIES
○ σc = 50 PSI
□ σc = 55 PSI
△ σc = 60 PSI
σ1-σ3 AND u (PSI)
AB
STRAIN %

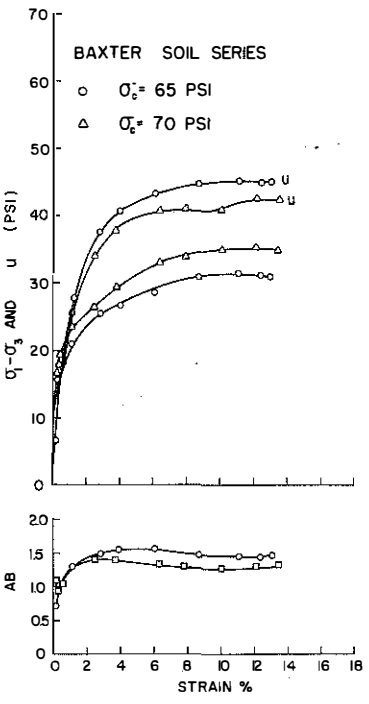
BAXTER SOIL SERIES
○ σc = 65 PSI
△ σc = 70 PSI
σ1-σ3 AND u (PSI)
AB
STRAIN %

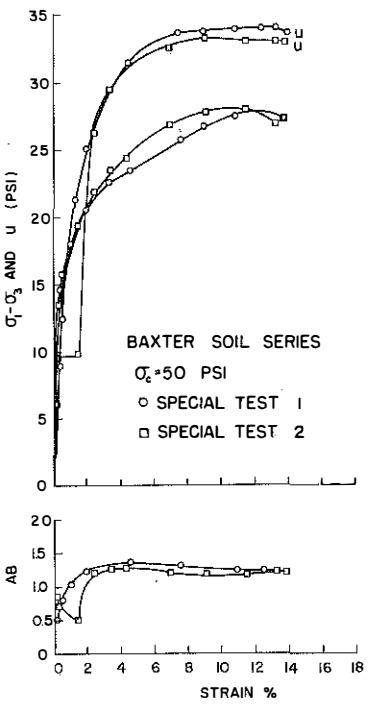
BAXTER SOIL SERIES
σc = 50 PSI
○ SPECIAL TEST 1
□ SPECIAL TEST 2
σ1-σ3 AND u (PSI)
AB
STRAIN %

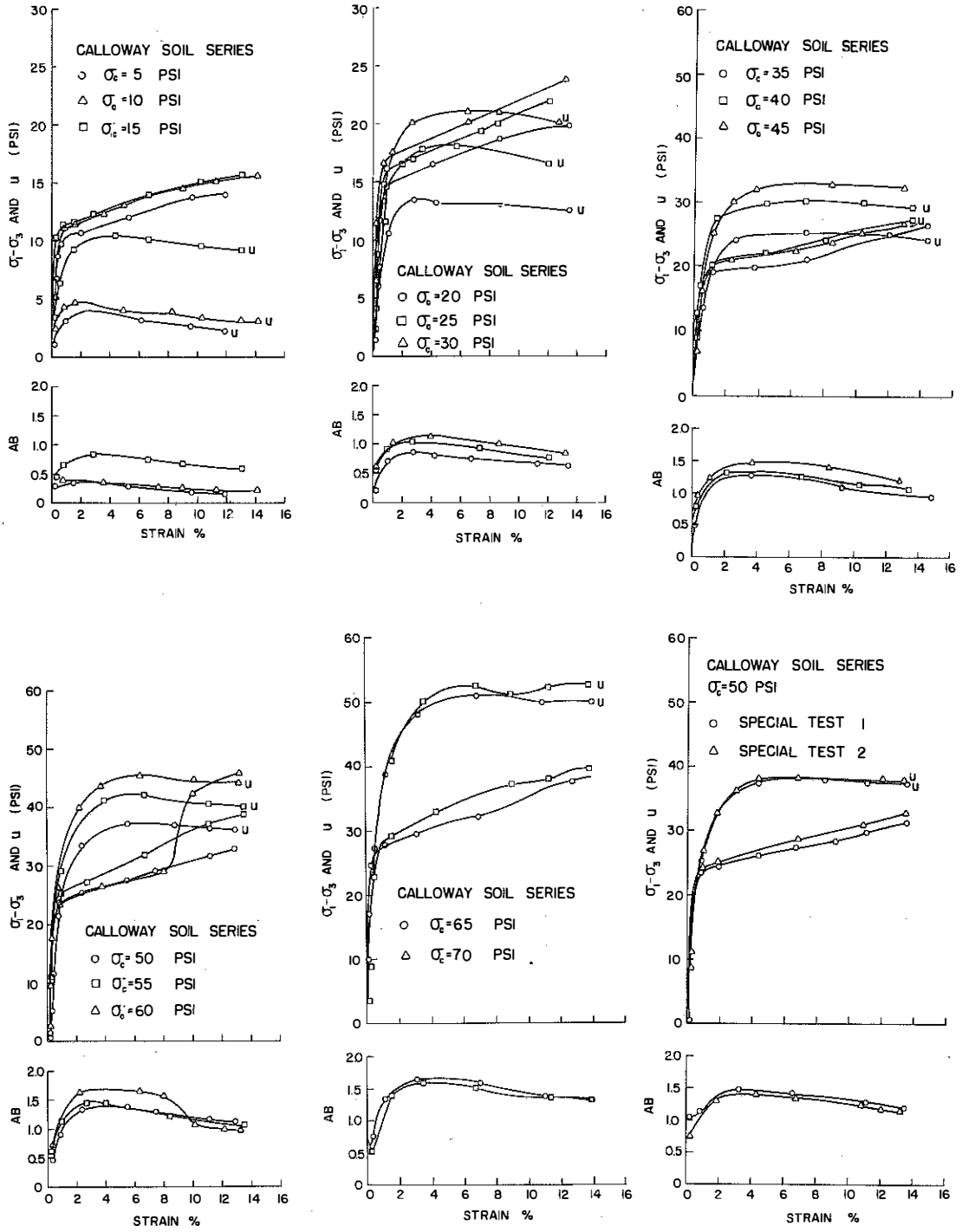
CALLOWAY SOIL SERIES
○ σc = 5 PSI
△ σc =10 PSI
□ σc =15 PSI
CALLOWAY SOIL SERIES
○ σc =20 PSI
□ σc =25 PSI
△ σc =30 PSI
CALLOWAY SOIL SERIES
○ σc =35 PSI
□ σc =40 PSI
△ σc =45 PSI
CALLOWAY SOIL SERIES
○ σc = 50 PSI
□ σc =55 PSI
△ σc =60 PSI
CALLOWAY SOIL SERIES
○ σc =65 PSI
△ σc =70 PSI
CALLOWAY SOIL SERIES
σc =50 PSI
○ SPECIAL TEST 1
△ SPECIAL TEST 2
σ1-σ3 AND u (PSI)
AB
STRAIN %
u

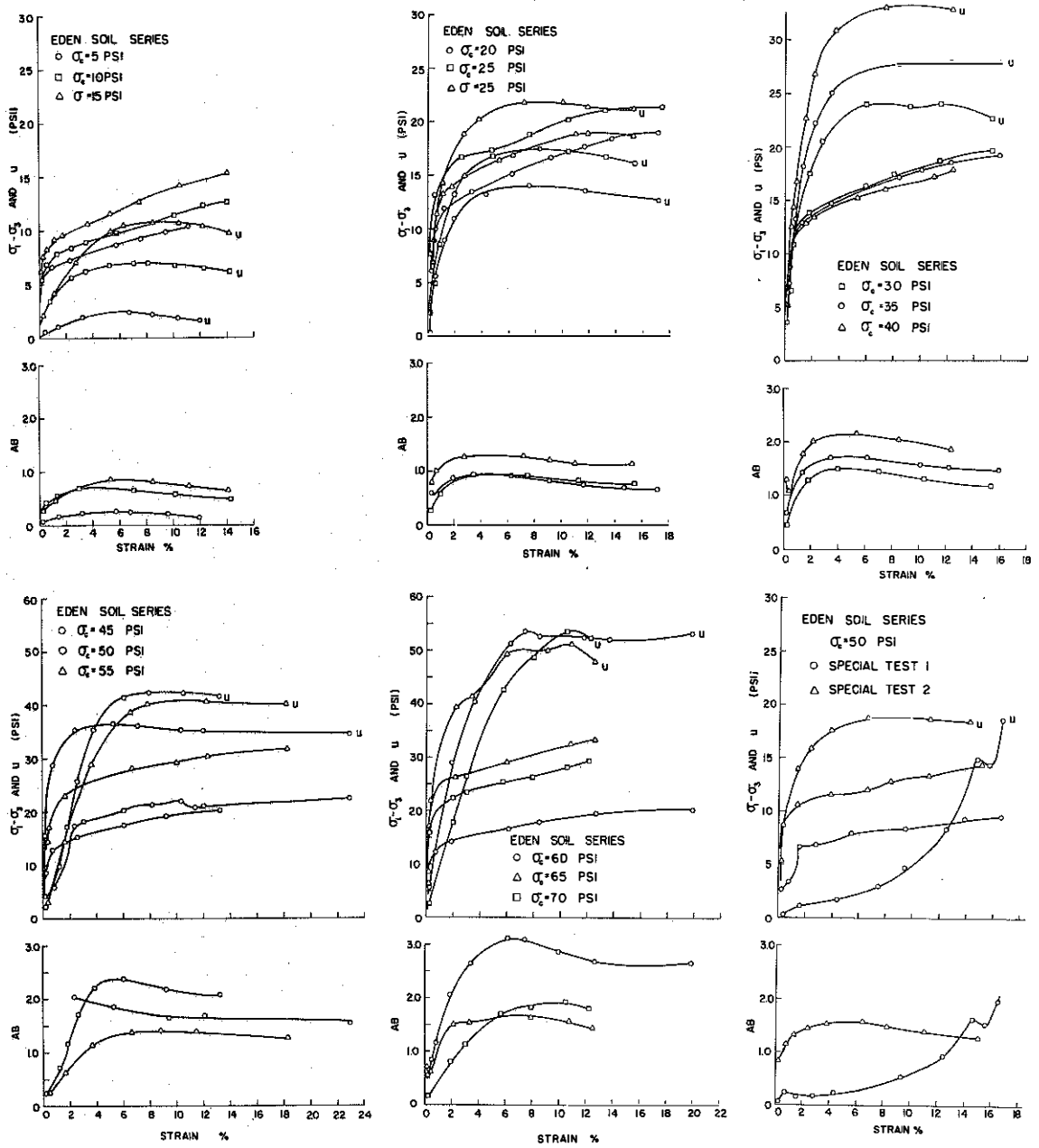
EDEN SOIL SERIES
σc=5 PSI
σc=10PSI
σ =15 PSI
σc=20 PSI
σc=25 PSI
σ =25 PSI
σc=30 PSI
σc=35 PSI
σc=40 PSI
σc=45 PSI
σc=50 PSI
σc=55 PSI
σc=60 PSI
σc=65 PSI
σc=70 PSI
SPECIAL TEST 1
SPECIAL TEST 2
σ1-σ3 AND u (PSI)
AB
STRAIN %
u

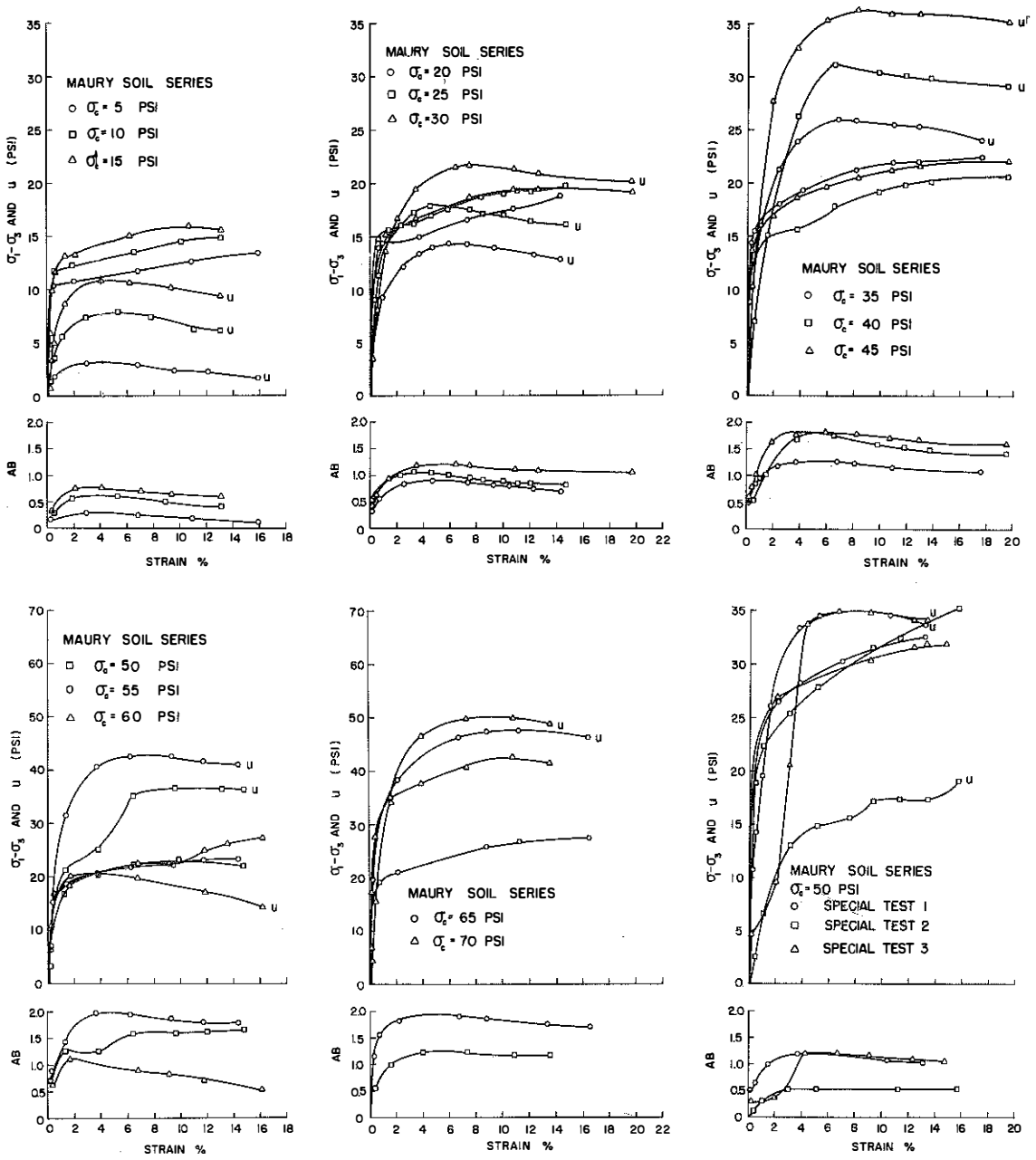
MAURY SOIL SERIES
○ σc = 5 PSI
□ σc = 10 PSI
△ σc = 15 PSI
MAURY SOIL SERIES
○ σc = 20 PSI
□ σc = 25 PSI
△ σc = 30 PSI
MAURY SOIL SERIES
○ σc = 35 PSI
□ σc = 40 PSI
△ σc = 45 PSI
MAURY SOIL SERIES
□ σc = 50 PSI
○ σc = 55 PSI
△ σc = 60 PSI
MAURY SOIL SERIES
○ σc = 65 PSI
△ σc = 70 PSI
MAURY SOIL SERIES
σc = 50 PSI
○ SPECIAL TEST 1
□ SPECIAL TEST 2
△ SPECIAL TEST 3
σ1-σ3 AND u (PSI)
AB
STRAIN %
u

APPENDIX B

RELAXATION MODULUS (PSI) X 10⁴
TIME (MIN.)
PORE PRESSURE (PSI)
KAOLINITE (0.3% STRAIN)
σ = 5 PSI
σ = 10 PSI
σ = 15 PSI
KAOLINITE (0.3% STRAIN)
σc = 35 PSI
σc = 40 PSI
KAOLINITE (0.3 % STRAIN)
σc = 20 PSI
σc = 25 PSI
σc = 29 PSI
KAOLINITE (0.3 % STRAIN)
σc = 50 PSI
σc = 55 PSI

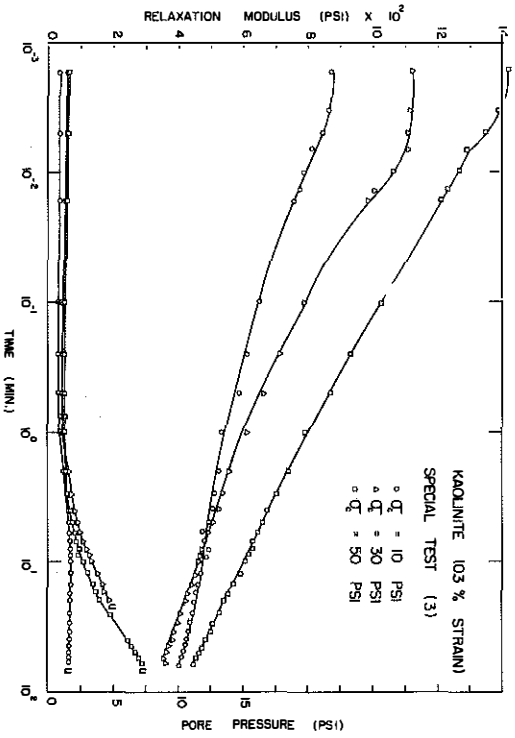
KAOLINITE (0.3 % STRAIN)
SPECIAL TEST (3)
σ3 = 10 PSI
σ3 = 30 PSI
σ3 = 50 PSI
RELAXATION MODULUS (PSI) X 10²
PORE PRESSURE (PSI)
TIME (MIN.)

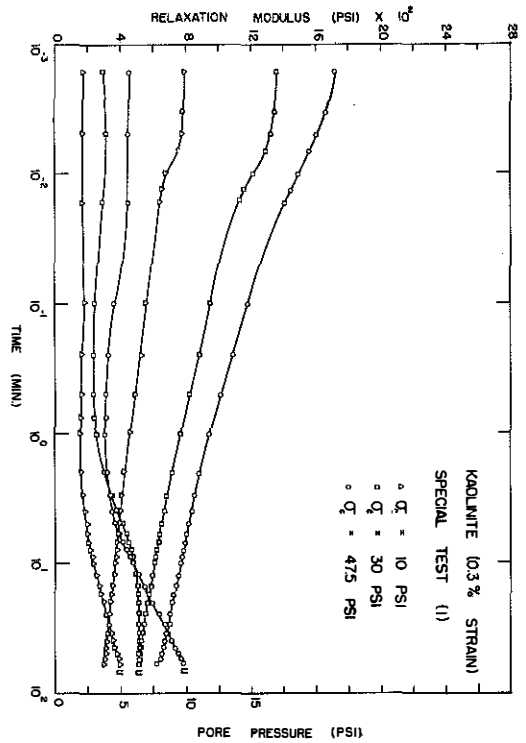
KAOLINITE (0.3 % STRAIN)
SPECIAL TEST (1)
σ3 = 10 PSI
σ3 = 30 PSI
σ3 = 47.5 PSI
RELAXATION MODULUS (PSI) X 10³
PORE PRESSURE (PSI)
TIME (MIN.)

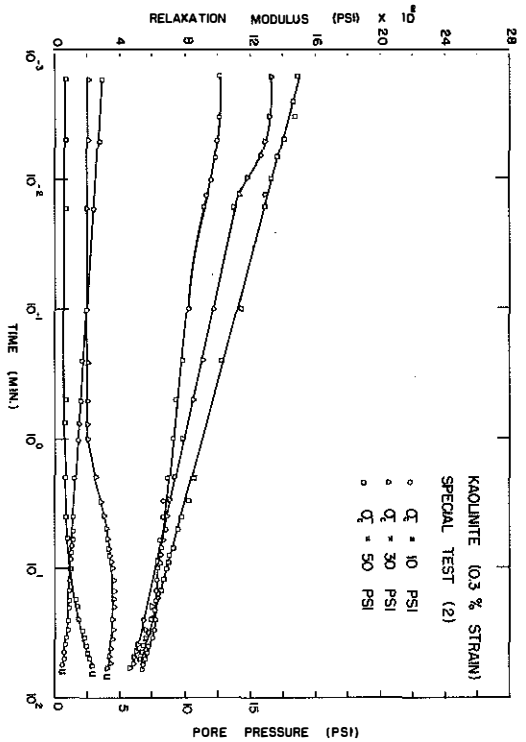
KAOLINITE (0.3 % STRAIN)
SPECIAL TEST (2)
σ3 = 10 PSI
σ3 = 30 PSI
σ3 = 50 PSI
RELAXATION MODULUS (PSI) X 10³
PORE PRESSURE (PSI)
TIME (MIN.)

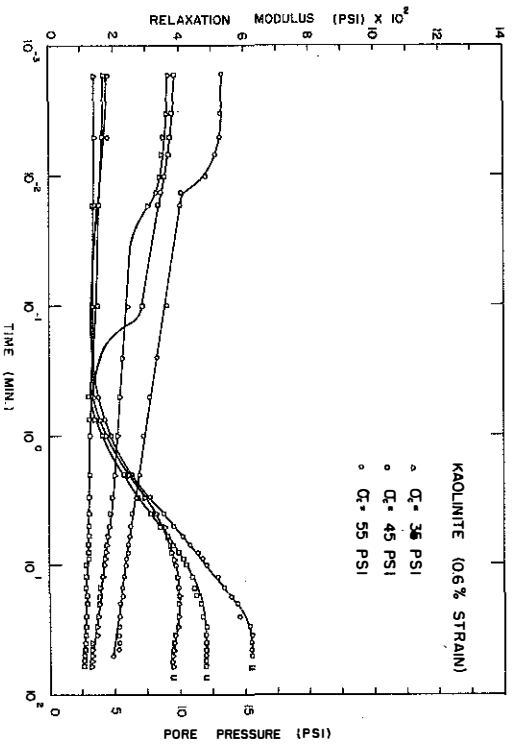
RELAXATION MODULUS (PSI) X 10²
TIME (MIN.)
PORE PRESSURE (PSI)
KAOLINITE (0.6% STRAIN)
○ σ₃ = 35 PSI
□ σ₃ = 45 PSI
◇ σ₃ = 55 PSI

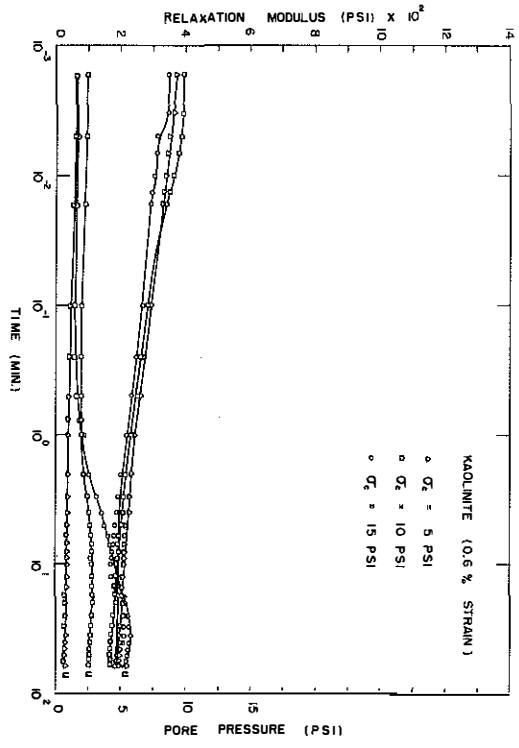
RELAXATION MODULUS (PSI) X 10²
TIME (MIN.)
PORE PRESSURE (PSI)
KAOLINITE (0.6 % STRAIN)
○ σ₃ = 5 PSI
□ σ₃ = 10 PSI
◇ σ₃ = 15 PSI

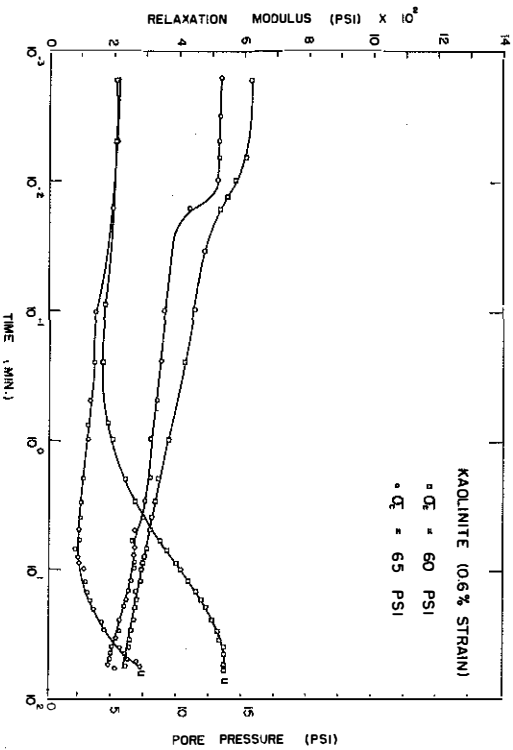
RELAXATION MODULUS (PSI) X 10²
TIME (MIN.)
PORE PRESSURE (PSI)
KAOLINITE (0.6% STRAIN)
□ σ₃ = 60 PSI
◇ σ₃ = 65 PSI

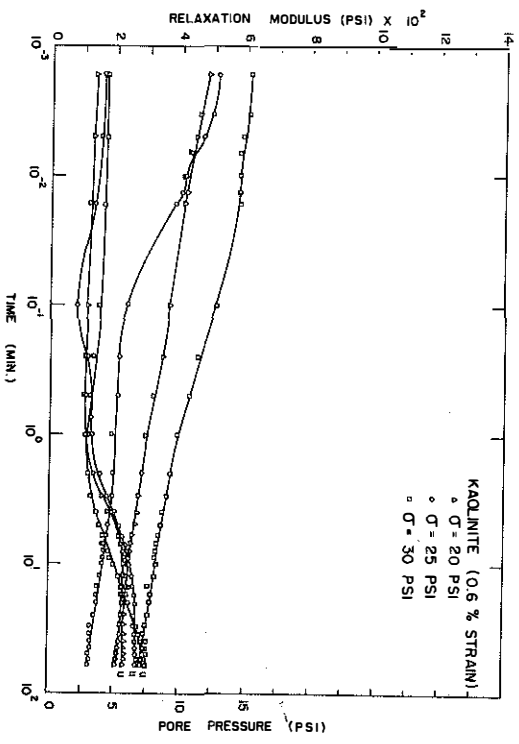
RELAXATION MODULUS (PSI) X 10²
TIME (MIN.)
PORE PRESSURE (PSI)
KAOLINITE (0.6 % STRAIN)
○ σ = 20 PSI
◇ σ = 25 PSI
□ σ = 30 PSI

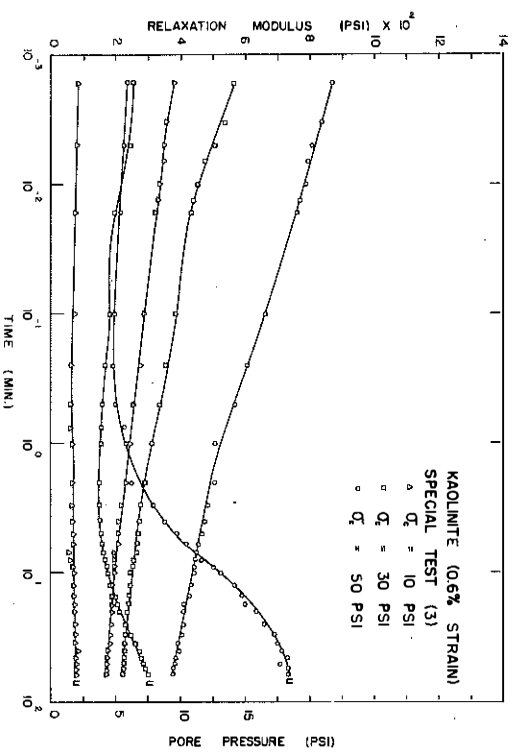
KAOLINITE (0.6% STRAIN)
SPECIAL TEST (3)
Δ σc = 10 PSI
□ σc = 30 PSI
○ σc = 50 PSI
RELAXATION MODULUS (PSI) X 10²
TIME (MIN.)
PORE PRESSURE (PSI)

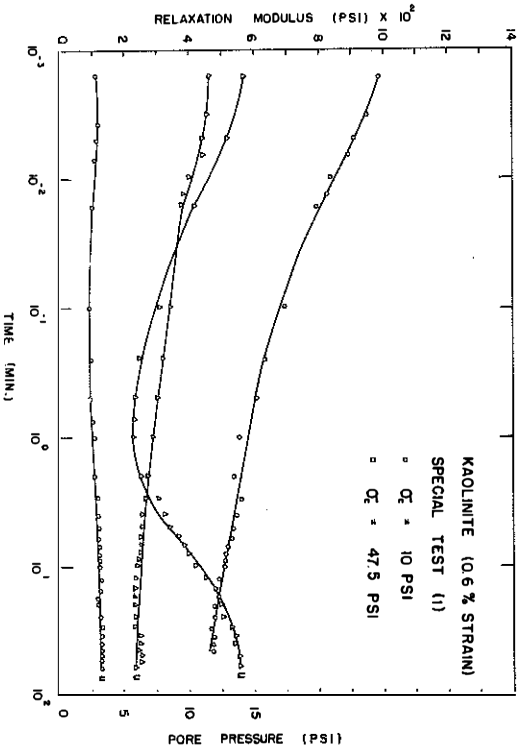
KAOLINITE (0.6 % STRAIN)
SPECIAL TEST (1)
□ σc = 10 PSI
□ σc = 47.5 PSI
RELAXATION MODULUS (PSI) X 10²
TIME (MIN.)
PORE PRESSURE (PSI)

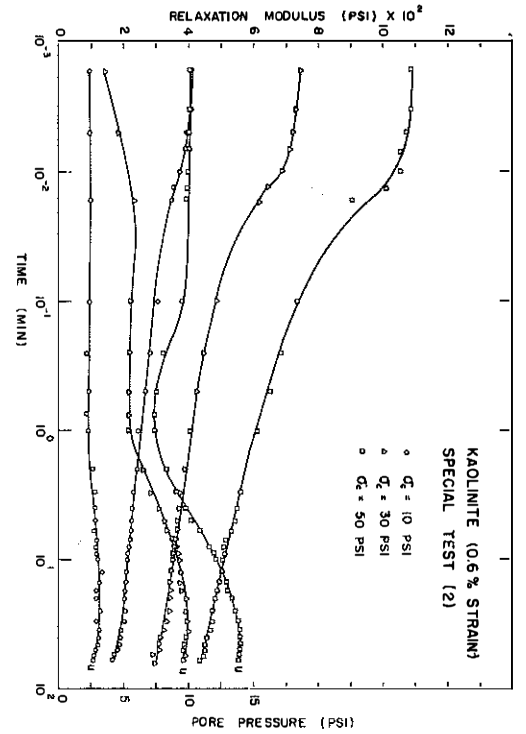
KAOLINITE (0.6 % STRAIN)
SPECIAL TEST (2)
○ σc = 10 PSI
Δ σc = 30 PSI
□ σc = 50 PSI
RELAXATION MODULUS (PSI) X 10²
TIME (MIN)
PORE PRESSURE (PSI)

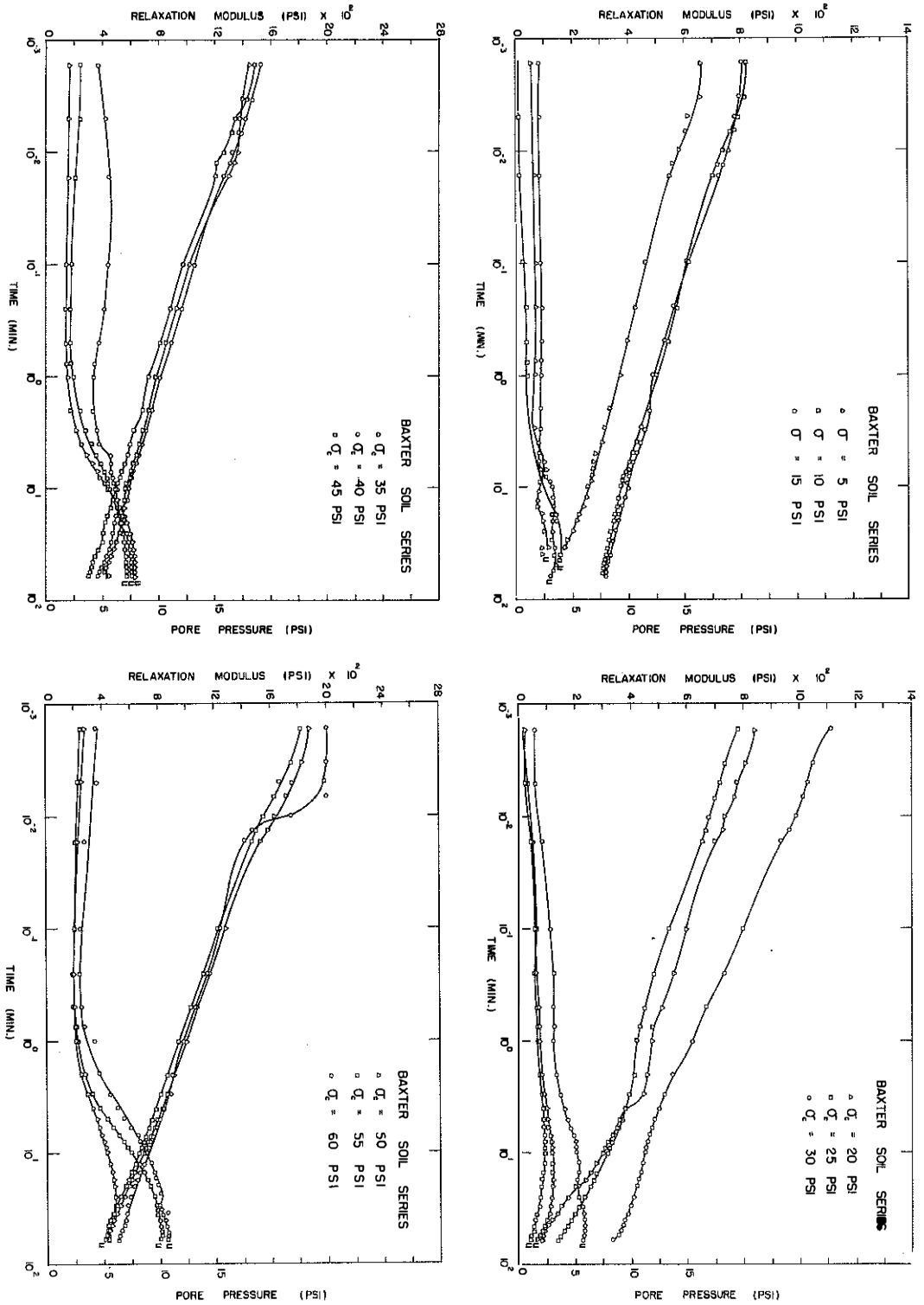
RELAXATION MODULUS (PSI) X 10⁶
TIME (MIN.)
PORE PRESSURE (PSI)
BAXTER SOIL SERIES
○ σ₃ = 5 PSI
□ σ₃ = 10 PSI
△ σ₃ = 15 PSI
BAXTER SOIL SERIES
○ σ₃ = 20 PSI
□ σ₃ = 25 PSI
△ σ₃ = 30 PSI
BAXTER SOIL SERIES
○ σ₃ = 35 PSI
□ σ₃ = 40 PSI
△ σ₃ = 45 PSI
BAXTER SOIL SERIES
○ σ₃ = 50 PSI
□ σ₃ = 55 PSI
△ σ₃ = 60 PSI

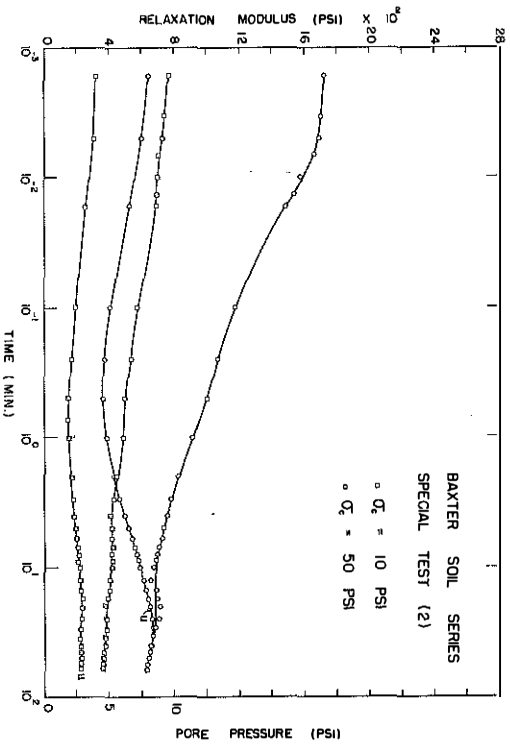
BAXTER SOIL SERIES
SPECIAL TEST (2)
○ σ_c = 10 PSI
● σ_c = 50 PSI
RELAXATION MODULUS (PSI) X 10^2
PORE PRESSURE (PSI)
TIME (MIN.)

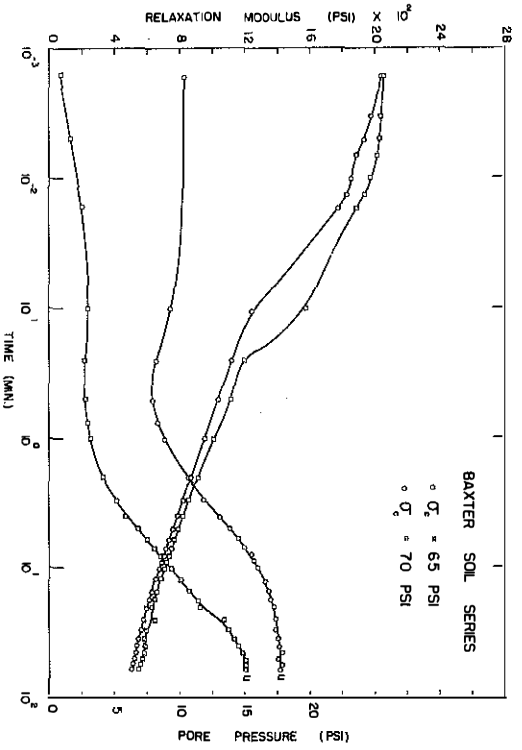
BAXTER SOIL SERIES
○ σ_c = 65 PSI
● σ_c = 70 PSI
RELAXATION MODULUS (PSI) X 10^2
PORE PRESSURE (PSI)
TIME (MIN.)

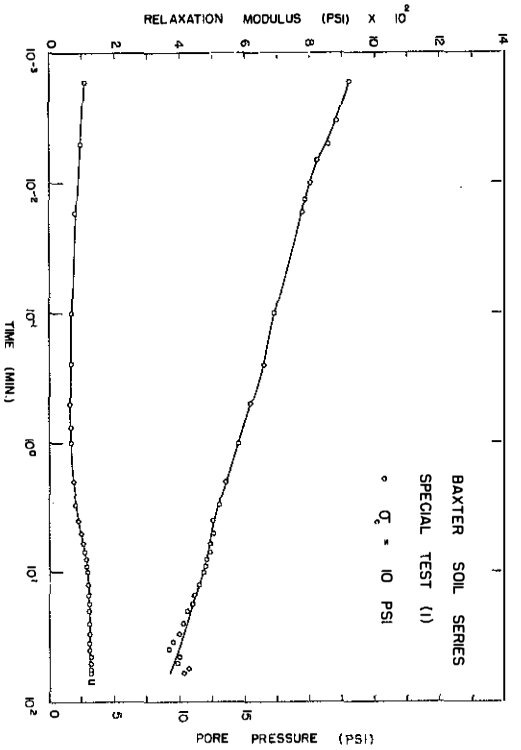
BAXTER SOIL SERIES
SPECIAL TEST (1)
● σ_c = 10 PSI
RELAXATION MODULUS (PSI) X 10^2
PORE PRESSURE (PSI)
TIME (MIN.)

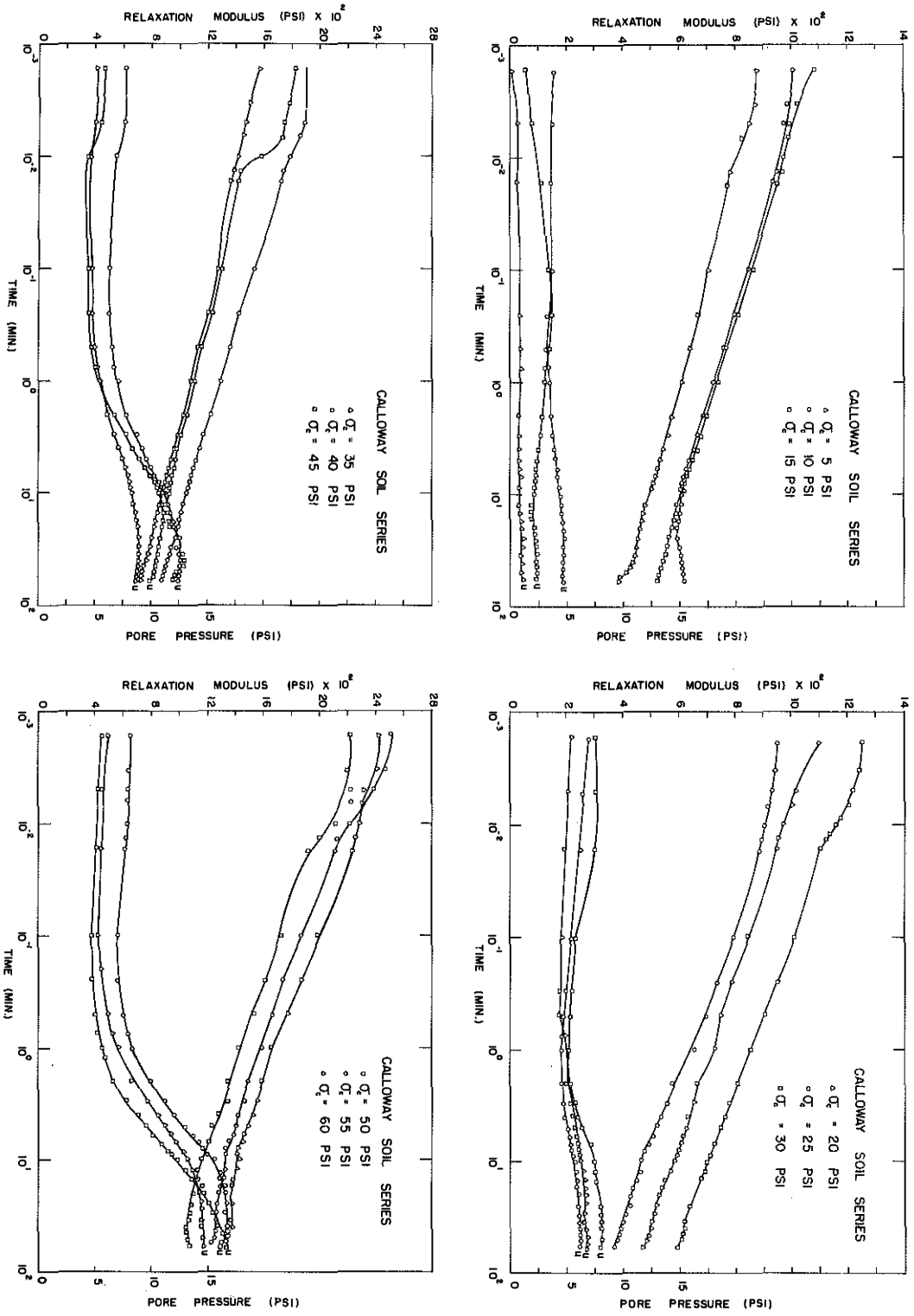
RELAXATION MODULUS (PSI) X 10²
PORE PRESSURE (PSI)
TIME (MIN.)
CALLOWAY SOIL SERIES
Δ σ₃ = 5 PSI
○ σ₃ = 10 PSI
□ σ₃ = 15 PSI
CALLOWAY SOIL SERIES
Δ σ₃ = 20 PSI
○ σ₃ = 25 PSI
□ σ₃ = 30 PSI
CALLOWAY SOIL SERIES
Δ σ₃ = 35 PSI
○ σ₃ = 40 PSI
□ σ₃ = 45 PSI
CALLOWAY SOIL SERIES
□ σ₃ = 50 PSI
○ σ₃ = 55 PSI
Δ σ₃ = 60 PSI

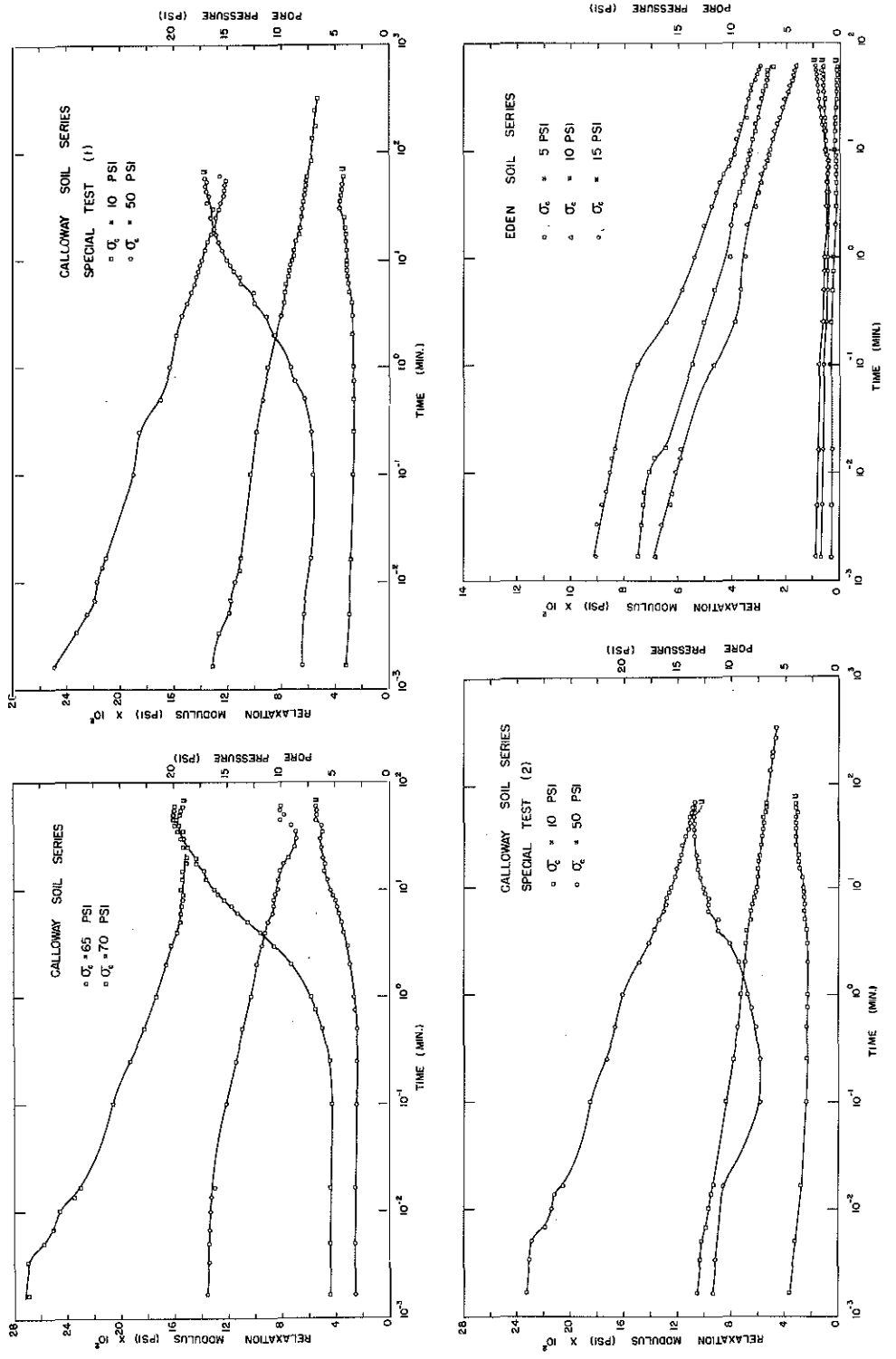
CALLOWAY SOIL SERIES
SPECIAL TEST (1)
□ σc = 10 PSI
○ σc = 50 PSI
CALLOWAY SOIL SERIES
○ σc = 65 PSI
□ σc = 70 PSI
EDEN SOIL SERIES
□ σc = 5 PSI
△ σc = 10 PSI
○ σc = 15 PSI
CALLOWAY SOIL SERIES
SPECIAL TEST (2)
□ σc = 10 PSI
○ σc = 50 PSI
RELAXATION MODULUS (PSI) x 10⁴
PORE PRESSURE (PSI)
TIME (MIN.)

EDEN SOIL SERIES
σc = 20 PSI
σc = 25 PSI (A)
RELAXATION MODULUS (PSI) X 10²
PORE PRESSURE (PSI)
TIME (MIN.)

EDEN SOIL SERIES
σc = 25 PSI
σc = 30 PSI
σc = 35 PSI
RELAXATION MODULUS (PSI) X 10²
PORE PRESSURE (PSI)
TIME (MIN.)

EDEN SOIL SERIES
σc = 40 PSI
σc = 45 PSI
σc = 50 PSI
RELAXATION MODULUS (PSI) X 10²
PORE PRESSURE (PSI)
TIME (MIN.)

EDEN SOIL SERIES
σc = 55 PSI
σc = 60 PSI
RELAXATION MODULUS (PSI) X 10²
PORE PRESSURE (PSI)
TIME (MIN.)

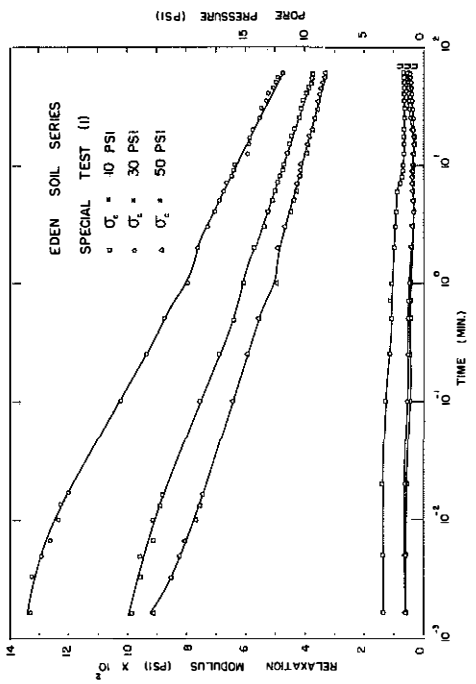
EDEN SOIL SERIES
SPECIAL TEST (1)
σc = 10 PSI
σc = 30 PSI
σc = 50 PSI
RELAXATION MODULUS (PSI) x 10⁴
PORE PRESSURE (PSI)
TIME (MIN.)

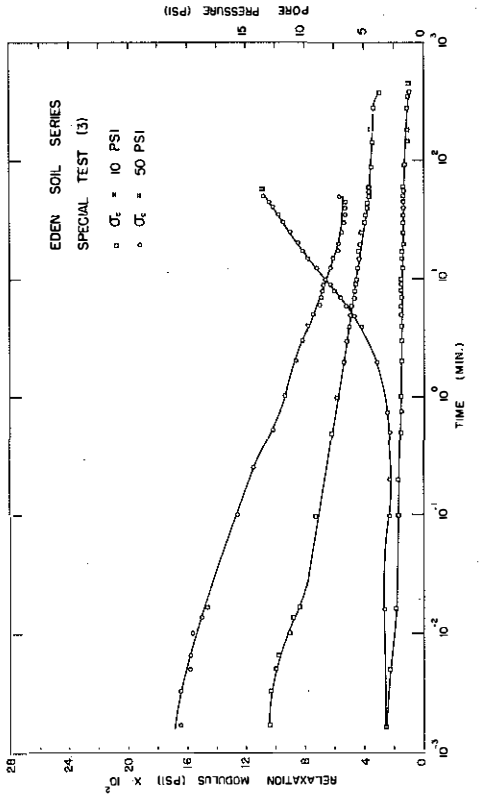
EDEN SOIL SERIES
SPECIAL TEST (3)
σc = 10 PSI
σc = 50 PSI
RELAXATION MODULUS (PSI) x 10²
PORE PRESSURE (PSI)
TIME (MIN.)

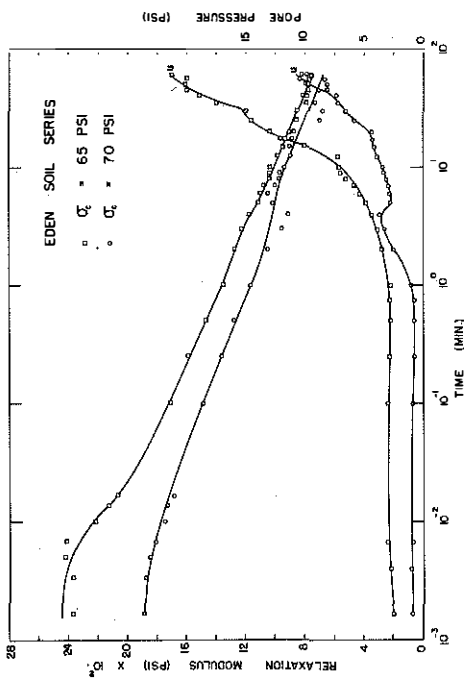
EDEN SOIL SERIES
σc = 65 PSI
σc = 70 PSI
RELAXATION MODULUS (PSI) x 10⁴
PORE PRESSURE (PSI)
TIME (MIN.)

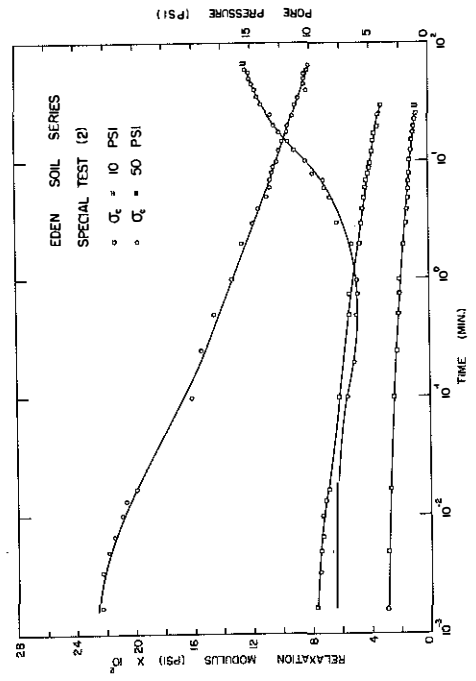
EDEN SOIL SERIES
SPECIAL TEST (2)
σc = 10 PSI
σc = 50 PSI
RELAXATION MODULUS (PSI) x 10²
PORE PRESSURE (PSI)
TIME (MIN.)

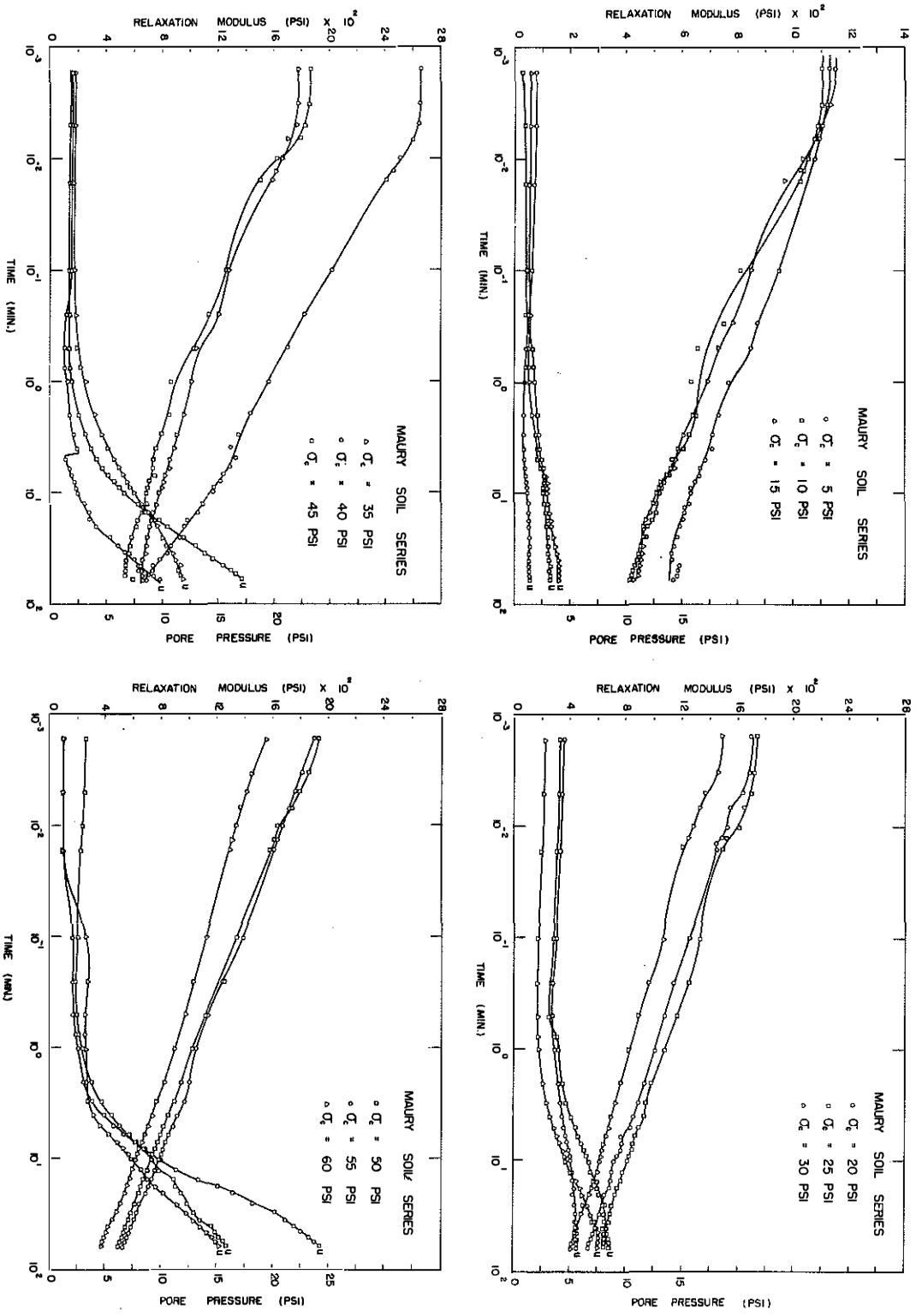
RELAXATION MODULUS (PSI) X 10²
TIME (MIN.)
PORE PRESSURE (PSI)
MAURY SOIL SERIES
○ σ₃ = 5 PSI
□ σ₃ = 10 PSI
△ σ₃ = 15 PSI
MAURY SOIL SERIES
○ σ₃ = 35 PSI
□ σ₃ = 40 PSI
△ σ₃ = 45 PSI
MAURY SOIL SERIES
○ σ₃ = 20 PSI
□ σ₃ = 25 PSI
△ σ₃ = 30 PSI
MAURY SOIL SERIES
○ σ₃ = 50 PSI
□ σ₃ = 55 PSI
△ σ₃ = 60 PSI

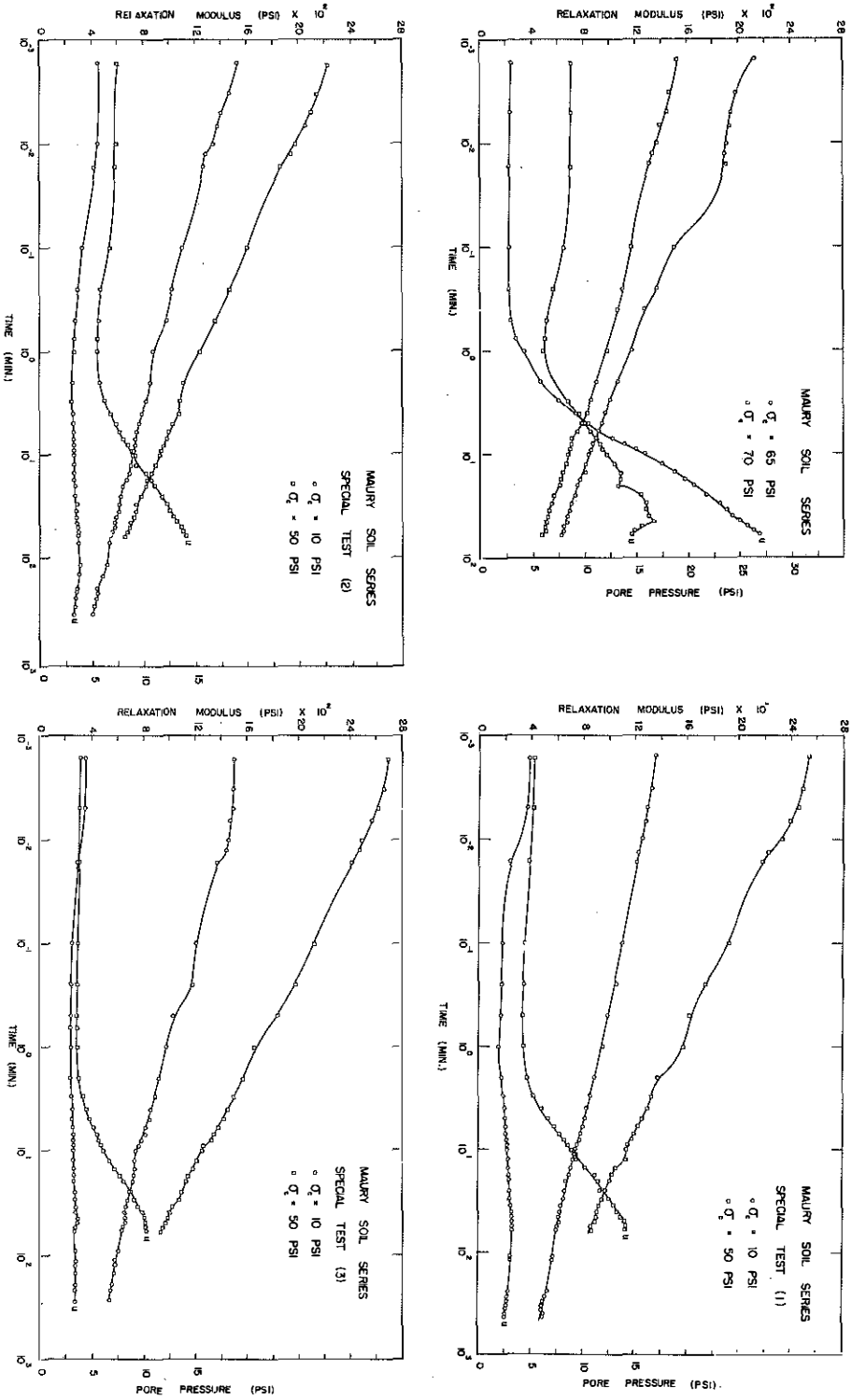
MAURY SOIL SERIES
SPECIAL TEST (1)
σ3 = 10 PSI
σ3 = 50 PSI
RELAXATION MODULUS (PSI) X 10⁻²
PORE PRESSURE (PSI)
TIME (MIN.)
MAURY SOIL SERIES
σ3 = 65 PSI
σ3 = 70 PSI
RELAXATION MODULUS (PSI) X 10⁻²
PORE PRESSURE (PSI)
TIME (MIN.)
MAURY SOIL SERIES
SPECIAL TEST (3)
σ3 = 10 PSI
σ3 = 50 PSI
RELAXATION MODULUS (PSI) X 10⁻²
PORE PRESSURE (PSI)
TIME (MIN.)
MAURY SOIL SERIES
SPECIAL TEST (2)
σ3 = 10 PSI
σ3 = 50 PSI
RELAXATION MODULUS (PSI) X 10⁻²
TIME (MIN.)

REFERENCES

1. Alfrey, T., Jr., **Mechanical Behavior of High Polymers**, Interscience Publishers Inc., New York, 1948.

2. Alfrey, T., Jr. and Doty, P., *"The Method of Specifying the Properties of Voscoelastic Materials,"* **Journal of Applied Physics**, Vol. 16, 1945.

3. Alfrey, T., Jr. and Gurnee, E. F., *"Dynamics of Viscoelastic Behavior,"* **Rheology, Theory and Applications**, Vol. I, edited by Eirich, F. R., Academic Press Inc., New York, 1956.

4. Biot, M. A., *"Theory of Stress-Strain Relations in Anisotropic Viscoelasticity and Relaxation Phenomena,"* **Journal of Applied Physics**, Vol. 15, 1954.

5. Biot, M. A., *"Theory of Deformation of a Porous Viscoelastic Anisotropic Solid,"* **Journal of Applied Physics**, Vol. 27, 1956.

6. Ferry, J. D., *"Experimental Techniques for Rheological Measurements on Viscoelastic Bodies,"* **Rheology, Theory and Applications**, Vol, II, edited by Eirich, R. F., Academic Press Inc., New York, 1958.

7. Folgue, J., *"Rheological Properties of Compacted Unsaturated Soils,"* **Proceedings**, Fifth International Conference on Soil Mechanics and Foundation Engineering, Vol. I, Paris, 1961.

8. Goldstein, M. N.; Misumsky, V. A. and Lapidus, L. S., *"The Theory of Probability and Statistics in Relation to the Rheology of Soils,"* **Proceedings**, Fifth International Conference on Soil Mechanics and Foundation Engineering, Vol. I, Paris, 1961.

9. Havens, J. H. and Daniels, W. F., *"Constitution and Characterization of Paving Asphalts,"* **Bulletin 118**, Highway Research Board, 1956.

10. Havens, J. H. and Deen, R. C. *"A General Survey of Highway Construction Materials, Jefferson*

County," Kentucky Department of Highways, 1965.

11. Hoskins, B. D. and Lee, E. H., *"Flexible Surfaces on Viscoelastic Subgrade,"* **Proceedings,** American Society of Civil Engineers, Vol. 85, No. EM 4, October 1959.

12. Lara-Thomas, M., *"Time-Dependent Deformation of Clay Soils Under Shear Stress,"* **Proceedings,** International Conference on the Structural Design of Asphalt Pavements, University of Michigan, August 1962.

13. Leaderman, H. ,*"Viscoelastic Phenomena in Amorphous High Polmeric Systems,"* **Rheology, Theory and Applications,** Vol. II, edited by Eirich, F. R., Academic Press, Inc., New York, 1958.

14. Lee, E. H., *"Stress Analysis in Viscoelastic Materials,"* **Journal of Applied Physics,** Vol. 27, 1956.

15. Lee, E. H., *"Viscoelastic Stress Analysis,"* **Structural Mechanics, Proceedings,** First Sumposium on Naval Structural Mechanics, edited by Goodier, J. N. and Nicholas, J. Jr., Pergamon Press, New York, 1960.

16. Leonards, G. A. and Girault, P., *"A study of the One-Dimensional Consolidation Test,"* **Proceedings,** Fifth International Conference on Soil Mechanics and Foundation Engineering, Vol. I, Paris, 1961.

17. Lo, K. Y., *"Secondary Compression of Clays,"* **Proceedings,** American Society of Civil Engineers, Vol. 87, No. SM 4, August 1961.

18. Mitchell, J. K., *"Shearing Resistance of Soils as a Rate Process,"* **Proceedings,** American Society of Civil Engineers, Vol. 90, No. SM 1, January 1964.

19. Mossbarger, W. A., Jr., *"Rheological Investigation of Asphaltic Materials,"* Division of Research, Kentucky Department of Highways, January 1964, (MSCE Thesis, University of Kentucky, unpublished).

20. Murayama, S. and Shibata, T., *"Rehological Properties of Clays,"* **Proceedings,** Fifth International

Conference on Soil Mechanics and Foundation Engineering, Vol. I, Paris, 1961.

21. Pister, K. S., *"Viscoelastic Plate on a Viscoelastic Foundation,"* **Proceedings**, American Society of Civil Engineers, Vol. 87, No. EM 1, February 1961.

22. Pister, K. S. and Williams, M. L., *"Bending of Plates on a Viscoelastic Foundation,"* **Proceedings**, American Society of Civil Engineers, Vol. 86, No. EM 5, October 1960.

23. Schmertmann, J. H. and Osterberg, J. O. *"An Experimental Study of the Development of Cohesion and Friction with Axial Strain in Saturated Cohesive Soils,"* **Proceedings**, Research Conference on Shear Strength of Cohesive Soils, American Society of Civil Engineers, 1960.

24. Schiffman, R. L., *"The Use of Viscoelastic Stress-Strain Laws in Soil Testing,"* **STP No. 254**, American Society for Testing and Materials, 1959.

25. Tan, T. K., Discussion on: *"Soil Properties and Their Measurement,"* **Proceedings**, Fourth International Conference on Soil Mechanics and Foundation Engineering, Vol. 3, London, 1957.

26. Tan, T. K., Discussion on: *"Soil Properties and Their Measurement,"* **Proceedings**, Fifth International Conference on Soil Mechanics and Foundation Engineering, Vol. 3, Paris, 1961.

27. Tan, T. K., *"Consolidation and Secondary Time Effect of Homogenous, Anistropic Saturated Clay Strata,"* **Proceedings**, Fifth International Conference on Soil Mechanics and Foundation Engineering, Vol. 1, Paris, 1961.

28. Terzaghi, Karl, *"Discussion,"* **Proceedings**, Research Conference on Shear Strength Cohesive Soils, American Society of Civil Engineers, 1960.

29. Vislov, S. S. and Skibitsky, A. M., *"Problems of the Rheology of Soils,"* **Proceedings**, Fifth International Conference on Soil Mechanics and Foundation Engineering, Vol. 1, Paris, 1961.

30. Wilson, S. D. and Dietrich, R J., *"Effect of Consolidation Pressure on Elastic and Strength Properties of Clay,"* **Proceedings**, Research Conference on Shear Strength of Cohesive Soils, American Society of Civil Engineers, 1960.

BIBLIOGRAPHY

1. Bjerrum, L., *Third Terzaghi Lecture: Progressive Failure in Slopes of Overconsolidated Plastic Clay and Clay Shales,* **Journal of the Soil Mechanics and Foundations Division,** American Society of Civil Engineers, Vol. 93, SM 5, September 1967.

2. Goldstein, M., Lapidus, L. and Misumsky, V., *Rheological Investigation of Clays and Slope Stability,* **Proceedings,** Sixth International Conference on Soil Mechanics and Foundation Engineering, Vol. 2, 1965.

3. Haefeli, R., *Creep and Progressive Failure in Snow, Soil, Rock, and Ice,* **Proceedings,** Sixth International Conference on Soil Mechanics and Foundation Engineering, Vol. 2, 1965.

4. Mitchell, J. K., Campanella, P. G. and Singh, A., *Soil Creep as a Rate Process,* **Journal of the Soil Mechanics and Foundations Division,** American Society of Civil Engineers, Vol. 94, SM 1, January 1968.

5. Pagen, C. A., and Jagannath, B. N., *Effect of Gyratory Compaction on the Rheological Characteristics of Clay,* **Engineering Experiment Station, Report No. EES248-3,** The Ohio State University, Columbus, Ohio, July 1968.

6. Pagen, C. A., and Jagannath, B. N., *Resilient and Residual Mechanical Properties of Compacted Kaolinite Clay,* **Engineering Experiment Station, Report No. 248-5,** The Ohio State University, Columbus, Ohio, July 1968.

7. Pagen, C. A., Wang, C. L., and Jagannath, B. N., *Effect of Compaction and Increase of Saturation after Compaction on the Engineering Properties of Compacted Clay,* **Engineering Experiment Station, Report No. EES248-6,** The Ohio State University, Columbus, Ohio, July 1968.

8. Saada, A. S., *Stress-Controlled Apparatus for Triaxial Testing,* **Journal of the Soil Mechanics and Foundations Division,** American Society of Civil Engineers, Vol. 93, SM 6, November 1967.

9. Saito, M., *Forecasting the Time of Occurrence of a Slope Failure,* **Proceedings,** Sixth International

Conference on Soil Mechanics and Foundation Engineering, Vol. 2, 1965.

10. Schmid, W. E. and Kitago, S., *Shear Strength of Clays and Safety Factors as a Function of Time,* **Proceedings**, Sixth International Conference on Soil Mechanics and Foundation Engineering, Vol. 1, 1965.

11. Singh, A. and Mitchell, J. K., *General Stress-Strain-Time Function for Soils,* **Journal of the Soil Mechanics and Foundations Division**, American Society of Civil Engineers, Vol. 94, No. SM 1, January 1968.

12. Ter-Stepanian, G., *In-Situ Determination of the Rheological Characteristics of Soils in Slopes,* **Proceedings**, Sixth International Conference on Soil Mechanics and Foundation Engineering, Vol. 2, 1965.

13. Vyalov, S. S., *Plasticity and Creep of a Cohesive Medium,* **Proceedings**, Sixth International Conference on Soil Mechanics and Foundation Engineering, Vol. 1, 1965.

14. Wu, T. H., Resendiz, D. and Neukirchner, R. J., *Analysis of Consolidation by Rate Process Theory,* **Journal of the Soil Mechanics and Foundations Division**, American Society of Civil Engineers, Vol. 92, SM 6, November 1966.